Examination of ancient artefacts from Europe (2200 BC-1200 AD) using material analysis techniques

August 25, 2023

Dissertation

Submitted to obtain the degree of
DOCTOR OF ENGINEERING (Dr.-Ing.)

at
FACULTY OF ENGINEERING-KIEL UNIVERSITY

INSTITUTE FOR MATERIAL SCIENCE

Khurram Saleem

born in Lahore

Academic advisor:

Prof. Dr. Lorenz Kienle
Faculty of Engineering-Kiel University
Institute for Materials Science
Synthesis and Real Structure
Kaiserstraße. 2-24143 Kiel
lk@tf.uni-kiel.de

Reviewer:

Prof. Dr. Claus von Carnap-Bornheim
Institute of Pre- and Protohistory
Johanna-Mestorf-Straße 2-6-24118 Kiel
claus.carnap@landesmuseen.sh

Date of Oral Examination: 11.12.2023

Abstract

Field of Archaeology has long benefited from the technological developments in order to provide unique viewpoints on ancient finds. In the light of technological developments for the study of ancient artefacts, material analyses plays an important role to examine the heritage materials and document the history of production, provenance and the craftsmanship of the ancient societies. This approach provides unique scientific results and perspective while contextualizing archaeological finds. In this dissertation, a methodology for the nano analytical analysis of the inorganic (metal alloys and stones) and organic (amber) ancient artifacts is presented. A detailed microchemical analyses is demonstrated in four pilot studies. The first pilot study includes comparing 11th-12th century archaeological objects from two distant regions: former East Prussia and Ostriv cemetery. They include several types of penannular brooches and flat ladder brooches, as well as spiral neck rings. For material analysis nine metal samples were chosen from the Berlin part of the collection and five samples from the Ostriv cemetery from central Ukraine. The series contains four ring-form brooches, three penannular brooches with connected star-shaped terminals, one penannular brooch with widened terminals, four flat ladder brooches and fragments of two neckrings. The second pilot study includes a detailed surface examination of a Neolithic copper axe coming from an Eskilstorp village in present day Sweden. The axe's chemical analyses is conducted to identify the intrinsic and extrinsic elements and authenticate whether a surface treatment of the axe was conducted. The study was conducted to highlight if a reclassification of the Neolithic axe's is needed on the basis of the presence of a decorative silver coating on these Neolithic axes from South Scandinavia. The third pilot study was conducted to study the weathering and degradation of Baltic amber exposed to the environment over decades and analytically comparing Baltic ambers collected from Denmark and Russian origins. The last pilot study consisted of identifying metallic traces on flint and testing the reliability of the trace element analysis methods. The trace element analyses is linked to examine the possibility of identifying whether metallic knapping tools were available in late Neolithic Denmark to produce flint sickles and daggers with intricate shapes. The tools used for the analytical studies included transmission electron microscopy (TEM), scanning electron microscopy (SEM), Raman spectroscopy and fourier transform infrared spectroscopy (FTIR). TEM investigation is enabled by utilising focus ion beam milling (FIB) to prepare thin slices of a specimen from a depth of approximately 30-40 µm from the surface of the artefact. Overall, the artefacts analysed in this study belonged to the different regions of Europe and time periods between 2200 BC and 1300 AD. The chemical and structural information attained from the material analysis techniques have been linked to answer the fundamental archaeological research questions related to provenance, technological development, trade networks and connectivity between the regions.

Kurzfassung

Die Archäologie profitiert seit langem von den technologischen Entwicklungen, die ihr einzigartige Einblicke in antike Funde ermöglichen. In Anbetracht der technologischen Entwicklung bei der Untersuchung antiker Artefakte spielen Materialanalysen eine wichtige Rolle bei der Untersuchung des Kulturerbes und der Dokumentation der Produktionsgeschichte, der Herkunft und der Handwerkskunst der antiken Gesellschaften. Dieser Ansatz liefert einzigartige wissenschaftliche Ergebnisse und Perspektiven und kontextualisiert archäologische Funde. In dieser Dissertation wird eine Methodik für die nanoanalytische Untersuchung von anorganischen (Metalllegierungen und Steine) und organischen (Bernstein) antiken Artefakten vorgestellt. Eine detaillierte mikrochemische Analyse wird in vier Pilotstudien demonstriert. Die erste Pilotstudie umfasste den Vergleich von archäologischen Objekten aus dem 11. bis 12. Jahrhundert aus zwei weit entfernten Regionen: dem ehemaligen Ostpreußen und dem Friedhof von Ostriv. Es handelt sich dabei um verschiedene Arten von Federfibeln und flachen Leiterfibeln sowie um spiralförmige Halsringe. Für die Materialanalyse wurden neun Metallproben aus dem Berliner Teil der Sammlung und fünf Proben aus dem Gräberfeld von Ostriv in der Zentralukraine ausgewählt. Die Serie enthält vier ringförmige Fibeln, drei Federfibeln mit verbundenen sternförmigen Enden, eine Federfibel mit verbreiterten Enden, vier flache Leiterfibeln und Fragmente von zwei Halsringen. Die zweite Pilotstudie umfasste eine detaillierte Oberflächenuntersuchung eines neolithischen Kupferbeils, das aus einem Dorf in Eskilstorp im heutigen Schweden stammt. Die chemischen Analysen des Beils wurden durchgeführt, um die intrinsischen und extrinsischen Elemente zu identifizieren und festzustellen, ob eine Oberflächenbehandlung des Beils durchgeführt wurde. Die Studie sollte zeigen, ob eine Neuklassifizierung der neolithischen Äxte auf der Grundlage des Vorhandenseins einer Silberbeschichtung auf diesen neolithischen Äxten aus Skandinavien erforderlich ist. Die dritte Pilotstudie untersuchte die Verwitterung und den Abbau von baltischem Bernstein, der über Jahrzehnte hinweg der Umwelt ausgesetzt war, und verglich baltische Bernsteine aus Dänemark und Russland analytisch. Die letzte Pilotstudie bestand in der Identifizierung von Metallspuren auf Feuerstein und der Prüfung der Methoden der Spurenelementanalyse. Die Spurenelementanalysen sind mit der Untersuchung der Möglichkeit verknüpft, festzustellen, ob im späten Neolithikum in Dänemark metallische Klingenwerkzeuge zur Herstellung von Feuersteinwerkzeugen mit komplexen Formen verfügbar waren. Zu den für die analytischen Untersuchungen verwendeten Instrumenten gehören die Transmissionselektronenmikroskopie (TEM), die Rasterelektronenmikroskopie (SEM) und die Fourier-Transformations-Infrarotspektroskopie (FTIR). Die TEM-Untersuchung wird durch den Einsatz des Focus Ion Beam milling (FIB) ermöglicht, um dünne Scheiben einer Probe aus einer Tiefe von etwa 30-40 µm von der Oberfläche des Artefakts zu präparieren. Die in dieser Studie untersuchten Artefakte stammen aus verschiedenen Regionen Europas und Zeiträumen zwischen 2200 v. Chr. und 1300 n. Chr.. Die durch die Materialanalyse gewonnenen chemischen und strukturellen Informationen wurden miteinander verknüpft, um die grundlegenden archäologischen Forschungsfragen in Bezug auf technologische Entwicklung und Verbindungen zwischen den Regionen zu beantworten.

Acknowledgement

Firstly, I would like to thank Prof. Dr. Lorenz Kienle for giving me the opportunity to pursue my PhD and write the thesis in the Sythesis and Real Structure Group. I am very grateful to the honorable Prof. Lorenz's continues guidance during the entire period of PhD and consistent availability during group seminars, science days and focus group meetings. I am also grateful to Prof. Claus von Carnap-Bornheim for establishing a link with the museums to source the archaeological artefacts, his guidance and mentorship during the research activities. Thank you for trusting me without any formal background in the field of archaeology and giving me the scientific freedom during the course of this thesis work.

This thesis has been accomplished under the overarching project ROOTS "Cluster of excellence"-social, environmental and cultural connectivity in the past societies funded by Deutsche Forschungsgemeinschaft (DFG). ROOTS is designed to operate under a broad interdisciplinary conceptual framework involving archaeology, history, linguistics, materials science, information technology and several other fields. I would like to thank Prof. Dr. Johannes Müller who is project speaker, for his relentless efforts in making ROOTS excellent. I would also like to mention the scientific coordinator Dr. Mara Weinelt who also served as young academy speaker and resolved administrative matters of the phDs in ROOTS. This thesis would not have been completed without the scientific and non-scientific advice of my colleagues both current and former and I would like to mention few names: The foremost name is Dr. Ulrich Schürmann whose support helped me accomplish many scientific milestones ranging from learning the complicated material analysis techniques, brainstorming research tasks to manoeuvring through the administrative responsibilities and issues. I would also specifically like to appreciate and thank Ms. Christin Szillus for teaching me the sample preparation techniques and always being there for the technical support.

I would like to thank my colleagues who created a conducive and friendly environment in the group for scientific discussions: Niklas Kolmann, Marius Kamp, Niklas Wolff, Redwan-ul-Islam, Ole Gronenberg, Marie Elis, Hendrik Groß, Lennart Voß, Katrin Brandenburg, Julian Strobel, Torben Dankwort and Ahmed Takriti. I would also like to thank my counterparts in the archaeology who helped fill the knowledge gaps. Worthy mentions are Dr. Roman Shiroukhov, Dr. Jutta Kneisel, Dr. Oliver Narkoinz, Moiken Henrich, Dr. Berit Erikson, Henry Skorna, Anna Loy, Benjamin Serbe and Dana Zentgraf. I am grateful to the administration of "Museum for Pre- and Early History Berlin" and "Centre for Baltic and Scandinavian Archaeology (ZBSA)" for trusting us with the valuable artefacts.

Last but not the least I would like to thank my family and friends for the encouragement through my PhD journey and providing unconditional support.

Contents

List of Figures

List of Tables

1 Introduction

Cultural heritage materials are an important aspect of human history that reflect the identity and history of a particular society. In order to understand these materials and their historical context, it is important to employ an interdisciplinary approach that combines the expertise of various fields such as archaeology, history and material science to name a few. One of the key aspects of understanding cultural heritage materials is determining their provenance or the history of ownership and location of an artifact [3]. This information can provide important insights into the cultural, social and technological context of the materials and can help to establish authenticity of the artefacts and connectivity between the regions. In order to determine the provenance of cultural heritage materials, various techniques can be employed. Stylistic examination is one such technique that involves the examination of the aesthetic and design elements of an artefact, such as motifs and decoration, as well as the methods and materials used in its creation [4]. By comparing these attributes with those found in other artefacts from the same period and region, it is possible to establish a likely place of common or distinct origin and establish cultural context for the artefact. In addition to stylistic examination, various scientific techniques can be employed to determine the provenance of cultural heritage materials and chronocultural sorting can be done [5]. In the past several decades intensive and multi-disciplinary research has been carried out at the interface of archaeology and solid state analysis. However, new procedures and methods are now being developed to analyse ancient materials more actively. Scanning electron microscopy (SEM), fourier transform infrared spectroscopy (FTIR) and Raman spectroscopy are some of the more commonly used techniques in the field of cultural heritage science depending on the kind of analysis required. SEM is a microscopy technique that enable the examination of materials at a microscopic scale. Comparatively, transmission electron microscopy (TEM) is less frequently used in the context of archaeological research but carries a huge potential for providing atomic scale composition and structural information of the artefacts [6]. It uses a beam of electrons to produce an image of the internal structure of the material at much higher resolution compared to SEM [7]. Combination of SEM and TEM techniques can provide important information on the microstructure from surface and intrinsic material of the objects [8]. On the other hand, FTIR and Raman spectroscopy are techniques that allow for the identification of the chemical components of organic artefacts such as amber, textile items, pollen and others [9] [10]. These techniques can provide important information on the materials and can be used to identify the source of raw materials, estimation of plant origins, paleoclimatic conditions and the relative age of the artefacts based on the degree of polymerisation of molecules. The natural environment can often be detrimental to cultural heritage materials, leading to a) degradation and deterioration of the valuable assets and b) making the analytical studies difficult or misleading [11][12] [13]. Fazio et al. (2019) conducted the material analyses of the Roman Orichalcum coins. The authors found dezinfication on the corroded surface, hence, giving a false indication of the underlying base metal components [14]. Therefore, it is also important to understand the processes of degradation in order to develop effective conservation methods and understand the original artefacts' composition in order to reach the precise conclusions

related to the materials of the artefacts [15] [16] [17].

In this dissertation, an interdisciplinary approach that combines the expertise from the field of material science techniques and archaeology are employed to examine the cultural heritage materials and societies of the past. The research work included in this thesis is focused on four different materials: medieval metallic brooches, metallic Neolithic axe, late Neolithic flint stone and amber. One of the main contribution of this work is the application of TEM in combination with SEM to investigate the intrinsic and extrinsic material related features in the metallic artefacts. The sample preparation for the TEM studies is conducted via focused ion beam milling (FIB) from these metallic samples. FIB allows reaching internal structure to prepare a nano sized sample. This sample preparation strategy helps to keep the process extremely minimally invasive. The main points in this work can be highlighted as follows: i) To provide chemical compositions of the metallic and organic artefacts included in the study ii) To demonstrate that focused ion beam milling in combination with TEM has the ability to provide micro chemical analysis of the ancient artefacts in a quasi non destructive manner iii) To contribute to a better understanding of the degradation on metallic artefacts exposed to natural environments for a prolonged period of time. iv) Demonstrate combined usage of FTIR and Raman to classify amber and to trace changes in its chemical fingerprint when it degrades by heat exposure v) To differentiate between the extrinsic and intrinsic material properties of the heritage materials provided by SEM and TEM analysis. All of these mentioned points are organised in six sections within the framework of this thesis work. These sections provide a structured approach from state of the art literature in archaeometry to conclusions of relative sections. A brief overview of the individual sections is provided in the following paragraphs.

Section 1 is the literature review and provides the recent developments and state of the art in the material analysis techniques mainly related to the electron microscopy and methods for the heritage materials. Multiple time periods ranging from stone age to medieval times across several typological artefacts are included in the review. The studies involve methods for base metal identification and trace elements analysis. The base metal and trace elements are then linked to answer historical research questions. The studies involve diverse group of ancient locations from South America to Northern Europe and Central Asia. Some of the studies are not directly related to the ancient artefacts but are instrumental in understanding the changes that take place in archaeological items over decades. It covers the phenomenon of secondarily deposited corrosion layers on the soil buried artefacts and related chemical processes. It provides comprehensive details of specialised case studies that give the literature framework for the interpretation of analytical results of the artefacts examined as part of this thesis.

Section 2 presents the methodology combining the stylistic interpretation approach from arts and material science for the comparative analyses of the metallic artefacts. Moreover, instrumentations, test parameters, theoretical description and step by step procedure of the analytical tools is also covered under this section. Certain limitations of the chemical

analyses and the analytical equipment are also highlighted here.

Section 3 begins with the pilot study 1 describing mobility and migration patterns between the East Baltic population in the Central European regions of present day Kiev, Ukraine. The possibility of common origins of the population is explored by laboratory analyses. This section provided the chemical fingerprints of metallic artefacts from Prussian Collection and Ostriv cemetery. Moreover, the stylistic features and physical morphology such as typology and dimensions are utilised for comparison between the artefacts from the two distinct regions. The Prussion Collection is received from the Museum of Pre and Early history Berlin whereas the artefacts from Ukraine are received from Kiev (Ukraine). The set of artefacts are from 11th-12th century AD and are selected based on typological commonalities. The section includes metallic ring brooches, horseshoe brooches with star shaped terminals, flat ladder brooches, penannular brooches with widened terminals and spiral neckings. Focused ion beam milling was used to prepare TEM samples and major part of the chemical analysis is conducted in the TEM. Whereas SEM is also used to analyse the artefacts described above for surface analysis.

Section 4 consists of second pilot study that is conducted on a low flanged Neolithic copper axe. The axe was excavated in a village Eskilstorp in Sweden and dates between the years 1800-2200 BC. The axe is believed to be produced locally and found in a Pile type hoard. The Pile type hoard contained several copper axes of various categories and non of them is believed to have surface decorations. This pilot study involves a combination of SEM and TEM analyses to conduct a detailed surface analysis and examination of this late Neolithic copper axe. Moreover, a corrosion experiment on the experimental alloy simulating the possible selective surface deterioration phenomenon is also included in this section.

Section 5 is the pilot study in an attempt at finding chemical fingerprint of Baltic amber. Moreover, it involves degradation experiments under heat and UV light to observe the changes in the chemical information. The amber items included in this study are from Kalliningrad Russia and Skallingen Vejers Denmark. For the analysis FTIR and Raman spectroscopy techniques are utilised. The chemical features attained using FTIR and Raman spectra are used to identify features specific for Baltic amber and then pristine and heat treated amber samples are compared with each other. The study focuses on exploring provenance studies of Baltic amber and the effects on its molecular structure under intense environmental conditions such as heat or UV radiations. It provides a comparative organic material analysis of such artefacts using FTIR and Raman.

Section 6 the last pilot study presented in this section involves flint stone samples. The hypothesis tested in this section is that the flint made in late Neolithic time period in the region of Denmark was prepared using metallic knapping tools. For this, we attempt to find metallic traces on experimental replicas prepared in 2018 using copper knapping tool. A two step methodology involving identifying the metallic traces using digital microscopy and SEM EDS analyses to differentiate between false positives is presented in this study.

This section further explores the reliability of this technique by heat treating the flint experimental replicas in order to observe if the oxidised metal remains on the surface and is detectable.

2 Literature Review-Developments in the field of Archaeometry

Overview

The literature review is divided into two sections, which provides a summary of the current literature in the field of archaeometry. The first section summarizes the articles that focus on non-destructive testing of archaeological materials in order to analyze corrosion/patina layers on metallic artifacts, sample preparation techniques as well as technical considerations for the analysis of heritage materials [18]. The second section includes specialized articles (case studies) that will serve as references throughout the remainder of this thesis.

This approach to literature review not only summarizes current knowledge but also develops a workable methodology that can be cross-referenced during the interpretation of the results in this thesis work. Given that the overall nature of the results presented in later sections is highly visual, with electron images, elemental maps, and spectra, we will incorporate relevant images from the articles under review to serve as a point of reference for visual analysis. The topics covered in the thesis include provenance studies using elemental data, hypothesized ancient surface treatment processes, corrosion phenomena of copper metal, and analyses of organic (amber) materials and their degradation studies.

Physical, chemical, and biological analytical methods have been long used in the archaeology, history, and arts. The tendency of analytical methods to provide a well rounded chemical analysis is especially instrumental when studying ancient objects and items such as ornaments, manuscripts, paintings, and sculptures. This approach provides unique scientific results with new dimensions to scientific research in the field of archaeology. In most cases, archaeological research is concerned with questions such as: where, when, by whom, and for what purpose a given artifact was manufactured, what material an artefact was made of, what are the ways a particular artefact was fabricated, and what are the historical contexts of the researched artefact given its geographical information.

The choice of an analytical method or a combination of complementary methods for the analysis is determined by the type of artefacts' material and the objectives of its study. Items of study can be categorised into several basic types: items produced with inorganic composites (stone, ceramics, glass, and metal alloys) and organic materials (parchment, wood, tissue, plants, bones including elephant ivory, paper, cardboard, and pigments). Heritage materials and archaeological artefacts are analyzed in order to determine the compositional properties of the materials, their production technology, and the possible geographic region where these objects were imported or exported. Analytical techniques are also applied in order to confirm the authenticity of an archaeological object. Additionally, to study the problems related to the recovery of the objects and their preservation from the destructive and often corrosive effects of the environment to conserve the objects displayed in the museum.

Among a great many modern and powerful methods of analytical studies, electron microscopy holds an important stature. For this purpose, scanning electron microscopy techniques are widely utilised and their applications in archaeological research are increasing in recent times. This is due to the simplicity of these methods and the opportunity of studying valuable ancient objects without their initial preparation and conservation of a sample even after the analysis. The workable size of the analysed regions can vary from several tens of centimetres to several nanometres. These techniques also provide the possibility to easily change the magnification from several tens to several millions, and attaining information about the surface morphology of the analysed regions and the elemental composition from the intrinsic structure of the specimen.

Electron microscopic techniques can be used in practically all studies of cultural objects, from determining the composition of stone or medieval age tools, decorative ornaments or items of particular social status. Advantages of using SEM include its large focal depth, which exceeds that of optical microscopes by a factor of about 300. Due to this, one can obtain clear images of sample surface areas and attain precise information. Another electron microscopy technique is transmission electron microscopy (TEM). This technique is used much more rarely because it requires complex sample preparation since the thickness of the specimen should not exceed 10 - 100 nm (depending on the material) due to the necessity electron transparency. However, this technique provides data on the crystal structure of the sample material and its composition with a high spatial resolution i.e. up to the sub-angstrom level. TEM has not very widely utilised in archaeology because of complex sample preparation. However, several researchers have utilised TEM in the recent past to identify features on a nanoscale which helped decode optical properties of archaeological artefacts. More on this topic is presented in the specialised case studies section. In the context of this thesis work FIB and TEM are applied for the first time on the medieval artefacts from Prussian Collection and typologically similar artefacts from Ostriv (Central Ukraine). More details are covered in the following sections.

2.1 Non-destructive Testing, Corrosion Characterization and Sample Preparation Techniques

Non-destructive testing (NDT) has played a role in identifying the internal morphological and physical properties of artefacts without damaging the artefacts. These physical properties and morphologies remained hidden in the past because destructive analysis prevented their examination due to ethical concerns i.e. damage of ancients items of historical significance. Fortunately, techniques of various types such as scanning electron microscopy (SEM), transmission electron microscopy (TEM), focused ion beam (FIB), x-ray fluorescence (XRF), fourier transform infrared spectroscopy (FTIR) and Raman spectroscopy have aided researchers to develop the pathway for examining the morphological and physical properties of the artefacts without damaging the health of the items. The NDT data has the potential to provide complementary data from different techniques or different modes in a technique to cross correlate the chemical fingerprints. In archaeology, determination of the original alloy composition is important to know the true structure of the centuries old soil buried artefacts. Monetary theories or theories about the technological advancement and economic development can be made only after analyzing the internal compositions. Such studies require analysis of the archaeological artefacts from different time periods to follow the material evolution over the time period [19][20]. Research into the original structure of the ancient artefacts however present major challenges owing to the corrosion or restoration of the artefacts [21]. In copper alloy objects, secondary alterations cause surface modifications due to patination and corrosion. As a result, differently colored layers appear on the surface of the artefact comprising of various chemical compounds making investigations of the internal structure of the artefact challenging. Black patina can form on any copper surface as a result of corrosion, however, intentional patina of the metal archaeological artefacts have also been found on ancient artefacts. Intentional high temperature oxidation to obtain a dark patina on Egyptian and Roman artefacts was reported by Aucouturier et al. (2010) [22]. Many laboratory studies have been performed to elucidate the one or more processes that control copper solubility and speciation in soil. The obvious examples include studies on the effect of pH, degree of contamination, dissolved organic matter in soils, and soil type effects on the solubility of copper in soils which will be discussed in later section.

Archaeological materials have also been often investigated using x-ray flourescence (XRF), particle induced x-ray emission (PIXE) and x-ray diffraction (XRD) methods [23]. With each technique having its advantages and limitations, a combination of these techniques is often utilized to attain detalied microchemical analysis [24]. XRF, PIXE and SEM, are known for surface limited analysis techniques. In SEM the chemical information from only a depth of 2.5 µm is attainable for copper based alloys even at 30 keV [25]. Constantinescu et al. (2007) reported on the classification of Apollonia and Dyrhachium silver drachmae (currency of Greek) found on Romanian territory by using SEM EDS and PIXE. They acquired chemical composition of the drachmae and drew conclusions about the connections between the coins composition and historical economic aspects of the corresponding period. The authors associated hard economical and political situation

with the increased Cu content of drachmae [26].

Similarly, Ghoniem et al. (2011) utilized combination of SEM EDS and XRD to reveal the corrosion products and contaminents such as Ca, C, S, Cl, Si, Al and Mg on Egyptian bronze statue. The authors reported higher percentages of the actual composition such as Cu, Sn and Pb in the internal layer and lower concentration in the corrosion layer on the surface of the artefacts [27]. Therefore, to reach higher depths and attaining chemical information from inside the ancient artefacts, a more sophisticated sample preparation technique is crucial in archaeology. For this purpose focused ion beam milling could be utilized which is not frequently used on archaeological samples so far. Focussed ion beam (FIB) milling offers the more advantageous means of obtaining access to the bulk composition with a non-noticeable extremely minimal invasion into the artefact. With several micromanipulators, FIB extracts a thin free standing slice from roughly 5-40 µm depth of the material using ion beam [10]. For nanoscopic elemental investigation, transmission electron microscopy (TEM) is performend on such thin slices of the material giving access to the internal structure of the artefacts [28].

2.2 Specialized Case Studies

This section provides an overview of the literature in the field of non-destructive testing (NDT) techniques applied on the archaeological artefacts within Europe and around the world. Some of the studies are also from non-archaeological samples which help understand the material changes under influence of the environment which can help understand the paleoclimatic conditions as well. The section aims to highlight the uses and applications of material analyses technologies on archaeological artefacts for examining the surface treatments, identifying geographical connectivities, environment impacts on the artefacts and usage of raw materials for the production. The case studies presented here consist of titles of the research articles, authors and are followed up by the findings from the researchers.

Vindel et al. 2018, "The contribution of transmission electron microscopy (TEM) to understand pre-Columbian goldwork technology." Journal of Archaeometry 60, 2 (342-349)

The first study presents the usage of a combination of material analysis techniques such as XRF, SEM EDS and TEM to analyse the gilding and silvering methods on pre-Columbian gilded objects. Two gilded rods were analysed in this research work belonging to the archaeological sites of Atacames in the region of Esmeraldas, Ecuador. The objects were dated between AD 750 and 850 which was the early phase of Atacames culture in the Esmeraldas. The archaeological site, as described by the authors is in a rainy tropical environment and the objects were covered with brown-green corrosion of cuprite. For sample preparation, a cross section of 0.25 mm thickness was cut with a diamond wire in order to investigate the inner area. The cross section revealed that the rod was com-

posed of an internal black and an external metallic part. The authors report that the outer metallic part did not tightly adhere to the inner core and is separated fairly easily. The sample from the core of the rod was prepared by the drop casting method on a Cu grid. The external section on the other hand was too ductile to be ground, therefore, ion milling was used to prepare an electron transparent sample. The investigation on the cross sections using SEM imaging and EDS analysis demonstrated higher gold content (17 at.%) on the outer part of the artefacts, which was occasionally very low (1.64 at.%) and sometimes not detected at all in the inner core. Additionally, the inner core consisted of regions having copper and very high chlorine content (40 at.%) and some regions had copper with low chlorine content (3.43 at.%).

Summarising the results, TEM combined with SEM EDS suggested that gilding process was applied to the surface of the rod. One reason for the presence of chlorine is proposed to be the result of corrosion, however, the authors propose an alternate hypothesis for such high chlorine content, they state that it could be a hint of the chemical and annealing processes conducted on these object. The study further explains that the grain boundary diffusion of Au in Cu is facilitated with an acid solution. This type of diffusion is a characteristic between elements with complete solid solubility but with a difference in the atomic radii. Taking into account that above 350°C solubility of gold increases on chloride rich systems, the formation of chloride complexes ($AuCl_2$), eventually could have contributed in the mobilisation of the Au in an aqueous solution. A drop in the temperature at the surface might have resulted in deposition of the metallic gold on the surface region. The authors concluded the study by stating that the gold smith probably heat treated the rod to obtain a very thin Au-enriched surface layer by this process pointing towards the craftsmanship of the worker [29].

Roxburgh et al. 2018, "A comparative compositional study of 7th to 11th century copper alloy Pins from Sedgeford, England, and Domburg, the Netherlands." Journal of Medieval Archaeology

This study compares the medieval pins from Norfolk (England) and Domburg (Netherlands), 19 pins from Domburg and 14 pins from Sedgeford were analysed. This research presents a comparative analysis based on the style, manufacturing process and raw materials of the early medieval pins. The authors quote that ancient copper alloys have been a subject to typological interest and comparisons since over two centuries, however, the ability to study from the compositional aspects of the artefacts was only developed after 1950s. With the invention of elemental analysis techniques, alloy studies have already shed light on the compositions and technical choices available to ancient craftworkers. In this study, the researchers found that the main alloying agents of copper were tin and zinc with or without lead. Alternatively, a mixture of tin, zinc and copper was found as well, namely 'Gunmetal´. Also, a correlation between the type of the aretfact and the artefact's composition was observed. The authors suggested, that different type of pins were possibly produced separately at single or multiple sites with a deliberate control of the compositions at occasions.

The authors regard bronze as the material mostly found in early medieval Britain, however, a significant amount of bronzes at that time were not pure, often mixed with other alloying ingredients. The other major alloying element was zinc, to make brass, possibly favoured in medieval times for its distinctive gold colour. This may have created a cultural value between the brass and the bronze. Brass alloys involving more elaborate cold working such as hammering and bending became the metal of choice for high status jewellery, may be also these pins.

Bronze on the other hand, especially leaded, was easier to cast into thinner objects, so probably suitable for mass production as suggested by the authors. In this study the corrosion process was also evaluated and was noted that zinc is the principle element lost during the corrosion process, creating the patina and permanently altering the original surface. In the copper zinc ratio, the zinc loss was clearer between the corroded and non-corroded surfaces. Due to the presence of tin mining areas in south western England, the authors hypothesize that bronze pins might have been made closer to these areas and then distributed. Fresh brass on the other hand might have entered England in ingots via the North Sea trade network. The main entry points for regular supplies would most likely be ports of Ipswich and Hamwic. Whereas the large scale production of the pins happened in the urban centres. The pins from Domburg showed the similar pattern where majority of the pins were produced in a bronze alloy with a smaller group of brass. However, the pins from Domburg had small content of zinc as well when compared to Sedgeford bronze pins. So, a less pure bronze was used in Domberg and could also be classified as tin dominant gunmetal. It could be because zinc scrap was added into the mixture or zinc was deliberately entered as corrosion inhibitor in bronze. However, the small zinc content could also have come from the leftovers in the crucibles. So the alloy of choice at Domburg (Netherland) was bronze (or tin rich gunmetal) and the small minority of brass might have come from a different production centre, possibly from a site where production in brass was a norm. The richer, more gold like brass pins that might have been imported in Domburg, may have provided competition for locally produced pins [30].

Miśta et al. 2019, "Material description of a unique relief fibula from Poland." Archaeological and Anthropological Sciences (2019) 11:973–983

The authors present a stylistic and elemental study of an artefact from 6th century Radziejów, Poland. The authors point towards the possibility of the artefacts as the imported item from Scandinavia or the middle Rhein area. Two specimen were taken and their surfaces were etched with one part of perchloric acid $HClO_4$ and two parts of acetic acid anhydride $C_4H_6O_3$ solution for 10 s. SEM EDS, µ-XRF, XRD and Vickers hardness tests were part of the analyses in this study. Irregular cloudy shapes were found on the surface of the artefact that the authors attributed to the corrosion and soil contaminants on the structure. The main elements determined by SEM– EDX, on the other hand, were copper (63.95 ± 1.06 at.%), zinc (15.98 ± 0.73 at.%) and tin (18 ± 1.49 at.%), while lead

was present as a trace element (0.9 ± 0.82 at.%). The authors argue that the addition of lead was to improve the machineability of the alloy [31]. Other examined trace elements were silver (0.9 ± 0.06 at.%) and iron (0.59 ± 0.08 at.%) in the alloy. A higher amount of tin, silver and lead was present on the surface compared to the interior of the artefact which is attributed to the possibility of dipping the artefact in the molten tin during the production process. The molten tin solution perhaps also has silver from the ore (galena PbS) [32].

Drozdov et al. 2021, "Lycurgus cup: the nature of dichroism in a replica glass having similar composition", Journal of Cultural Heritage, Vol 51, Page 71-78

The nature of the very unusual optical properties of the Roman Lycurgus cup carved with a scene of Lycurgus death has interested researchers over last several years. It has a vine red colour in transmitted and olive green colour in reflected light. The optical properties of the Lycrugus cup were previously associated with a colloidal Au/Ag nanoparticle by Freestone et al. (2007) [33]. However, recently Drozdov et al. (2021) suggested bimetallic Au and Ag nanoparticles being responsible for the red colour appearance only. Experimental replicas prepared by the authors showed the light absorbance by iron ions and light scattering due to silica rich phase as reason for the olive green colour [34].

Nicolopoulos et al. 2018, "Novel characterization techniques for cultural heritage using a TEM orientation imaging in combination with 3D precession diffraction tomography: a case study of green and white ancient Roman glass tesserae", Heritage Science

FIB has not been frequently used in archaeology for sample preparation, however, there are some publications where this technique was used. For instance, Nicolopoulos et al. (2018) used FIB to prepare electron microscopy samples in order to characterise green and white ancient Roman glass tesserae by advanced electron diffraction techniques to reveal insights into the ancient ceramic pigments. The authors utilised a combination of automated 3D diffraction tomography and ASTAR techniques (for orientation and crystallographic phase mapping) in order to reduce dynamical effects and obtain nanocrystallites and space group symmetries with great precision. The results revealed the presence of $Pb_2Sb_2O_7$ cubic and $CaSb_2O_7$ trigonal structures responsible for green and white colours. Moreover, STEM EDX analysis showed trace elements of Cu, Co and Fe. It was revealed that same space groups with variation in amount of copper or cobalt caused the glass to look either green (yellow to green) and white (blue to white) in their respective nanocrystals inside the glass matrix [35].

Ghoniem et al. 2011, " The characterisation of a corroded Egyptian bronze statue and a study of the degradation phenomenon", International Journal of conservation science, Volume 2, Issue 2

The authors conducted the examination on the surface and cross section specimen of

the Egyptian bronze statue excavated in Sais, Egypt. The research employed optical microscopy, SEM EDS and XRD to analyse the patina, corrosion products, elemental investigation and the corrosive effects on the alteration processes. The analyses revealed bronze as the primary alloy with lead and tin content. It was further stated that three layers of altered products with varying compositions and morphologies were found on the artefact. The SEM EDS demonstrated the presence of Cu, Sn and Pb (associated with ancient bronze), along with carbonates, sulphates, chlorides and contamination products such as Ca, C, S, Cl, Si, Al and Mg. The researchers made the distinction between the layers based on the higher concentration of primary alloy in the substrate while prevalent presence of containments on the outer layer. Conversion of copper into cuprite (Cu_2O, detected by XRD) was also observed, which was stated as an electrolytical membrane allowing the transport of oxygen and chloride ions inwards and cuprous ions outwards. Copper chloride (CuCl) is regarded as sandwiched between cuprous oxide layer and substrate layer. Warraky et al. (2004) also showed consistency with this phenomenon in their study [36]. The authors state that lead was possibly added to improve the cast process whereas choice of bronze was associated with its high corrosion resisting properties and reproducibility, keeping the decorative details on the artefacts intact [37].

Zeren et al. 2016, "Using Raman spectroscopy of counterfeit amber examinations", International journal of multidisciplinary R and D, Vol 3, Pages 216 to 219

In this study, the authors demonstrated the use of Raman spectroscopy to differentiate natural amber from artificial amber. The spectral patterns attained via Raman served as fingerprints to find the chemical composition of the substance and to provide the quantitative or semi-quantitative information. The author recorded Raman spectrum of ten samples that were plotted between the range of 720 and 1800 cm^{-1}. The strong features appearing at 776, 846, 998, 1259, 1435 and 1608 cm^{-1} were then used to authenticate the real amber from the artificial amber [38].

2.3 Specialized Case Studies based on non-archaeology materials

By examining the interactions between materials and their environments, an understanding can be developed about the factors like temperature, humidity and the chemical components that contribute to corrosion of the archaeological artefacts. This section provides the case studies related to the corrosion phenomenon of the copper based materials.

Siano et al. 2009, "Use of neutron diffraction and laser-induced plasma spectroscopy in integrated authentication methodologies of copper alloy artefacts", Journal: Nuovo Cimento della Societa Italiana di Fisica B, Vol 124, Page 671-686

Siano et al. (2009) did micro chemical analyses to authenticate the copper based artefacts. They utilised a methodology in which they employed micro chemical analysis techniques such as time-of-flight neutron diffraction (TOF-ND) and laser induced plasma spectroscopy (LIPS) in an attempt to differentiate between the time dependent and time independent surface alterations. The analyses highlighted the enrichment of the elements on the original surface of the artefacts (Sn in this case) and the penetration of burial ramifications in the form of Cl, Si and Ca [39].

Hong et al. 1997, "Corrosion and Leaching of Copper Tubing Exposed to Chlorinated Drinking Water", Journal of Water, Air, and Soil Pollution

The study examined how free chlorine in the form of hypochlorous acid and hypochlorite ions affects the amount of copper present in water that comes into contact with the solid metal, and suggested an explanation for copper leaching based on oxidation and dissolution processes. The proposed mechanism to explain the leaching includes two phases: (1) initial direct oxidation of the solid metal surface by free chlorine forming cupric oxide, and (2) subsequent dissolution of the partially oxidized copper surface, which depends on the solubility of the copper mineral products at a specific pH. The copper metal can dissolve in the water forming various complexes, a comprehensive list of the complexes is given by the authors in the article. The study also showed that the leaching was enhanced with increase in chloride and carbonate concentrations [40].

Bella et al. 2002, Degradation of power contacts in industrial atmosphere: silver corrosion and whiskers, electrical contacts", Proceedings of the Annual Holm Conference on Electrical Contacts

The authors studied the behaviour of electrical contacts (copper parts plated with silver) in a corrosive environment of H_2S. It was found through morphology and composition analysis via SEM EDX that there occurred extensive growth of silver whiskers (thin needle-like filaments) after the formation of thin silver sulfide (Ag_2S) layer. The silver whiskers practically grew everywhere but the growth occurred more abundantly near the edges and corners of the contacts. The whiskers are elongated single crystals of pure

metal that have been reported to grow more than 4 mm in length with a diameter of 0.3 to 10 micrometer. They have been reported to be straight, kinked, hooked or forked and some are reported to be hollow as well. Temperatures around 50°C or moisture are proposed to be more suitable conditions for the growth of these whiskers. The SEM elemental analysis (shown in the article) shows the newborn whiskers which start to extrude from the flakes as a group of thin straight or curly filaments of different thicknesses. The chemical composition of the whiskers revealed predominantly >90 % silver content with presence of sulphur (some instances upto 9 %). The amount of sulphur also correlated with the dull dark colour of the whiskers [41]. This is an important case study in the context of this thesis work which shows the morphology of the corrosion product of silver to be whiskers or hair like. It is a phenomenon that is also observed on the late Neolithic copper axe, more on this in the later section.

Warraky et al. 2004, "Anti-corrosion methods and materials emerald article: Pitting corrosion of copper in chloride solutions", Journal of Anti-Corrosion Methods and Materials

Warraky et al. (2004) conducted corrosion experiments and drew conclusions about the mechanism of the pitting corrosion on copper in different concentrations of chloride solutions. From the results it was concluded that pitting corrosion of copper occurs when a protective film of Cu_2O exists on its surface which corrodes further in presence of chloride solutions. The author devised the Cu_2O formation on the surface as a result of cathodic reaction of copper reduction. The initiation of pits on sites where CuCl was trapped under the overlying Cu_2O layer at higher NaCl concentrations was reported in this study [36]. This study is linked with the interpretation of the results when examining the surface of the Neolithic copper axe which also showed evidence of the pitting corrosion.

Overall, the specialised case studies provide a basic frame work to help interpret our findings. The later section provides the details about the methodology employed in the scope of this work.

3 Methodology

3.1 Overview

This section represents the design of the research, experimental methodology, methods, instrumentation and technical considerations.

3.2 Empirical Research

The research design of this thesis is mainly structured around the principles of empirical research. Empirical research obtains data and generates knowledge via indirect/direct observations, rather than from theory [42].

In the context of this thesis, stylistic analyses, surface investigations by means of macrophotography and scanning electron microscopy (SEM) represents the preliminary or surface investigations, whereas the advanced analyses conducted by transmission electron microscopy (TEM) represents the main phase of investigations attaining the information from the internal structure. Moreover, organic samples are analysed under FTIR and Raman spectroscopy.

3.3 Experimental Methodology

As literature suggests, the analysis of the ancient finds still remains an important scientific challenge that requires methodology and a criterion. Rabbiola and Porter [1] in their research proposed two pertinent approaches to examine cultural materials one being historical and artistic and the second being material science approach. The historical and artistic approach concentrates on the study of style and typology as well as the history of the artefacts. While the material science approach focuses towards the identification of the tangible characteristics of the metals such as composition, primary and secondary alterations, patinas/corrosions and fabrication techniques. This dual approach of historical artistic and material science is the mixed methodological approach this thesis incorporates.

The historical and artistic approach attributed to (a) stylistic analyses (b) typology and the material science approach includes (a) metallurgy, composition, structure, technology and fabrication and (b) patina, corrosion and surface characterisation. The research work in this thesis aims to achieve the maximum inter-disciplinarity by integrating contributions from human sciences and technological fields. The material science approach will be the center of focus which is based on understanding the material composition and comparing it with the available data set or artefacts originating from similar areas or with identical stylistic attributes. Thus, the major, minor and trace elements are determined to link the compositions of the artefacts with a known reference. Moreover, the material analyses database developed during this research work can potentially serve as

the reference database for similar typological, stylistic and temporal artefacts in future excavated items. One aspect of the material science approach is to investigate the patinas, whose compositional and microstructural analysis can provide information about the corrosion products and point out whether they are consistent with the bulk. It can also possibly indicate the state of the corrosive environment, possible surface treatments and help reorient interpretation of decorative surfaces on the artefacts.

A schematic representation of authenticating the artefacts from the works of Robbiola and Portier is used to compare the artefacts in our research [1]. The schematic is shown in Figure 1.

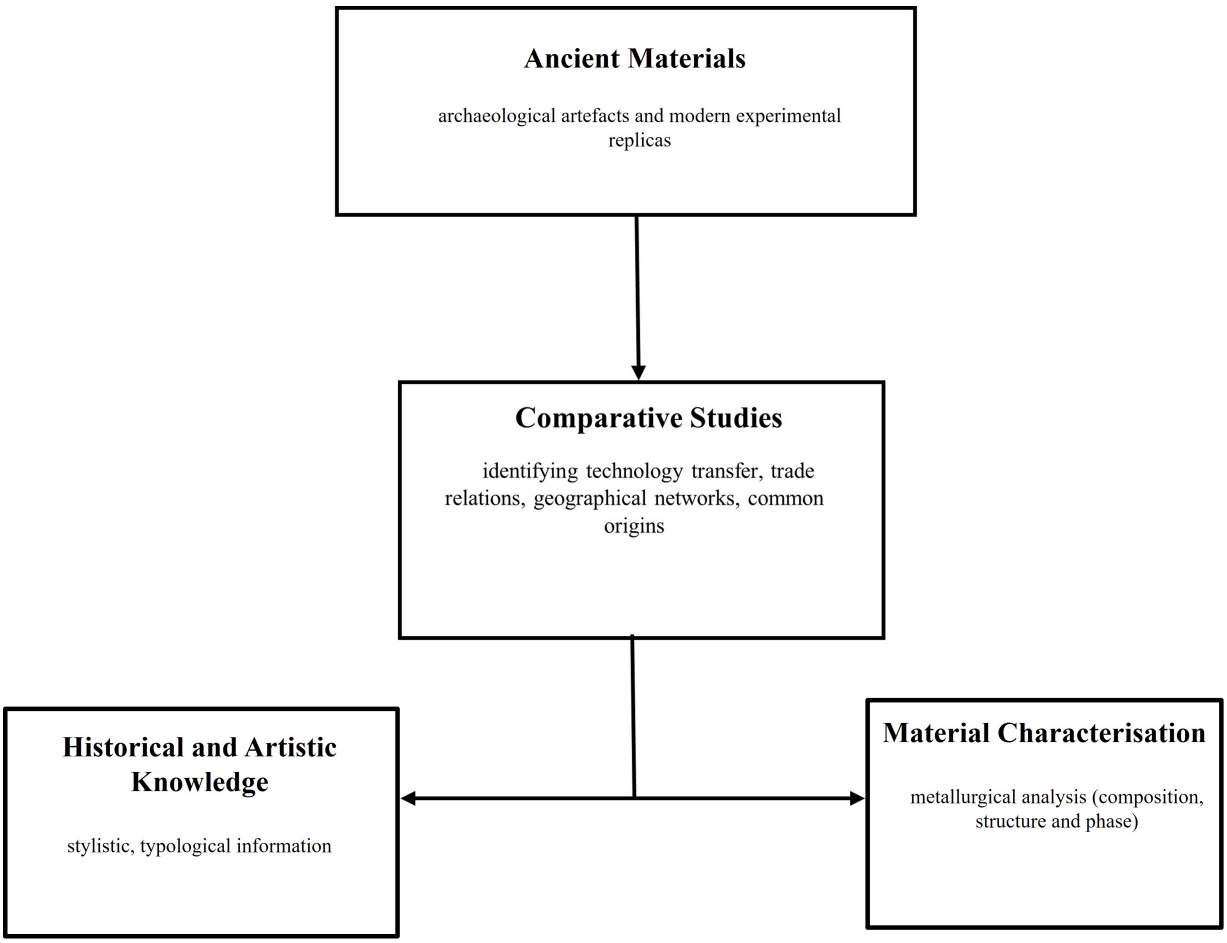

Figure 1: Schematic process of investigation, inspired from the work of Robbiola et al. (2006), to compare the ancient metallic materials [1]

In practical cases, the material samples and in turn the analysis is taken such that it pro-

duces the minimum invasiveness and using techniques that provide the most meaningful data. Siano et al. (2009) employed three step study for the archaeological specimen authentication. 1) Archaeological context and archival information 2) Observation and interpretation of crafting procedures through naked eye analysis 3) Material analysis of the bulk and alteration layers [39]. In the scope of this thesis work, the process to devise the interdisciplinary conclusions is explained in the following 3 bullet points.

1. Literature Review
   Historical Contextualization

2. Stylistic Interpretation

3. Chemical analyses

Within this framework the main focus will be/should be given to the material analysis. The material science results can then be contextualized by using the knowledge of history, typology, archaeological and stylistic data from the artefacts. The benefits of this multidisciplinary approach and its practicality is further illustrated in the section of relevant studies.

3.4 Characteristic Features Identification and Comparison

This section gives an overview of the material analysis techniques that will be used on the selected pool of artefacts. The composition of the materials, structure, manufacturing techniques are all capable of providing criterion for the comparison of the artefacts. In order to identify these characteristic features, (a) material analysis techniques will be used and (b) the interpretation of the results will be done through comparison.

Analytical Techniques

The analytical techniques are based on the following chronological order. In addition organic artefacts will be analysed using Raman and FTIR spectroscopy techniques:

Metallic Artefacts

1. Stylistic analysis. This process will rely on the photographic and visual analysis and the literature available online.

2. Surface investigation using SEM, this will be done on the metallic samples before deciding to use the TEM, if the size of the samples is appropriate.

3. Bulk material analysis via TEM after FIB preparation to identify the intrinsic material composition by comparing the results from the SEM analyses of representative objects.

Organic Artefacts

1. Organic artefacts analysis using the Raman and FTIR spectroscopy and comparing the spectra for understanding the chemical fingerprints which can be used to classify the amber, evaluate the relative age and paleoclimatic effects on the amber.

Comparative Analysis

After the characteristic features have been identified, the artefacts will be compared based on the identified features with each other and literature examples if available. Examples will be incorporated based on the bulk material compositions, age, origin and stylistic attributes [43]. The criterion is listed as follows:

1. Surface Analysis: (a) style (b) decoration (c) size (d) workmanship

2. Material science: (a) internal material composition (b) major components (c) minor components (d) trace elements (e) surface analysis

3.4.1 Importance of the Chemical Analyses

The chemical analysis of the archaeological materials is performed within the scope of archaeometry. The researchers have used the analytical data to identify the origins of archaeological metals using the analysis of trace elements. For example, along with the main elements of brass (Cu and Zn) or bronze (Cu and Sn), the compositions of the trace elements (such as iron, cobalt, nickel, arsenic, zinc, lead, antimony, selenium, tellurium, gold and bismuth) provide unique profile to analyse the archaeological artefacts. The research can provide information about the metal sources (mining), trade (local or international) and technologies (fabrication). The information can in turn be contextualised for archaeological research conclusions such as social structures, ancient population immigration patterns and specific decoration trends [44].

For the authentication of the metal artefacts, the chemical analysis of the alloy composition and the corrosion serves as important tool. As the corrosion is the product of the natural chemical alterations of the underlying metal, it can be analysed to indicate the original base alloy composition [26]. The information about the elemental composition is of great value because this can serve to understand relative dating as well since the metallurgical additives were often period specific. Fortes et al. (2005), utilised the chemical composition of Bronze and Iron age metallic artefacts to conduct chrono-cultural sorting of objects [5]. The chemical and physical process can also aid in finding the region of the artefact since the compositions are directly linked with the raw material used in the production which can, in turn, be linked with the mining and the trade route identification. Moreover, the elemental composition of raw material and the manufactured object along with the thermal conditions (via microstructural and phase diagram analyses) can shed light on the ancient production mechanism. This information can be used to identify the possible origins of raw materials, provide insights on manufacturing methods and

also identify local or international trade routes. The spectra analysed from the organic artefacts can be used to classify different artefacts and understand the degradation behaviours attributed to climatic conditions.

3.5 Methods, Instrumentation and Test Parameters

This section provides an overview of the methods and techniques that are utilised for the preparation and analyses of the artefacts. The more detailed explanations are as follows:

3.5.1 Sample preparation for TEM: Focused Ion Beam (FIB)

FIB was used as a technique to prepare electron transparent specimens which is a prerequisite for TEM measurements. It is a combination of a microscope with a large depth of focus and a cutting tool for the site specific and precise preparation of cross-sections. FIB offers excellent new opportunities for the investigation of the structure and geometry of archaeological samples in the micrometre range. FIB works with dual beam in which imaging using electron beam is essentially same as SEM, whereas ion beam (Ga ions) is used to cut the specimen by sputtering (milling). It is not only used to remove the material, it can also be used to deposit material using the gas assisted deposition (GAD) system with a precursor gas.

Focused ion beam was utilised in the scope of this thesis to prepare the specimen which were later analysed under TEM. FIB used a beam of gallium ions to extract a $10 \times 10\ \mu m^2$ lamellae. The technique helped preparing TEM ready specimen in a quasi non-destructive manner. The extracted lamellae were smaller than the visibility range of typical human eye [45].

The equipment used to prepare the samples was an FEI Dualbeam Helios Nanolab. The samples were prepared following the steps as mentioned below and are shown in the Figure 2.

(a) Deposition of small amount of Platinum (Pt) in the area of interest to protect the top portion of the sample.
(b) Milling the trenches in the sample area on both sides of the top protective layer.
(c) The polishing of the trench by cleaning cross section.
(d) Undercutting of the trench.
(e, f) Cut-off and lift-out of the prepared lamella with the help of Omniprobe. Omniprobe is used for microscale handling of the lamella in the FIB.
(g) Final thinning of the lamellae after welding it to the Molybdenum (Mo) TEM grid.

Same steps were followed for all the specimens to produce electron transparent thin slices.

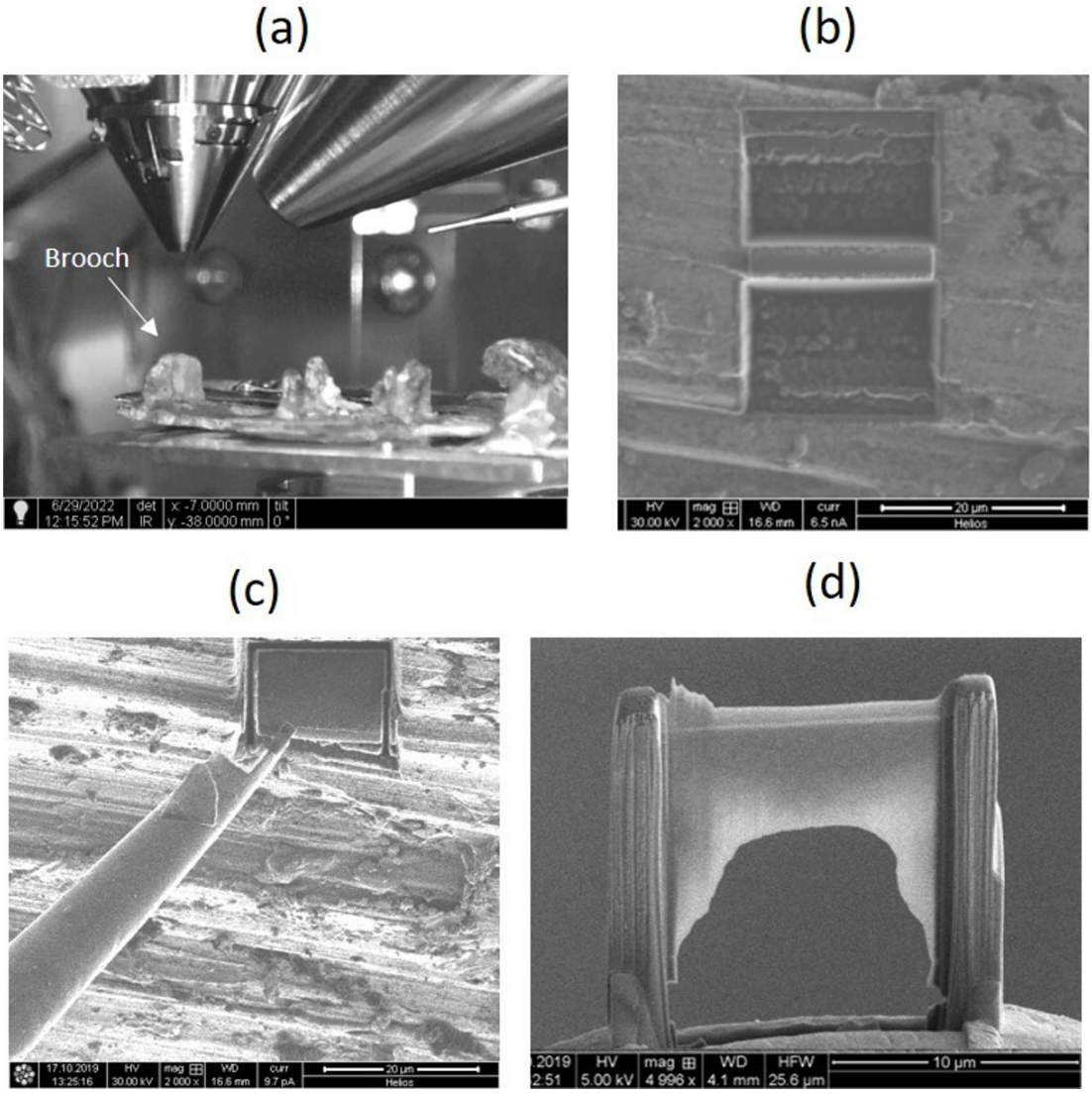

Figure 2: Demonstration of the FIB cutting (a) a flat ladder brooch inside the chamber (b) cutting the trenches (c) lifting with omniprobe and (d) placing and fine thinning on the Molybdenum TEM grid (By K. Saleem)

3.5.2 Surface Analyses: Scanning Electron Microscopy (SEM)

The SEM equipment used for the surface analysis was Ultra 55 Plus, with Software SmartSEM 5.04 from ZEISS. The instrument uses beam of electrons operating in the accelerating voltage ranging between 5-20 kV. The SEM is equipped with multiple detectors and depending on the detected signal (secondary electron, backscattered electrons and x-rays) several types of analyses are possible. These signals originate from specific depths of the sample when the primary beam interacts. The images via secondary electron only provide information about the surface morphology in the form of electron images. The energy dispersive x-ray (EDX or EDS) detector detects the x-ray signals and generate elemental analyses in the form of point measurements or maps. The electron beam penetration is dependent on the atomic number of the specimen under analysis. For metallic samples, it is limited up to approximately 3 µm from the surface, so the analysis is limited to the surface or sub-surface of the specimen.

SEM is a non destructive analysis technique however the SEM chamber only allows samples smaller than 5 cm in width, 5 cm in length and 1.2 cm in height inside the analyses chamber. The FIB SEM on the other hand allows relatively larger samples inside the analysis chamber, the width should be smaller than 8 inch, the length should also be less than 8 inch. During the analysis, the objects were fixed onto the sample stage with the help of sticky copper tape and inserted inside the analyses chamber with a transfer rod. After the appropriate vacuum conditions, the object was positioned under the electron beam. The detector was set at secondary electron (SE) mode from the detectors tab and electron images from the surface were recorded. Then in the second monitor, EDX Aztec ® software was used to conduct EDX point measurements and elemental maps. The area for the elemental map was selected such that the physical features and surface information could be documented.

3.5.3 Transmission Electron Microscopy (TEM)

Invented by Ernst Ruska, TEM is a very powerful tool for micro and nanostructural characterisation of the prepared sample. Jeol JEM 2100 (LaB_6, 200 kV, Cs = 1.0, Oxford SDD EDX detector) was used to conduct the TEM analyses on the lamellae extracted form the objects. FEI Tecnai F30 G^2 STwin equipped with an EDX detector (Si/Li, EDAX) was also used for several samples. In the TEM measurements, high resolution electron images (HRTEM) and EDX spectra were recorded in the bright field (TEM BF) mode. Then high-angle annular dark-field (HAADF) scanning TEM mode was used for EDX mapping and point measurements. Furthermore, selected area electron diffraction (SAED) was conducted to attain electron diffraction patterns from the lamellae. TEM employs a high voltage beam of electrons in order to create images that are magnified upto 2 million times. It has the capability of resolving the features to subatomic level and uses electromagnetic lenses which focus the beam on a very small area. This beam while transmitting through the specimen, interacts elastically and inelastically with the specimen, providing chemical and structural information at atomic resolution. Since, the

electron beam penetrates through the specimen, it requires an extremely thin specimen (<100 nm).

3.5.4 Raman Spectroscopy

WITec Alpha300 RA Raman spectroscopy was utilised to attain the Raman spectra of the organic specimen (amber in our case). Raman uses inelastic scattering of monochromatic light as a result of interaction of the laser with the sample and records frequency changes in the vibrational, rotational and other low frequency modes after interaction with the specimen. The monochromatic light source is focused onto the sample and the scattered light is collected in a detector. The incident beam's wavelength is fixed and chosen such that the sample does not absorb the beam. Otherwise, there occurs a fluorescence effect which increases the background noise and makes the measurement very challenging. It is equipped with two laser sources which operate at different excitation wavelengths 532 nm and 633 nm. Depending on the type of material, one of these sources can be selected. It is possible to measure metal oxides, organic samples or biological samples.

Limitations of Raman spectroscopy

The Raman effect is very weak, which leads to low sensitivity, so the substances with low concentrations cannot be measured with Raman. The specimen should not absorb the beam otherwise the noise to signal ratio will increase, making it difficult to measure useful data. This effect is called fluorescence. Higher wavelength light source can be utilised to minimize this effect. FT-Raman spectroscopy uses near infrared region light source and can successfully help analyse amber.

3.5.5 Infrared Spectroscopy

Bruker Vertex 70v ATR-FTIR was used to carry out the infrared spectroscopy on the amber specimen. Infrared Spectroscopy (IR) studies the interaction between the infrared radiation and the matter. The infrared radiation is an electromagnetic radiation (light) with the longer wavelength than visible light. The infrared light passes through the sample material and depending on the energy of the material, it triggers vibration of specific molecular bonds (absorption). The molecular vibration is infrared active if the dipole moment of the molecule modifies during the vibration. Hence, when illuminated with various frequencies, the molecule will selectively absorb the radiation matching its natural vibrational frequency. In doing so, the molecule transitions from one vibrational energy state to another and hence vibrates with increased amplitude. The most common vibrations are symmetric stretching vibrations, anti-symmetric stretching vibrations and deformation vibrations. These vibration types are dependent on the changes in the characteristic bond length between the atoms in the molecule and bond angle. The energy absorbed is consumed and thus missing from the original IR beam. The part of the light

that is transmitted carries the molecular information about the sample and it is collected by the detector to produce an electronic signal.

While measuring the IR spectra the environmental influences should be mitigated that might show in the spectra. Therefore, the initial spectrum is measured without the sample. This returns an IR plot of light intensity vs wavenumber (cm^{-1}), yielding a reference spectrum by fourier transformation. Now, the actual sample is placed in the beam path and the process is repeated, fourier transformation yields another single channel spectrum, this time from the specimen. Then the sample spectrum is divided by the reference spectrum and we have the classic view of FTIR transmission spectrum. This FTIR spectrum serves as a chemical fingerprint and enables the chemical identification of a variety of samples and is frequently used to characterise the material properties and verify known and elucidate unknown samples.

The representative amber were placed on the crystal on one-millimetre thick diamond window and flattened using a metal roller. Polariser filters were used to enhance the sample contrast and assist in targeted analysis. The measurements were conducted on a Vertex 70v ATR-FTIR spectrometer. The spectra were collected at a sum of 32 scans and 4 cm^{-1} resolution.

3.5.6 Andonstar ADSM302 digital microscope

Andonstar ADSM302 uses a digital camera to output the image into an LCD screen or monitor connected through HDMI. It uses LED light to illuminate the region of interest and magnifies small objects viewed on the monitor screen. This was used as a prerequisite to identify the metal-looking regions on the flint samples before loading the sample in the SEM for detailed elemental analysis on the regions identified through digital microscope. The advantages of using digital microscope was non-destructive nature of the instrument with no sample preparation required. Additionally, larger artefacts can be analysed as well. However, this technique can not do quantitative elemental analysis, therefore it was necessary that this step is followed up by the scanning electron microscopy with the energy dispersive x-ray spectroscopy.

The flint samples, were rigidly mounted onto the specimen holder in SEM using a conductive carbon tape. The samples were then tied onto the stage using the conductive copper tape as well which provided further integrity to the sample and helped drain the charge accumulation on the surface of the flint.

4 Pilot Study 1 Discovering Baltic Networks: Combination of stylistic and material science approach

Overview

The Ostriv-1 cemetery is an early medieval cemetery located near the village of Ostriv, approximately 80 km south of Kiev in present-day Ukraine. The objects found in the cemetery were markedly different from those of the contemporary Kievan Rus cultures. However, they had substantial stylistic similarities to those from the East Baltic region, specifically the Prussians, Curonians, and Scalvians.

It was hypothesized that the Ostriv population were immigrants who served as mercenaries during the reign of Jaroslow the wise in the 11^{th} century AD. Under the framework of "Baltic Migrants in Kyivan Rus", further research projects were planned to explore the mobility patterns of this Baltic population. The research began with the analysis of typological features of Ostriv and East Baltic artefacts, burial rites and 10^{th}–12^{th} century written sources. Later material analysis and stylistic interpretation of the atefacts, ancient DNA, radio carbon dating and dietary stable isotope analyses were also proposed to conduct a comprehensive laboratory analysis. These techniques were utilized to compare the grave goods and find the possible cultural and geographical origin of the population buried in Ostriv.

The material analyses of the artefacts was conducted in the TEM center in technical faculty, Kiel. TEM and SEM microchemical analysis were conducted on the received artefacts from Museum for Pre and Early history Berlin and Ukraine. The artefacts analysis and conclusions comparing the material aspects of the artefacts are included in this pilot study. It is important to note that the TEM has not been previously applied to the investigation of East Baltic and Ostriv artefacts.

4.1 Sample Group and Historical Context

Fourteen samples are analysed in this section from E1-E9 and O1-O5, as shown in the Table 1. The Table also shows the location and the type of the artefacts.

Before the stylistic and technical interpretation of the artefacts, it is important to consider the historic overview of the society where they were found and contextualise the items. This section aims at providing a brief overview of the nature, cultural context and history of the fibulas before proceeding towards the technological analysis. The medieval Ostriv cemetery was located at around 80 km of Kiev, at the south of River Rus between Ostriv and Puhashivka in the district of Rokytne. The researchers found 67 graves in an area spreading over 1400 square meter in this cemetery. The artefacts found in these graves had stark artistic resemblances to the chronologically identical artefacts of the East Baltic regions in present day Estonia, Latvia and Lithiuania. These East Baltic

Table 1: Archaeological samples serial numbers, geographical locations and shape details.

Lab ID	Region	Grave	Artefact
E1	Grebieten	-	Ring brooch
E2	Löberstoff	-	Ring brooch
E3	Popelken	-	Ring brooch
E4	Ekritten	-	Horse-shoe brooch with star-shaped terminal
E5	Trentitten	-	Horse-shoe brooch with star-shaped terminal
E6	Ramutten-Jahn	-	Flat ladder brooch
E7	Ramutten-Jahn	-	Flat ladder brooch
E8	Viehof	-	Flat ladder brooch
E9	Ramutten-Jahn	-	fragment of neck ring
O1	Ostriv	N02	flat ladder brooch
O2	Ostriv	N35	Pennanular brooch with widened terminals
O3	Ostriv	N41	Penannular brooch with star shaped terminal
O4	Ostriv	N51	Penannular ring-form brooch
O5	Ostriv	-	Halsring (totenkrone)

territories included tribes such as old Prussions, Curonians and Scalvians. The map of the East Baltic territories is shown in the Figure 3. Whereas the location of Ostriv cemetery is shown in the Figure 4. The researchers found that the head orientation of the buried population was towards North, which was uncommon in the Kievan Rus but a characteristic of 10^{th}-11^{th} century Baltic tribes. The territory of Kievan Rus was a point of interaction for centuries between the influential Byzantine empire and the Eastern Baltic regions. Local nomadic tribes and the young Kieven state were often engaged in confrontations which prompted the Kievan princes to fortify and build a defence line at the River Ros at the end of the 10^{th} century. By the second half of the 11^{th} century, the Southern border of the Kievan Rus was protected by several hillforts and sets of ramparts situated along the river. The settlement of Ros area was achieved through the relocation of the population from the interior of the Kievan state. The population settled at Kievan front was multicultural, and focused towards the need of the defence line to function. The settled population eventually comprised of nomads (Perchenegs, Torks and Kipchacks) and later joined by mercenaries (Masovians/Poles). The skeletal remains of the buried population at Ostriv cemetery were studied at the National Academy of Sciences of Ukraine (NASU). Most graves were buried with one individual, but there were also evidence of several individuals laid parallel to each other. Twenty four individuals were identified as adult males, eighteen were adult females and seventeen consisted of subadults which were under 14 years old. The largest pool of young adults died between 20-30 years of age. It was found that the average age of the male buried in the cemetery was 32 years and that of female was 34 years. The dental health indicators point towards mixed diet rich in protein and carbohydrates. Additionally, the DNA analysis of the buried population at Ostriv shows a close correlation to the individuals from East Baltic

population. The artefacts found at the Ostriv cemetery provide the first opportunity to identify the material attributes of the migrants settled in the Ros area. The following section provides more detailed characterisation of the received ornaments and devise the aims and objectives under the framework of this thesis work.

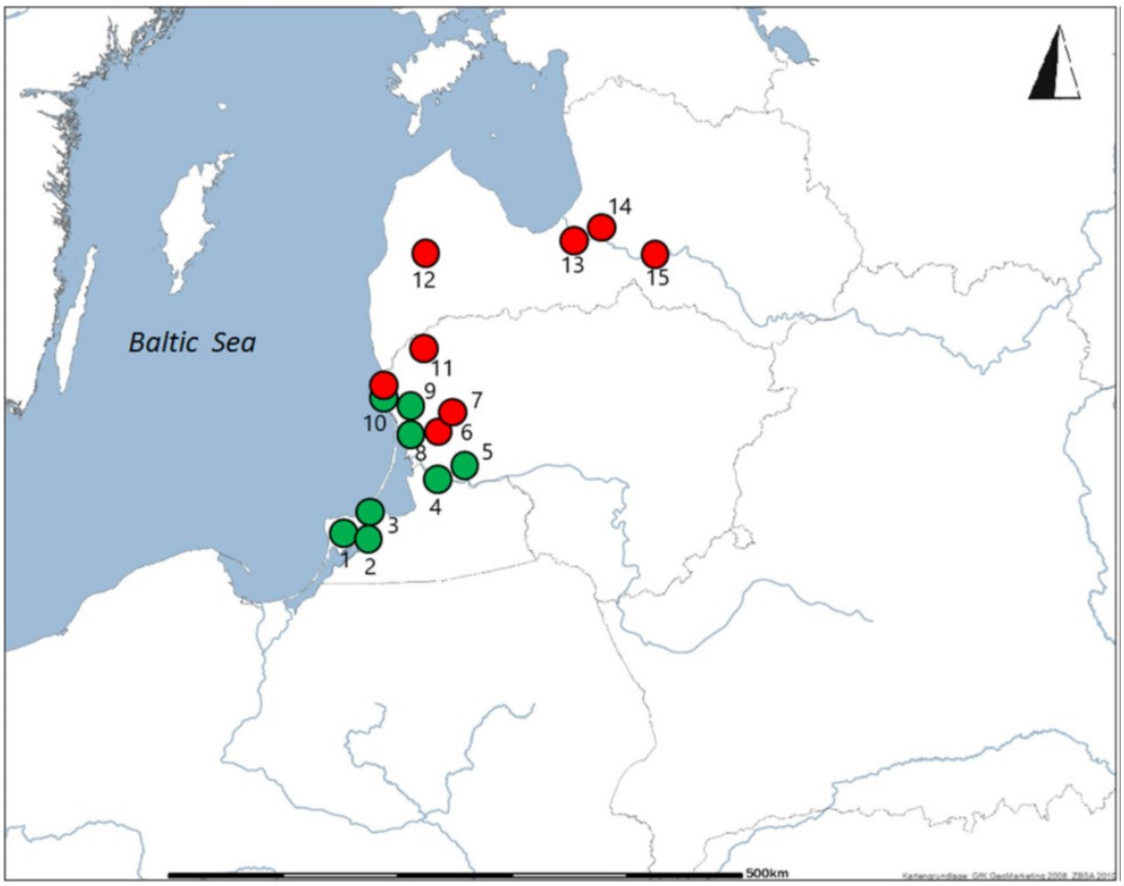

Figure 3: Green – the Prussian, Curonian and Scalvian cemeteries Red – Samogitian, Semigallian and Livs cemeteries [2].

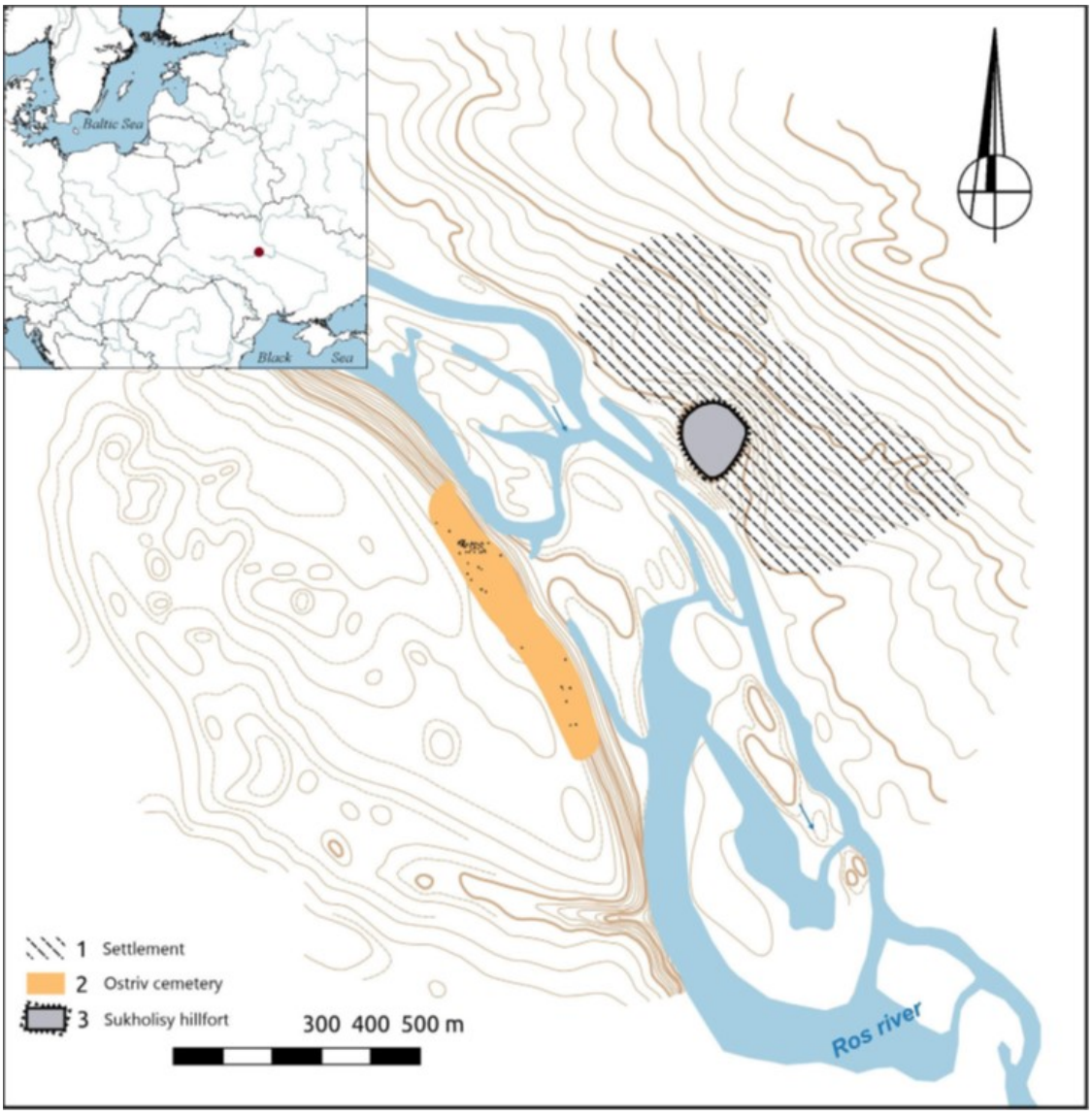

Figure 4: Location of the Ostriv cemetery in relation to the hillfort and settlement of Sukholisy [2].

4.2 Aims and Objectives

Research aims and objectives

In light of the experimental methodology (as outlined in the Section 3.3), the goal is to better understand these individual objects in light of their various components, state, material composition and function. To foster this understanding, we are employing the modern nano analytical techniques from materials science and try to answer specific set of critical questions, as follows:

1. Can we successfully differentiate between the intrinsic bulk material from the surface contaminants on the artefacts?

2. Can we utilise the cutting edge nano-analytical tools on archaeological artefacts and keep the analyses non-invasive?

3. Can we identify any characteristics or phenomenon in the physical structure and material composition of the sample group, which can help to compare and find common or separate origins of the artefacts?

4. Can we prove through stylistic and material science analysis comparison that the population buried at River Ros are Baltic migrants?

5. In the occurrence of these physical phenomenon, can we classify the artefacts based on the production methods?

Challenges of the study

It should be noted that the material analysis was consistently encountered with challenges and hence the limitations for handling the archaeological materials were formulated. One of the limitations was the necessity of keeping the process non-destructive and making sure the health of the artefact is intact even after the analysis. This very important prerequisite that meant that the samples can not be cut into smaller sizes where a cross sectional analysis could have been possible. The surface and bulk chemical properties of the artefacts are conventionally altered because of the environmental factors and burial conditions of the artefact. As a result, the analysis of the cross section to attain information from the intrinsic structure of the artefacts was crucial but not possible. Therefore, the prohibition from doing any sort of destruction of the artefact was a limitation and more sophisticated preparation was required. Another limitation was the total number of available artefacts, which is usually the case with the archaeological finds. The analyses and conclusions related to the analyses had to be drawn from the set of limited items that were provided from the museum. This decreases the number of data points which at times hinder reaching the concrete conclusions. The dimensions of the ornaments was also a limitation, since the processes had to be kept non-destructive, the whole artefact had to be loaded inside the analysis chamber. This meant that newly designed stage assemblies had to be produced and were tailor made for the course of the research.

4.3 Fibulas and Stylistic Interpretation

When the study was initially proposed, the intended focus fell exclusively on the analysis of the metallic fibulas using variety of non-destructive analysis techniques. The intended analysis methodology involved analysing using multiple complementary techniques which can contribute towards authentication of the results. A template of the samples width, height and depth was devised which could be successfully loaded in the chambers of the SEM microscopes. Several proposed techniques became non-viable because of the initial results. One such technique was x-ray diffraction (XRD) whose analyses were limited to the surface/corroded regions of the artefacts. An XRD profile measured on the neckring excavated from Ostriv, the profile is shown in Figure 54 in the Index Section 12. XRD provided the information about the crystal structure of the material by comparing the reflection positions at different angles with the reference database. The measured d-spacings associated with the planes were in exact agreement to the copper oxide (CuO). Hence, limiting the measurement only to the patinated region of the specimen. Although, the chemical composition of the corroded alloys can help estimate the base alloy as well but a direct measurement of the intrinsic elements was desirable. Hence, the focus shifted towards other non-invasive techniques such as scanning electron microscopy (SEM) and transmission electron microscope (TEM). As the pool of the viable techniques narrowed down, the limitations of the type of artefacts related to sizes, material and shape could also be clearly devised.

The suitable artefacts from the Prussia Collection received from the Museum for Pre- and Early History (Berlin) and the Ostriv Collection were included in the research. The collections have been dated to the medieval times of 11^{th} and 12^{th} century East Baltic regions and the medieval village of Ostriv (more description in Section 4.1). The collection from Ostriv consisted of artefacts with distinct stylistic features and sizes. For example, flat ladder brooches, penannular brooches with connected star-shaped terminals, rounded brooches with ribbed and spiral neckring. The artefacts from the Prussia Collection were selected such that they consist of resembling morphologies. As a result, the items from Prussia Collection also included flat ladder brooches, ring brooches, penannular brooches and spiral neck ring. The items from the Prussia Collection were in the range of 3-5 cm in size and around 1.5 cm in height in well preserved conditions beside the surface corrosion layer and minor casting defects. The artefacts from Ostriv were received in small fragments chipped from the excavated artefacts, which simplified the sample handling process to some extent.

The followed up sub-section introduces the objects under study in detail. The visual description is based on the attributes and physical features evident on the as casted items. For the ease of interpretation and comparison, the similarities in stylistic attributes have been considered and descriptions are arranged in sets of artefacts from both Ostriv and East Baltic regions.

4.3.1 Flat Ladder Brooches

Four flat ladder brooches constituting the largest set of samples that were received from the Prussia Collection are shown in Figure (5 to 7). These brooches are A1 spirgis subtype which are typical of the South Eastern Baltic cultures dating 10^{th}-11^{th} century AD. Despite being broken in several places; the brooches are well preserved. This group of artefacts are casted in geometrical patterns with rectangular holes through them. They were dimensionally the largest specimen with roughly 9 cm of width and 10 cm of length. The brooch can be hypothetically divided from the centre along the vertical length and symmetric features appear on either side of the line. A short 1.5 cm hump is also visible along the central line on the upper part of the brooch which is slightly higher compared to rest of the plane surface on the front side. The features on the backside of the brooch are partially broken, however, seems like a bow was present which is missing now. The surface of these flat ladder brooches is evenly covered with brittle looking, porous corrosion layer. The colour of the corrosion layer differs from light greenish to dark greenish black and sometimes slightly red in several areas on the item. This set of artefacts were not only the largest but also most intricate in shape. Therefore, they posed the highest challenge during their loading in the analyses chamber and care was needed to manoeuvre them inside the chamber. To compare the flat ladder brooches to East Baltic regions, one stylistically identical flat ladder brooch was included from the Ostriv artefacts' collection, shown in Figure 8.

Figure 5: Flat Ladder Brooch—E6 from Prussia Collection from the region Ramutten-Jahn with Front side A and Back side B (photographed and sketched by K. Saleem)

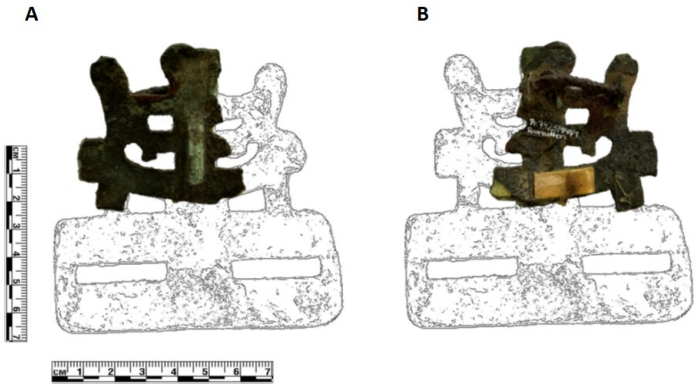

Figure 6: Flat Ladder Brooch-E7 from Prussia Collection from the region Ramutten-Jahn with Front side A and Back side B (photographed and sketched by K. Saleem)

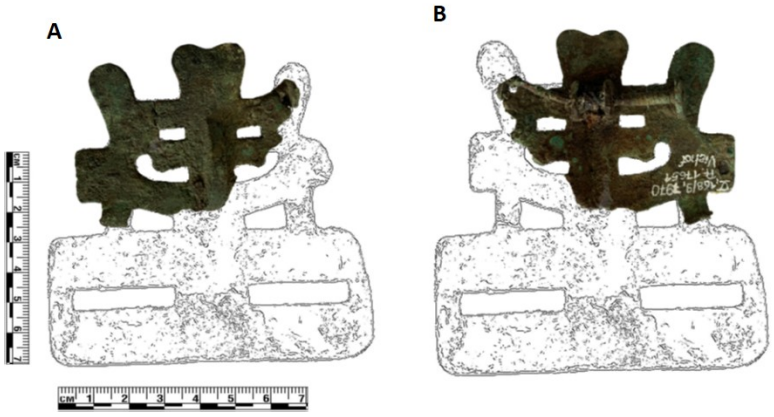

Figure 7: Flat Ladder Brooch-E8 from Prussia Collection from the region Viehof with Front side A and Back side B (photographed and sketched by K. Saleem)

Figure 8: Flat Ladder Brooch-O1 from the region Ostriv Ukraine found in grave 02 with only front side (photographed by I. Zocenko)

4.3.2 Penannular Brooches

Pennnular brooches are in ring form with a missing small part of the ring circumference. A pin runs through the circular ring and attaches to the back of the brooch. They constituted the second largest group of artefacts received from Prussia Collection and Ostriv. In the context of this research, the penannular brooches are further subdivided into two categorise i.e. Penannular horse shoe brooch with star shaped terminal and penannular brooch with widened terminals (only found in Ostriv). The description of the stylistic attributes of these brooches are as follows:

Penannular Horse Shoe Brooches with Star Shaped Terminal

Three penannular brooches of type horse shoe brooch with star shaped terminal especially typical of the Prussians were received consisting of two from Prussia Collection and one from Ostriv. These brooches are named as horse shoe brooch because of their shape resembling the horse shoe and its 4 sided terminals analogous to a star shape. The height and width of the artefacts is around 5 cm. On the front face of the artefact, decorative metal strides almost 2 cm distant from each other are visible which do not seem to have any functional value. On the back side, a horizontally extending pin is visible. This pin is fixed onto a metal hinge passing through the hole on one side of the pin whereas clamped under the pivot on the other side. The pin seems slightly bent towards the outer side, possibly as a result of pressure when wore on the cloak for a longer period of time. A homogenous covering of patina and corrosion layer is evident on the surface of these brooches as they stayed buried under the soil for above thousand years. Additionally, there are some modern time markings which were done by the museum staff to identify the brooches. Two brooches from the Prussia Collection of the East Baltic regions belong

to the regions of Trentitten and Ekritten and shown in the Figure 9 and 10 respectively. As mentioned earlier, one penannular brooch of star shaped terminal from Ostriv was also included in order to compare the stylistic resemblances. A smaller fragment was received from the brooch and its sketch is shown in the Figure 11. The brooch was found in the grave 51 in the Ostriv cemetery and correlates well with the stylistic description of the horse shoe from the Prussia Collection.

Figure 9: Horse shoe brooch with start shaped terminal – E5 from Prussia Collection from the region Trentitten with front side A and Back side B (photographed by K. Saleem)

Figure 10: Horse shoe brooch with star shaped terminal –E4 from Prussia Collection from the region Ekritten with front side A and Back side B (photographed by K. Saleem)

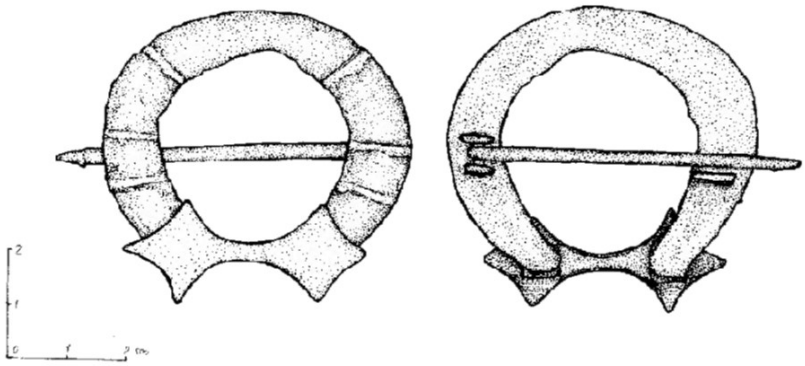

Figure 11: Horse showe brooch with star shaped terminal - O3 from the grave N51 from Ostriv (sketched by A. Suprun)

Penannular Brooch with Widened Terminals

This brooch is slightly elliptical in shape, has wide terminals and the only one received from this category. It consists of an adjustable pin fixed by bending around the brooch on one side and kept freely moveable on the other side. The size of the brooch is roughly around 5 cm in width and 1.3 cm in height. A small fragment from this brooch was received for the analysis. This brooch, shown in Figure 12, is stylistically not comparable with any other brooch from the batch. From the picture a yellowish coloured patina is evident and in some regions brownish corrosion layers can also be seen. On close observation decorative criss-cross features possibly made through a sharp object are also visible.

4.3.3 Ring Brooches

Three ring brooches were received from the Prussia Collection (Grebieten, Löberstoff and Popelken) and a fragment of one ring brooch was received from the Ostriv cemetery. The brooches from both the regions are shown in Figure (13 to 16). They are roughly 5 cm in length, 5 cm in width and around 1.2 cm in height. Stylistically, the front face of these artefacts consisted of strides around 1 cm distant from each other, casted as decorative design. Additionally, the back side of these brooches consisted of a pin, fixed on one side in the hinge and clamped under the pivot on the other side, from where it could be removed and adjusted. However, the pin is apparently missing from two of the excavated brooches from Prussia Collection. The decorative metal strides and the metal pin with its clamping function have stylistic resemblance with the earlier presented horse shoe brooches. Further more, a homogeneous corrosion layer is evident on the surface of the brooches which is distributed evenly throughout each of the artefacts. The colour of the surface patina on the brooches from East Baltic regions range from blackish green (E1)

Figure 12: Penannular brooch with widened terminals-O2 from Ostriv from grave N35 with only front side (photographed by I. Zocenko)

to greenish brown (E2). However, a different coloured patina i.e. yellow with goldenish cloud like morphology is present on the Ostriv ring brooch.

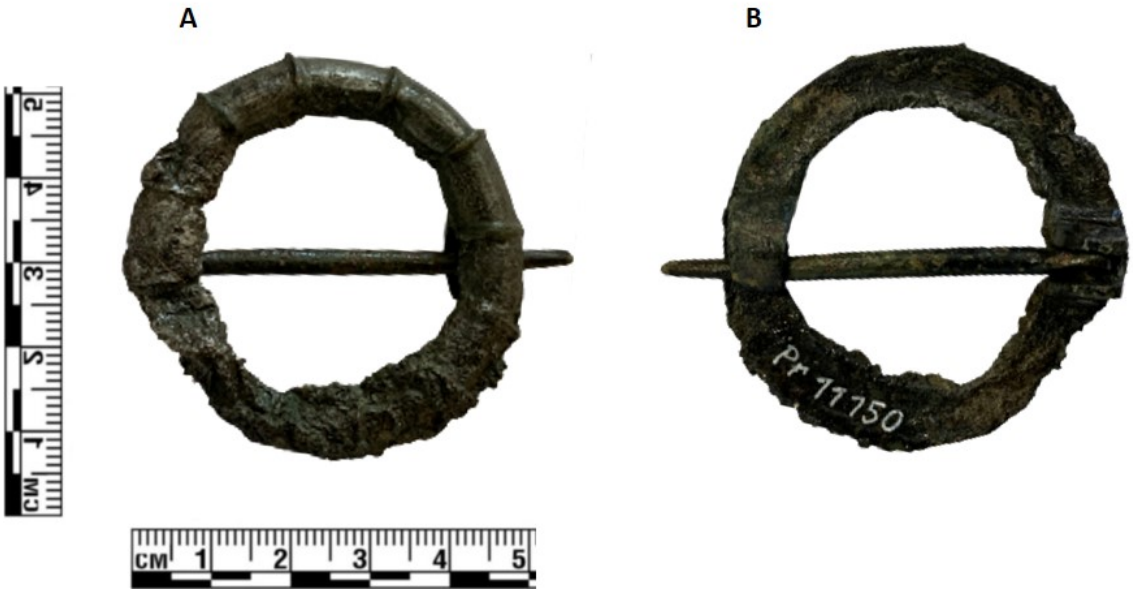

Figure 13: Round brooch—E1 from Prussia Collection from the region Grebieten with front side A and back side B (Photographed by K. Saleem)

Figure 14: Round brooch—E2 from Prussia Collection from the region Löberstorf with front side A and back side B (Photographed by K. Saleem)

Figure 15: Round brooch—E3 from Prussia Collection from the region Popelken with front side A and back side B (Photographed by K. Saleem)

Figure 16: Round brooch from Ostriv -O4 from grave N51 with only front side (photographed by I. Zocenko)

4.3.4 Spiral Neck Ring

Lastly, the spiral neck rings which were around 39 cm long were included in the study as well. These neck rings are typical of western Balts culture (Courinia, Semigallia and

Latgallia) and were a widely used form of ornaments in the Eastern Baltic regions. These are the twisted neck ring consisting of three twisted strings with a loop and a hook at the terminals for closing. Initially, three neck rings were received, two from the Prussia Collection and one from the Ostriv region. One of the neck rings was excluded from the research because of the large size i.e. 39 cm. Small fragments from the other two neck rings were received and made part of the analysis, one neck ring's fragment from Ramutten-Jahn region and one neck ring's fragment from Ostriv. The fragment from the Prussia Collection was roughly around 14 cm long and is presented in Figure 17. However, the fragment received from the Ostriv neck ring was very small so a photo is not shown here. Stylistically the neck rings from Ostriv and Prussian Collection seemed identical having close resemblance in physical features.

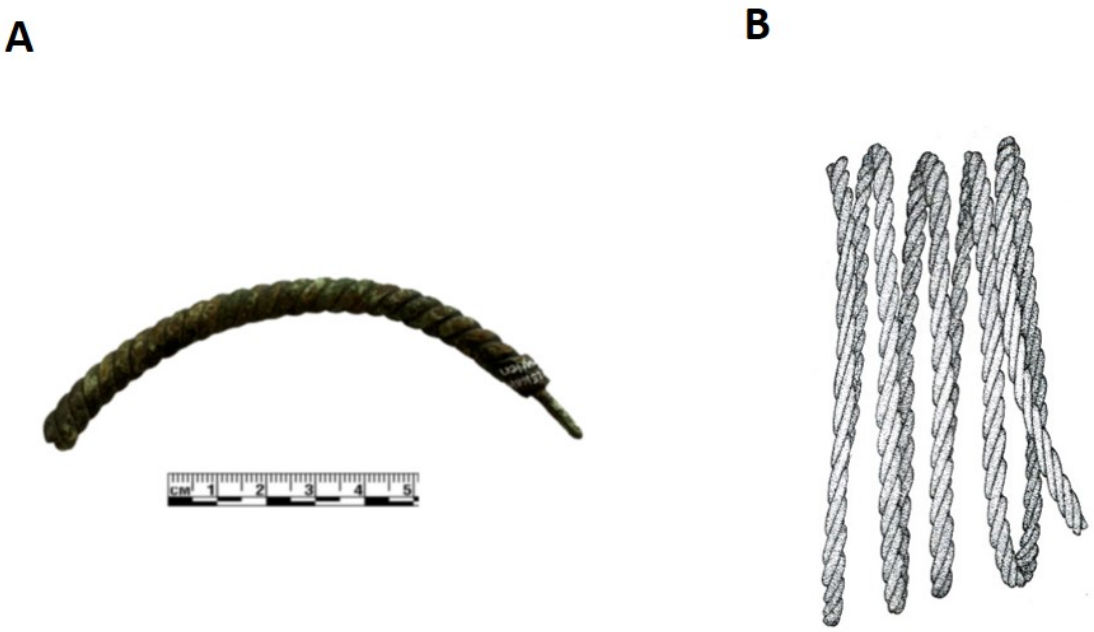

Figure 17: A Spiral neck ring fragment from Ramutten-jahn region-E9 from the Prussia Collections with only front side (Photographed by K. Saleem) and B is sketch of the spiral neck ring from Ostriv-O5 from grave N53 (sketched by A. Sorokun)

4.4 Chemical Analysis

The chemical analysis of the brooches from collection and Ostriv artefacts is presented in this section considering the above mentioned stylistic similarities in the physical features. Similar to previous section, the chemical and structural information of artefacts is conducted and documented in groups consisting of synchronous attributes in order to make comparison viable. The structural and chemical characterization was documented using

TEM performed on a thin lamellae prepared using FIB milling. As mentioned earlier, the surfaces of all the artefacts were homogeneously covered with corrosion products, hence, a micro drill was conducted to indent with a 0.3 mm diameter bit. This step removed the brittle patina from the region of interest and enabled extracting a slice (so-called nano-excavation) from the intrinsic structure of the artefact which reflected the original base alloys and trace elements.

Before exploring the analytical results in detail, it is important to know the preservation steps utilised on the excavated artefacts. The artefacts were mechanically cleaned by brush and processed with the tannin (chemical compound) to remove dirt, grime and visible surface contaminants, after that the artefacts were immersed in a solution containing benzotriazole to form a thin corrosion inhibiting layer which protects the heritage materials' surface by reacting with and neutralising new corrosive agents in the environment. Then, a paraloid B72 was applied on the items to form an adhesive coating to consolidate the surface flakes and prevent further surface deterioration. Paraloid B72 is a clear, colorless and odourless thermoplastic acrylic resin which was dissolved in ethanol and used to protect the surface of artefacts. The results of the TEM analysis are presented in the form of high resolution images, EDS point measurements, elemental mapping and SAED electron diffraction patterns. The EDS point measurements are presented in a table format in atomic percentages (at. %) and are averaged over 10 measurements to provide a statistic confirmation of the actual composition and trace elements. The high resolution electron images are presented for few artefacts in the Index Section 12.

The term trace elements is adopted in this thesis work from geochemistry reference with less than 0.1 % of the total composition of the alloy. In TEM, less than 1 at. % is an acceptable criteria to categorise an element as trace element. To avoid misinterpretations of results, the lower detection limit of the instrument is agreed at 0.2 at. % while further lower signals have higher chance of error. Furthermore, the carbon and the oxygen content is not included in the measurements because the signal of these elements could be from contamination after the excavation or during the measurements in the microscope. So, for the purpose of comparison these elements are left out. The variance of the atomic percentages was calculated according to the following equation.

$$S^2 = \frac{\sum_{i=1}^{n}(X_i - \overline{X})^2}{n-1}$$

The elemental compositions of the artefacts from the FIB lamella are given in atomic percentages in the Table (2, 3, 4 and 5). Copper (Cu) is present in all the artefacts which is the major component for all the base alloys used. Several artefacts also contain zinc (Zn), however, the content of Zn varies strongly between 8-20 (at.%) and few samples contain no Zn at all. Figure 18 shows the SAED pattern from the flat ladder brooch from Ostriv grave 2 sample O1 shown in (a) as a polycrystalline ring pattern and (b) the ring brooch from Popelken sample E3 shown as reflections. The flat ladder brooch corresponds to 2.1Å (111), 1.8Å (002), 1.2Å (022) and 1.1 Å (113) which fits well with

the crystal structure of face-centered cubic (FCC) Cu 80 at.% and Zn 20 at.% . The reflections from E3 sample correspond to 2.08 Å (111), 1.2 Å (022) and 1.09 Å (113) fitting well with the crystal structure of pure FCC copper. The reference dataset used is from Inorganic Chemistry Database (ICSD) [46]. Moreover, a comparison between the TEM EDX spectra from flat ladder brooches from Ramutten-Jahn (E6 and E7) of East Baltic region is shown in the Figure 19 (a and b), one is pure copper and the other is brass. A more detailed comparative analyses based on chemical examination of the typologically identical artefacts is included in the following sections.

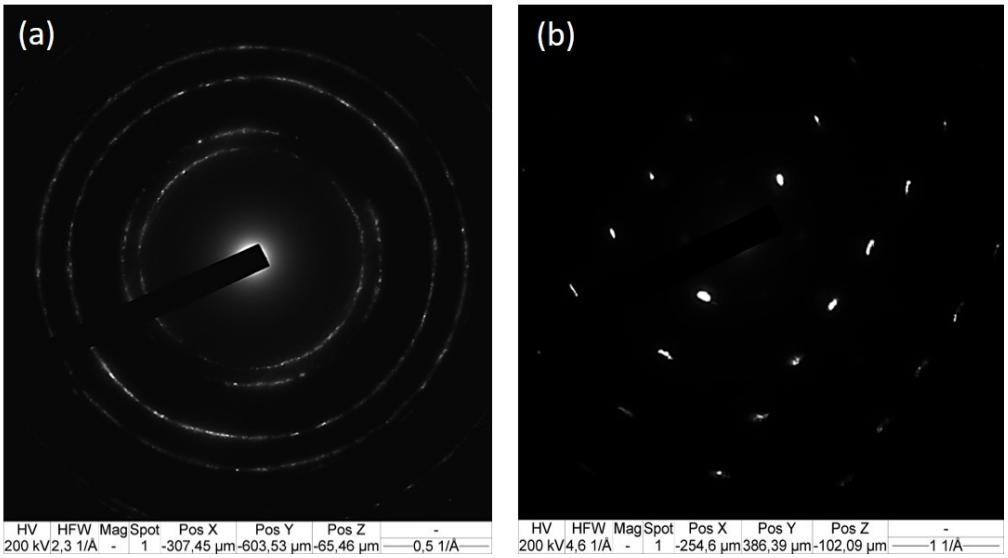

Figure 18: Shows the electron diffractions patterns with (a) ring pattern from specimen O2 corresponding to d-spacing of brass and (b) reflections from specimen E4 showing matches with pure copper (By K. Saleem)

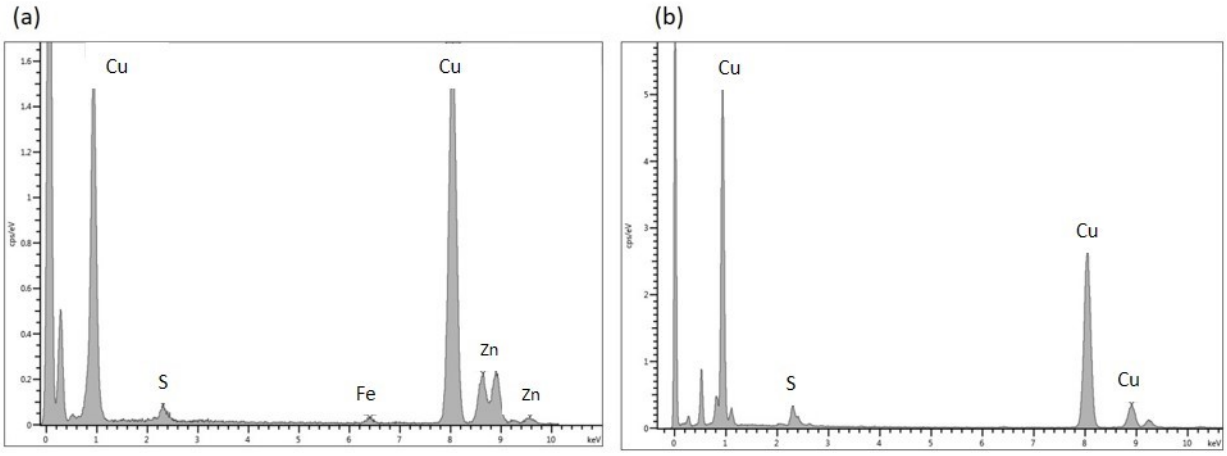

Figure 19: TEM EDS Spectra from flat ladder brooches from East Baltic regions (a) E6 showing brass and (b) E7 showing pure copper (By K. Saleem)

Flat Ladder Brooches

Five flat ladder brooches of A1 spirgis type were chemically analysed using TEM. Four belonged to the East Baltic regions (two from Ramutten-Jahn and one from Viehof) and one flat ladder brooch was analysed from Ostriv cemetery. The Table 2 presents the EDX point measurements (in at.%) recorded on the FIB lamellae extracted from the artefacts. The measurements confirm the presence of copper and zinc which are identified as base alloys with varying compositions in the flat ladder brooches. The two brooches of identical stylistic attributes from Ramutten-Jahn have discrepancy in the casted base alloy, one being pure copper and the other is brass (Cu and Zn). Whereas the flat ladder brooch from Viehof consists of brass and has comparable base alloy compositions with the brass brooch from Ramutten Jahn. Now, comparing these brooches with the flat ladder brooch found as a stray find at the Ostriv cemetery, which demonstrates brass as base alloy as well, the amount of Zn content is roughly 70% more than the East Baltic fibulas from Ramutten-Jahn and Viehof. Besides the base alloys, the measurements also reported multiple trace elements in the artefacts namely S and Fe.

The elemental distribution analysis of all the artefacts was also conducted and elemental maps illustrating the distribution of copper, zinc and trace elements are presented in the Figure 20. Since, the elemental maps of artefacts from Remutten-Jahn, Viehof and Ostriv contains brass, only one representative elemental map is displayed in the shown Figure. The electron image from where the mapping was recorded shows the lamella consisting of brighter contrast spots, possibly from dirt dislodged onto the sample during the preparation process. The other elements Cu, Zn, S and Fe are nearly consistently distributed over the whole range of lamella which is eventually representative of entire artefact assuming a uniform composition of the artefact. This assumption is valid because the flat ladder brooches are a one-piece casted artefacts except for the pin assembly. The

Table 2: EDX point measurements in scanning TEM mode on FIB slices taken from artefacts from Ramutten-Jahn, Viehof and Ostriv.

At.%	**E6**	**E7**	**E8**	**O1**
-	Ramutten-Jahn	Ramutten-Jahn	Viehof	Ostriv
Cu	86.8 ±1.0	94.3 ±1	87.1 ±0.5	80.62 ±3
Zn	10.8 ±0.2		10.3 ±0.2	18.28 ±1
Fe	0.5	0.2	0.4	0.2
Si				0.5
S	1.9 ±1.4	5.5 ±0.2	2.2 ±0.6	0.4

followed up section provides the analytical outcomes from the penannular brooches from the regions under study.

Penannular Brooches

Four penannular brooches from East Baltic and Ostriv regions were further sub-categorized as explained in the previous Section 4.3.2 with the chemical analyses results displayed in the Table 3. Two of the brooches were horse shoe brooches with star shaped terminals (E4—E5) from Ekritten and Trentitten locations of East Baltic regions, respectively. One horse shoe brooch with star shaped terminal and one with widened terminals from Ostriv cemetery were also analysed. As recorded by the STEM EDX point measurements, the underlying base alloy in the four brooches was brass with uneven atomic percentages of the Zn content. Furthermore, the horse shoe brooches from Trentitten, Ekritten and Ostriv demonstrated similar copper to zinc ratio i.e. 7.5, 10 and 7.3, contrasting with the atomic percentage of the brooch with widened terminals from Ostriv which displayed approximately double the amount of zinc content i.e. 20 at. %. Besides this, all the four brooches consisted of Fe as the trace element whereas S was also documented in the horse shoe brooches from Trentitten, Ekritten and Ostriv. Identical stylistic attributes and chemical composition was observed in the brooches from Trentitten and Ostriv brooch reflecting strong consistency.

Table 3: EDX point measurements in scanning TEM mode on FIB slices taken from artefacts from Trentitten, Ekritten and Ostriv.

At.%	**E5**	**E4**	**O3**	**O2**
-	Trentitten	Ekritten	Ostriv	Ostriv
Cu	87.28 ±0.3	85.45 ±3	87.2 ±1.3	79.02
Zn	11.5	7.9 ±0.3	11.2 ±0.4	20.5
Fe	0.2	0.3	0.3	0.3
S	1.02 ±0.3	6.35 ±2	1.3	-

An elemental mapping analysis was performed on the representative samples of penan-

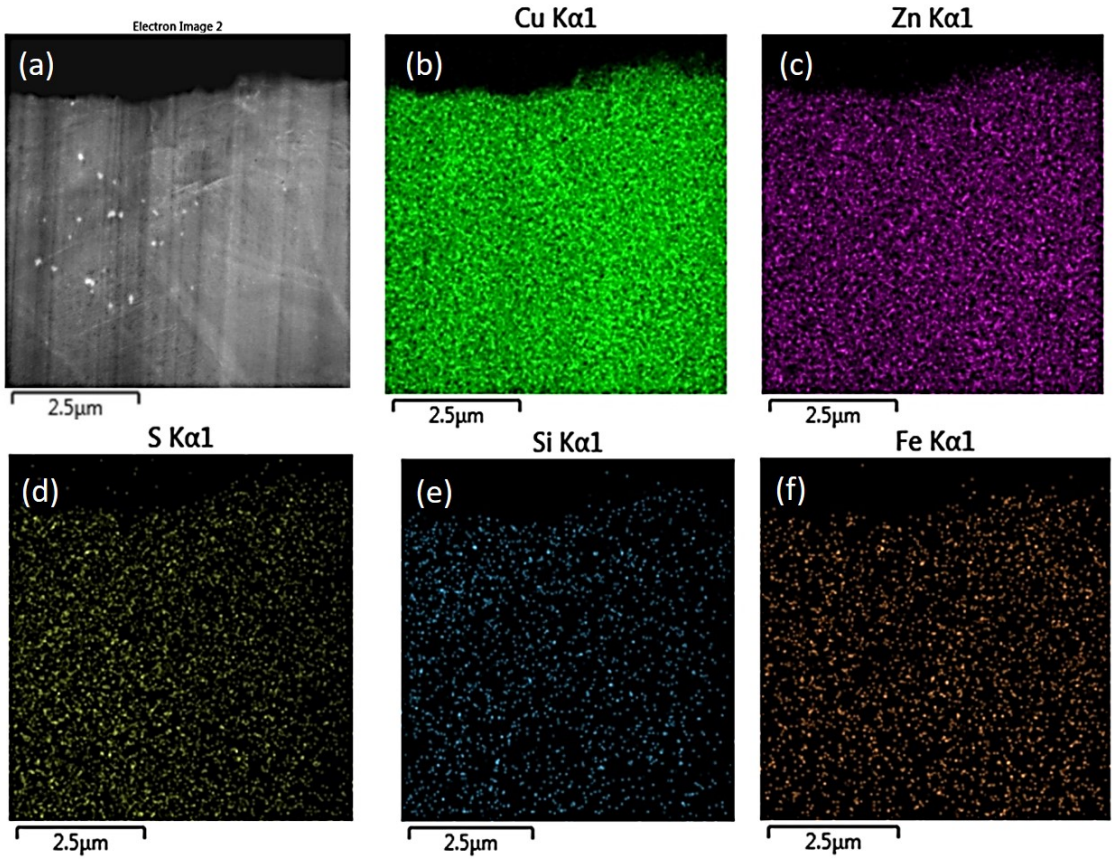

Figure 20: Measurements recorded in scanning TEM mode on lamella from flat ladder brooch with ID E6 a) electron image and b)-d) EDX elemental maps based on Cu, Zn, S, Si and Fe (By K. Saleem)

nular brooches from the East Baltic and Ostriv regions in order to investigate the distribution of the elements present. The results of this analysis are presented in Figure 21. Since, all three artefacts consist of copper and zinc as base alloy, the maps showed even distribution of the main base elements. Fe is also distributed in the entire lamella homogeneously showing that it was part of the original production process.

Ring Brooches

The sample group of ring brooches was significant comprising of equivalent number of artefacts as that of flat ladder and peannular brooches. Three of the brooches were excavated from East Baltic regions of the Grebieten, Löberstoff and Popelken whereas one brooch was also included from Ostriv. Copper was found as one of the base alloys in all the artefacts. The recorded elemental information is shown in Table 4. Interestingly, Zn content was not recorded in the two artefacts pertaining to the Löberstoff and Popelken territories. However, the consistency in the intrinsic elemental structure was noted in the brooches from Grebieten and Ostriv, both consisting of brass. Except, variation in Zn content was documented between Grebieten (8.9 at. %) and Ostriv (12.6 at. %), respectively. In the trace elements section, Fe was measured in the entire batch of ring brooches, additionally, Si was measured in the brooches from Popelken and Löberstoff. Moreover, traces of As were found in the artefacts from Löberstoff, Popelken and Ostriv as well. And lastly, Sulphur was found in the artefacts from Grebieten and Löberstoff in varying compositions.

Table 4: EDX point measurements in scanning TEM mode on FIB slices taken from artefacts from Grebieten, Löberstorf, Popelken and Ostriv.

At.%	**E1**	**E2**	**E3**	**O4**
-	Grebieten	Löberstorf	Popelken	Ostriv
Cu	87.5 ±0.3	90.3 ±3	95.9 ±1	90.9 ±0.1
Zn	12.6			8.9 ±0.1
Fe	0.2	0.3	0.2	0.2
Sn			3.5	
Si		0.2	0.2	
S	0.9	9 ±2.4	0.1	
As		0.2		

Spiral Neck Ring

The spiral neck ring from the East Baltic region of Ramutten-Jahn and Ostriv cemetery were analysed and an elemental comparison was documented. The elemental information is displayed in Table 5. Both the artefacts had copper and zinc (alpha brass), identified as the base alloys. The zinc content in both the artefacts was comparable with 14 atomic percent of zinc in the Ramutten-Jahn artefact and 11 atomic percent zinc in the spiral

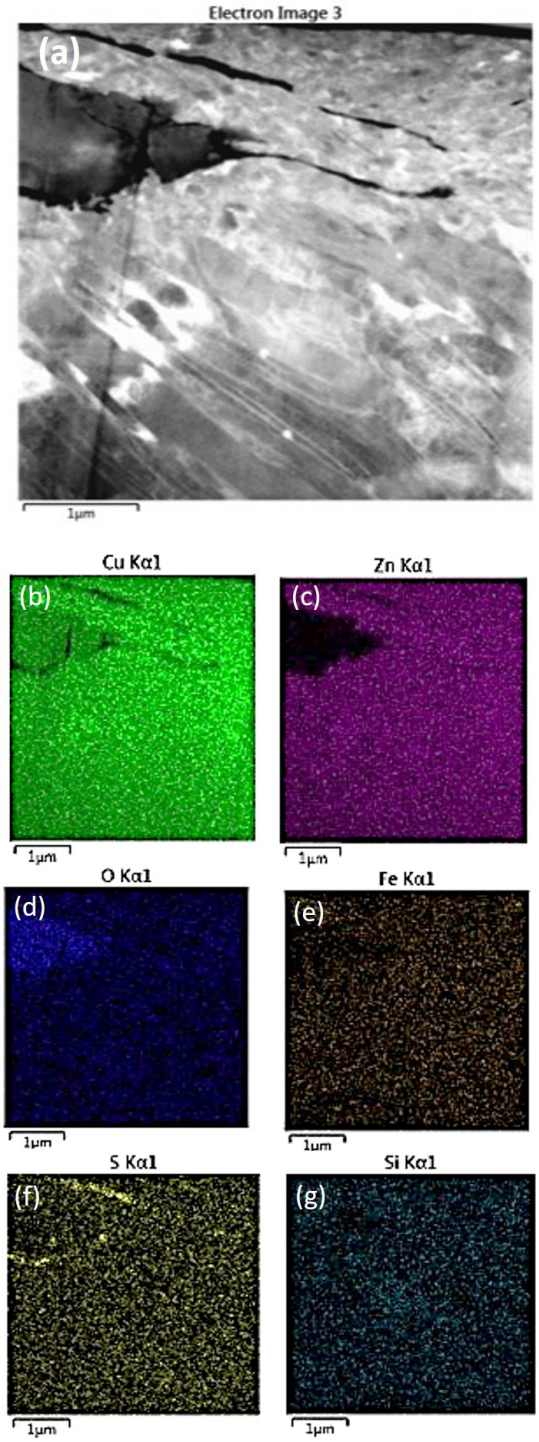

Figure 21: EDX elemental map recorded in scanning TEM mode on lamella from flat ladder brooch found at Ostriv with ID O1 with a) electron image and b-g) EDS elemental maps based on Cu, Zn, O, Fe, S and Si (By K. Saleem)

neck ring found in the Ostriv cemetery. Besides this, both the artefacts comprised of trace elements such as Fe and S in varying quantities.

Table 5: EDX point measurements in scanning TEM mode on FIB slices taken from artefacts from spiral neck ring from Ramutten-Jahn and Ostriv.

At.%	**E9**	**O5**
-	Ramutten-Jahn	Ostriv
Cu	84.5 ±0.5	88 ±0.5
Zn	14.2	11.4 ±0.9
Fe	0.4	0.2
S	0.9	0.4

4.5 Surface vs Bulk Analysis

The penannular brooch with widened terminal from Ostriv grave 35 has a complex corrosion crust, broken and discontinuous at certain regions as shown in the Figure 12. The environmental exposure possibly led to the formation of primary, secondary and tertiary compounds on the surface of the artefact. Thus, there is a difference in the exterior structure (analysed via SEM EDX) and the interior of the specimen (analysed via TEM). A comparison of the EDX spectrum taken through SEM and TEM is shown in the Table 6. SEM EDX spectrum revealed the elements in the corrosion crust such as Cu, Zn, Si, O, Fe, C, Pb and P. Whereas, the TEM-EDX spectrum only showed the presence of Cu, Zn with minute amounts of O and Fe, as analysis is taken at the depth of roughly 30-40 µm from the surface of the artefact. The corresponding EDX elemental map from SEM and TEM demonstrated the distribution of the compounds on the surface and bulk of the artefact and are shown in the Figure 22 and 23, respectively. The elemental maps show a visible difference between the surface and the internal structure of the artefact, where Pb, P, C, Si were limited to the surface and not documented in the bulk of the artefact. The elements established according to the TEM EDX spectrum were Cu, Zn as base alloys. Whereas the secondary chemical compounds in the uneven corrosion crust such Pb, P, C and Si are the microstructures from the soil and environment.

Table 6: Surface vs Internal structure (via SEM and TEM respectively) analysis documented in atomic percentages on the penannular brooch with widened terminals excavated from Ostriv (O2).

O2	**Cu**	**Zn**	**Si**	**O**	**Fe**	**C**	**Pb**	**P**
Surface	10.5	0.2	0.1	21.5	0.6	64.2	1	0.9
Lamella	78.2	19.2	-	1.2	0.2	-	-	-

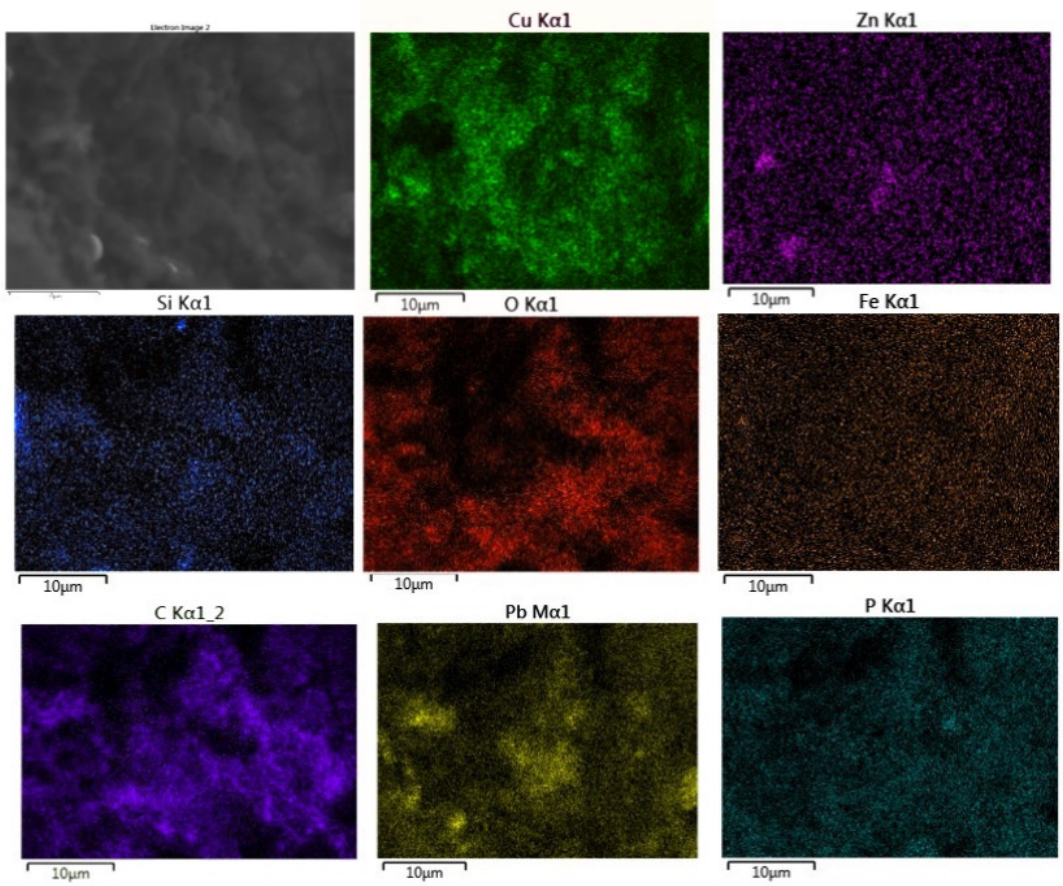

Figure 22: SEM-EDS Elemental map documented on the surface of the artefact O2 excavated from Ostriv (K. Saleem)

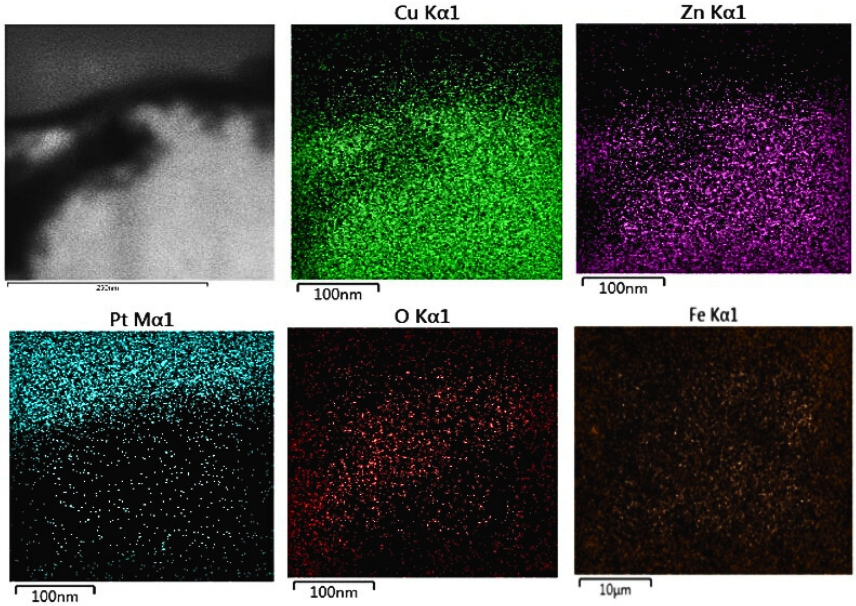

Figure 23: TEM-EDS elemental map documented on the FIB lamella of artefact O2 excavated from Ostriv (K. Saleem)

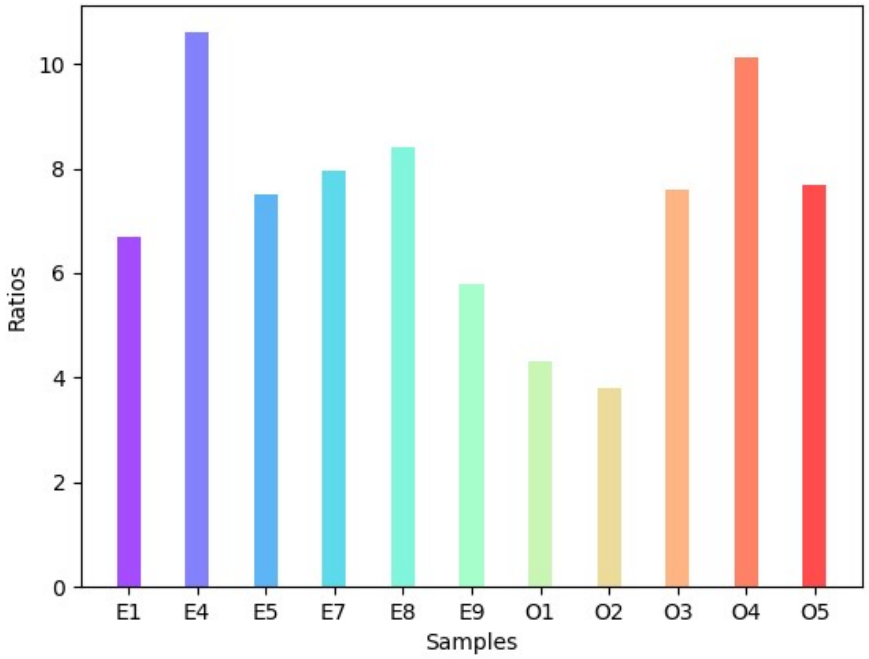

Figure 24: Copper and Zinc ratios of the East Baltic and Ostriv artefacts (K. Saleem)

4.6 Section Discussion

In total, fourteen artefacts from the Berlin part of the Prussia Collection and from the Ostriv cemetery were analysed in this study. Despite the fact that they come from regions far apart from each other, the East Baltic region and Central Ukraine, they are typologically similar and all refer to the same - Baltic – typological context. Eleven specimens of all the artefacts demonstrated brass as the primary alloy and two ring brooches from Popelken and Löberstoff showed evidence of pure copper used, additionally, one flat ladder brooch from Ramutten-Jahn was also pure copper artefact. However, the higher tendency of preferable zinc removal from the surface of the brass artefacts due to a phenomenon called 'dezincification' should not be ignored. Overtime, the zinc corrodes more aggressively in brass objects exposed to environments containing humidity and high temperatures, leaving zinc depleted surface layer [47]. This could point towards the need of extracting the representative lamella from further depth of the artefact. The correlation between the atomic percentage ratios of Cu and Zn is shown in the Figure 24. The zinc content in Ostriv artefacts ranged between 8 to 20 at. % . Meanwhile, the zinc content in the brass artefacts of East Baltic was between 7 to 14 at. %. An amount as high as 20 at. % as in case of widened terminal brooch from Ostriv is possibly a deliberate increment in the zinc content. While correlating the chemical composition with the stylistic interpretation of the penannular brooch with widened terminals, demonstrated in the Figure 12 and marked as O2 in the Table 3, the brooch has not only high zinc content but also criss-cross decorative lines ingrained on its surface. As pointed out by Roxburg et al. (2018) the brass based alloys were assumed to have higher cultural importance in medieval metallurgy in Sedgeford England owing to their superior mechanical properties. It became the alloy of choice and gave competition to the bronze- based jewellery which were harder but also more prone to fractures and cracks because of higher brittleness. Generally, brass even with 8 at. % zinc is tougher, stronger, malleable and also has higher ductility compared to bronze. This is because the crystal structure of the brass consists of copper and zinc atoms that have very low atomic radii difference. This allows them to form a tightly packed solid cubic crystal lattice of metal atoms which enables them to slide against each other when hammered, so the alloy hold together well under stress. Unlike most solid solution elements, the yield strength of brass increases with the amount of zinc content present [48] [31]. Therefore, in order to produce harder brass the craftsman possibly used higher zinc content as in case of the brooch with widened terminals. Using stylistic similarities and Cu to Zn ratio as a parameter to compare the artefacts further, it was noted that the penannular brooches with connected star-shaped terminals from Sambian Trentitten and Ostriv showed close stylistic and compositional attributes (Cu/Zn content as 87/11.5 and 88/11.2 at. %, respectively) providing an important evidence of the artefacts, which could be produced in the same region. But, we need some more archaeological arguments for those interpretations. Especially concerning some differences in production techniques (see Table 2, 3, 4 and 5) and lack of traces of long usage or repair for most of the Ostriv brooches.

Further regarding the copper and zinc ratio, most of the brass from the Prussia Collec-

tion and Ostriv cemetery have a 3 to 4 % difference in the amount of copper to zinc ratio. Here we would like to point out that the production of the brass artefacts and the composition could be influenced by several factors. Less is known about these medieval brooches production mechanism, however, historically brass production has been a complex task. There are multiple reasons for it, one is that zinc is not occurring in nature as a pure metal. It is very volatile-reactive and combines readily with other elements. It only occurs in compound ores such as zinc carbonates ($ZnCO_3$) or zinc sulphide (ZnS). The other major problem is that it vaporises and escapes into the atmosphere when heated above 907°C which is below melting temperature of copper. Therefore, melting copper and zinc together is not viable. As a remedy, first zinc oxide using ZnCO3 ore or zinc sulphide (ZnS) is produced which is more stable. The ZnO flakes could subsequently be used to produce brass following a process called cementation. The ZnO and copper fragments could be placed in a crucible, heated below the melting temperature of the copper (1084 °C) to make sure the small fragments of copper remain solid to offer higher surface area as the zinc vapours diffuse thought the copper surface. Furthermore, as the solid alloy becomes fully liquid, the temperature of the melt is dropped and requires to be regulated once again [31]. Hence, the brass making and copper zinc ratios are varied by several factors such as temperature control, the time of the whole process and the initial ratio of the ingredients. Even, if the same reproducible technology and high quality fresh metal was available, a difference of 3 to 4 at. % in medieval times artefact should not be the criteria determining separate origins of the artefacts.

Most copper ores contain Fe and S as major elements. We found nonhomogenous quantities of Fe trace elements in all the artefacts ranging from 0.2 to 0.5 at. %, however, it was measured around 0.3 at. % for majority of the brooches. The amount of sulphur was prevalent in the brooches from East Baltic regions, at times, around 9 at. % but were documented around 1 at. % for most of the artefacts. The principle task of smelting process is to separate copper from these two components. Hence, their concentration reflects on efficiency of the smelting and purification process. A relation between Fe content between copper ore and the raw copper metal exist with Fe reducing in every stage of smelting to minimum in the smelted metal, and so is the case with other trace elements such as S, As and Sb [49]. Ingo et al. (2006) also argue that the Fe could be indicator of the quality of the smelting process used to produce the raw copper metal. An amount of about 0.3 wt. % is typical of the early processes carried out under poor reducing conditions, while content less than 0.05 (wt. %) indicates a more efficient process and therefore, the iron content could evidence the level of technological competency and skill of the smelting operator. We would also like to highlight that the minor trace elements could also result from the contaminants from the walls of the crucible, which possibly was used for multiple batches during the production.

4.7 Section Conclusion

The study of archaeological objects from different regions with TEM analysis profoundly helped differentiate between the intrinsic chemical structures from the secondary alterations on the artefacts and unearth the true composition. However, it is worth mentioning that the TEM analyses relies on the quality of sample preparation method employed. The chosen method in this study i.e focused ion beam milling helped a) to produce the electron transparent slice from the intrinsic structure of the artefacts and b) fulfilled the most important criteria of keeping the process extremely minimally invasive. However, it is important to point out that the pre-drilling before the FIB is a critical step to remove the brittle patina. The successful non-destructive chemical analyse of the artefacts helped devise theories of likely production of the artefacts and the challenges of the process. It further helped to highlight the craftsmanship of the medieval East Baltic metallurgy industry. The difference in the alloying materials, at occasions pure Cu for three specimens could likely be a surface limited phenomenon, as a result of preferable zinc dissolution in the brass alloy leaving a zinc depleted surface layer due to corrosion. It points towards the need for higher depths required to reach in the artefact to extract a true representative lamella. However, if pure copper is documented in the future medieval East Baltic or Ostriv artefacts as well, then there might be a possibility to explore the availability of inconsistent raw materials or migration of technology and not necessarily the produced artefacts into the Kyivan Rus'. A difference in the amounts of zinc was documented in the artefacts, which was attributed to the complex nature of the brass production process. Whereas the addition of rough 20 at. % zinc was considered deliberate to achieve specific mechanical properties. Furthermore, the chemical analysis provided a strong evidence towards the common origin of the East Baltic artefacts and the artefacts found in the Ostriv cemetery. So, with small difference and identical stylistic attributes such as in ring brooches, flat ladder brooches, penannular brooches and the neck ring, the artefacts demonstrate more commonalities than differences. However, the data set on the chemical analyses of the artefacts from medieval Ostriv and East Baltic population should be increased with analysis of more artefacts to contribute evidence supporting this hypothesis. Further comparative chemical metal studies of similar jewellery objects from the Ros' and the Baltic regions are planned during the ongoing DFG project.

Acknowledgements The preparation of this paper was funded by the Deutsche Forschungsgemeinschaft (DFG, German Research Foundation) - Projektnummer 508078428 and under Germany's Excellence Strategy – EXC-2150 – 390870439).

5 Pilot Study 2 Neolithic Axe Surface Examination: Decorative coating or corrosion products?

5.1 Overview

The present study aims to provide a detailed understanding of the original surface of the Neolithic copper axe artefact that was excavated in Northern Europe. This section includes a brief overview of the theoretical background of copper axe, its historical context, and its stylistic categorization. Furthermore, the study will focus on the non-destructive chemical analyses of the surface of the artefact, which will allow for a comprehensive understanding of the original surface of the axe. The goal of this study is to provide a deeper understanding of the axe, its chemical composition and its place in the context of the Neolithic period from Scandinavia. The study will use a combination of analytical methods such as TEM and SEM EDS.

5.2 Sample Group and Historical Context

The Neolithic copper axe, as seen in Figure 25, was discovered in the Medieval village of Eskilstorp. It is important to consider the circumstances of the excavation in order to understand the factors influencing the surface condition of the axe. According to the observations made by Christian Horn in his publication [50], the axe was found in ploughed soil at the edge of a small drained bog, with no other Late Neolithic finds in the vicinity. However, several prehistoric and historic artifacts have been found in the region in separate excavations. Additionally, a cluster of Stone and Bronze Age grave monuments were located approximately 500 meters East of the excavation site, and the remains of two Late Neolithic houses were found roughly one kilometer south of the excavation site.

The axe was found in a well-preserved state, and it is referred to as a Pile type, named for a Pile type hoard that was found almost 5 kilometres Northwest of the Eskilstorp region, in present day Southern Sweden. Pile type axes are believed to have been used during the Neolithic period, which dates back to around 1800-2200 BC. Therefore, it is important to note the geographical proximity of the axe to the Stone and Bronze age grave monuments and Late Neolithic houses, as well as its well-preserved state, may provide insights into the use and cultural significance of the axe in the context of the Late Neolithic period [51].

Type and Dating of the Axe

Helle Vandkilde conducted extensive research [52] on Late Neolithic metalwork and classified the Pile type axes, including the Eskilstorp axe as belonging to the Late Neolithic II period, which is approximately dated to 1950-1700 BC. Specifically, Vandkilde classified the Eskilstorp axe as belonging to Class A "primitive low flanged axes" and assigned it to the subgroup type A3. The subgroup A3 is characterized by having parallel-sided curved flanges and is commonly referred to as the Gallemose type. Vandkilde also proposed that

this axe was likely produced locally in South Scandinavia, and it was not traditionally reported to have any decorative coatings [51][53].

Axe Dimensions

The Neolithic Cu axe is an artefact that is symmetrical and intact, with only slight signs of wear and tear. The total length of the axe is 115 mm, with a cutting edge width of 48 mm and a width of 20 mm from the butt side. The thickness of the axe is 11 mm and the flanges, or the raised edges on the sides of the axe, have a thickness of 14 mm. The butt area of the axe is semi-circular in shape, while the cutting edge of the axe is convex and there is a sign of damage with a missing piece of several millimetres in size. This missing piece of the axe could be due to ancient use or post-depositional damage.

Figure 25: Neolithic copper axe with (A) front side (B) back-side

A similar type of axe was also found in a hoard located 5 km away in the Tygelsjö parish region. It is thought that the axe was buried with one side facing downwards into the soil, which may have led to a difference in patination on the symmetrical faces of the axe. The downward facing side may have been better preserved due to a lack of oxygen, while the upward facing side may have been exposed to weathering and erosion. The burial of the axe for nearly 4000 years has also led to the accumulation of soil residues and a disfiguring crust of multicolored compounds on the surface of the axe, obscuring the original structure and composition of the artefact.

The corrosion products on the surface, as shown in Figure 25, are greenish in color with a tint of dark oxidized copper alloy as a result of long-term exposure to oxygen. This type of oxidation is common in copper-based alloys and is known as copper patina. Ad-

ditionally, a darker contrasting surface is visible on the majority of the axe, as well as near the butt of the axe. This darker surface is likely a result of the formation of copper compounds such as copper carbonates and copper sulfides.

The surface layers of the axe, which comprise of secondary chemical alterations and containments, may not reflect the original structure and composition of the artefact. Therefore, further analysis is needed to determine the original structure and composition of the axe. A darker contrasting surface is visible on the majority part of the axe and near the butt on both sides of the Figure 25.

Initial Analysis of the Axe

An initial analysis of the Neolithic copper axe was conducted by Horn et al. (2017) in which they employed digital microscopy techniques. The analyses revealed the presence of two distinct layers on the surface of the axe. The first layer, referred to as layer one, is believed to be the original surface of the axe. This layer is flaked off in some regions due to the build-up of underlying corrosion layers. The height of these regions is even and lower than the second layer. The second layer, referred to as layer two, is found at a higher height compared to layer one and is believed to be the original surface of the axe. Further analysis revealed the presence of marks of ribs and channels which are different in coloration. Horn et al. (2017) interpreted these ribs and channels as part of the decoration, as they were found on the original surface of the axe where the top layer had flaked off. Further research is needed to confirm the interpretation that the ribs and channels are part of the decoration, and that surface layer is the original surface of the axe. The corrosion layers and flaking of the surface can be caused by several factors such as environmental conditions, post-depositional damage or ancient use [51].

Initial metallographic analyses of the axe was conducted in order to find the surface cover composition. Two samples were prepared for this purpose, a small roughly 1 cm cross section was cut from the butt area of the axe and small flakes from the surface were removed. Both the samples were mounted in the epoxy resin. The analyses of the cross section showed the presence of a contrasting rim and a copper core. The core of this axe consisted of copper with several impurities i.e. silver, antimony, arsenic and nickel. The rim of the cross section showed the presence of homogeneously oxidised region from the copper core and outward. Near the edges, this oxidised copper consisted of small irregular patches of silver. This was unprecedented for Late Neolithic copper axes and built grounds for more detailed analyses to answer questions as stated in the following heading aims and objectives of this study.

5.3 Aims and Objectives

The aim of this study is to conduct a detailed chemical analysis from both sides of the axe which seem to be differently patinated. After identifying the chemical composition,

it is intended to differentiate between the original alloy and contamination from the surrounding environment i.e soil, air or water and impurity from within the casted alloy originating from the type of ore utilised. This is done in order to establish whether surface decorative layer is present and specifically observing whether silver surface coating is deposited on the copper axe. Furthermore, to understand the corrosion behaviour of the axe and deterioration of elements from the surface, experimental replicas are prepared. The prepared experimental replicas are further tested in soil like solutions for corrosion behaviour of copper and silver alloy. In this thesis, the research on the axe can be divided into following points:

a) What are the constituents of the axe's surface? Is there evidence of a decorative silver layer deliberately deposited on the surface of the axe?

b) Was the surface of the axe present when it was produced or was it the result of secondary alterations caused by its burial conditions and environment in the soil?

This is significant because the axe of this type are believed to have been produced in South Scandinavia and not known to have decorative silver coatings. The result of this study could emphasise categorisation of the Pile type axes once again.

5.4 Methods, Instrumentation and Test Parameters

Overview

Detailed studies based on the electron microscopy analysis of the axe was planned. The analysis was expected to reveal microstructures of silver present on the surface of the axe down to atomic scale, identify the compounds of copper metal and contaminants from the soil. As a result, SEM and TEM was utilised in the study where SEM could provide a comprehensive elemental understanding of the surface whereas TEM could help differentiate between the surface limited elements and primary base alloys in the intrinsic metal core. Additionally, TEM could provide information about the phases to atomic level preciseness.

Focused Ion Beam (FIB) for sample preparation

To keep the process non-destructive, FIB slices from the surface of the axe were taken following the process described in Section 3.5.1. Two FIB specimen were taken from the surface of the axe where the top layer was flaked off, as shown in the Figure 25B, which is the cleaner side of the axe as it was at the interface of the environment causing corrosion to be more aggressive. The corroded layer likely flaked off leaving a comparatively smooth surface underneath. The FIB cuts extracted from side B would be referred to as Lamella A and B. The second specimen was taken from the side A which was the top layer of the axe, shown in the Figure 25A. This side was facing downwards into the soil and possibly more protected from the environment due to less oxygen available for

the corrosion activity. As a result, arguably, corrosion on this side took place slower and the corroded surface layer did not flake off, rather stayed on the surface as a highly porous layer, supported from the soil underneath. This side provides more opportunity to investigating the original surface of the axe. However, this lamella was very porous and could not stay intact for the measurements. Nevertheless, SEM was conducted on this side and chemical information on this side in form of elemental mapping is available and discussed in results section.

Additionally, a cross-section taken from the butt of the axe was also received on which SEM analyses was conducted. So we have following 4 types of analyses.

a) Analyses on the two FIB slices taken from the side B (Figure 25B), representing the clean side, to attain chemical composition on this side, however, the axe was not pre-microdrilled and the FIB cuts were taken directly from the surface. These samples were analysed in TEM.

b) We have analysed the side A (Figure 25A) representing the dirty side under the SEM.

c) We have analysed cross-section taken from the butt area of the axe analysed under the SEM.

d) We have experimental replica that is used for corrosion test and understand the corrosion phenomenon of copper and silver alloys.

Electron Microscopy

TEM analyses was conducted on the prepared FIB lamellae using the steps mentioned in 3.5.3. TEM was used to record high resolution images in bright field mode. Then, while operating in the scanning TEM mode, EDX point measurements were conducted from the FIB lamellae. The EDX point measurements recorded the chemical information from the several regions on the lamella. Moreover, electron diffraction patterns were attained in the SAED mode to identify the phases on the lamellae.

The butt area that was previously cut from the axe was loaded vertically in the SEM chamber, so that the cross section area faces the electron beam. In this way, the core region and the surface regions were analysed. The SEM imaging and SEM EDS was conducted on the cross section. In SEM EDX mode, the point measurements were conducted from the core and the outward edges of the cross section. More details about the instrumentation can be found in Section 3.5.2.

5.5 Results

SEM analyses on the surface and cross section of the axe:

The electron imaging, EDX elemental mapping and EDX spectrum were conducted on the side A of the axe by using SEM. It is displayed in the Figure 26 and shows that this 'dirty' side has generally rough structures. The EDX signals from the irregular hill-like structures shows the presence of Fe whereas, the darker contrast regions show an interwoven pattern of Cu and Ag and copper is present in abundance. At a closer inspection it can be seen that the signals of Ag are rather isolated instead of homogenously distributed within the Cu and only present in the surface layer of the axe. So, a free copper layer is covered with isolated microscopic silver beads. Another region on the clean side was also analysed under the SEM EDS and elemental mapping was recorded. The results showed spiral filament like silver corrosion product and shown in Figure 27. A study covered in the literature review section shows the presence of these whiskers on silver surface, that grow rapidly over time in warm environments with SO_2 and are silver corrosion products [41].

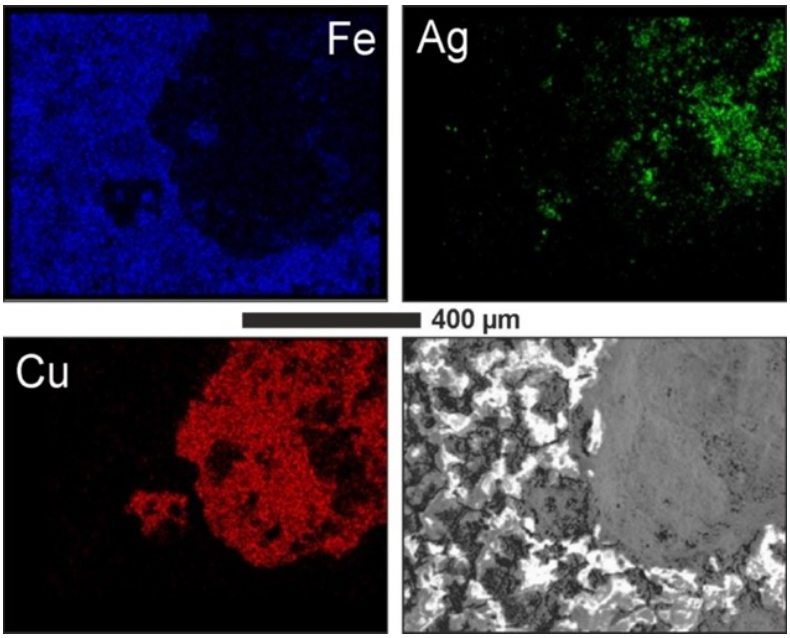

Figure 26: Elemental analysis on the surface of Face A of the axe using SEM-EDX (analysis credit: Christin Szillus, CAU Kiel)

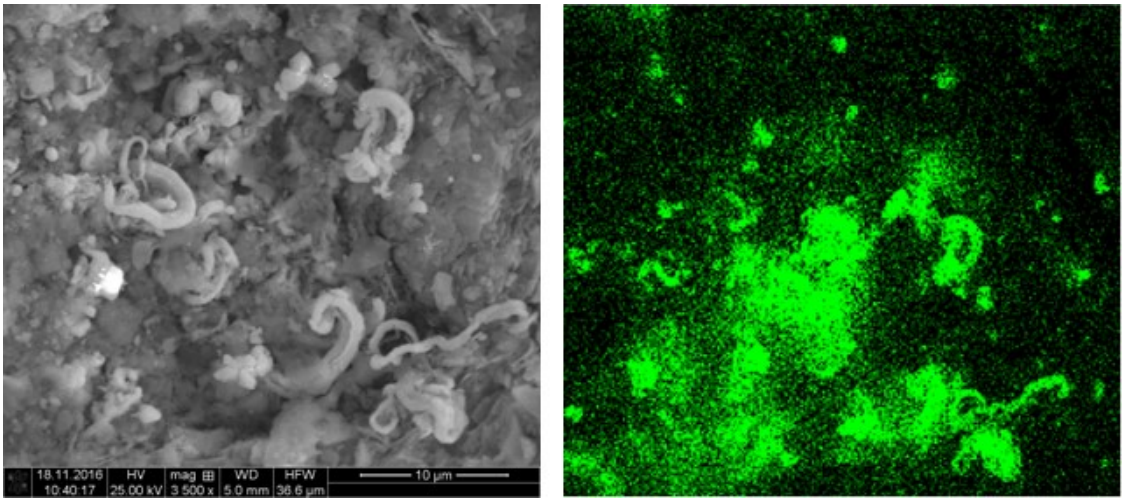

Figure 27: Electron image and SEM EDX elemental mapping on the Face A of the axe showing spiral silver structures (analysis credit: Christin Szillus)

SEM analysis from the cross section of the axe was also conducted and displayed in the Figure 28 showing contrasting morphologies on two sides (clean and dirty side) of the axe cross section. The SEM EDS elemental mapping on these two sides show the presence of Cu and O on the clean side and Cu, O, Ag and Fe on the dirty side. So, a top corroded layer is present on the dirty side of the axe consisting of metallic compounds which is probably the outcome of the one-sided contact of the axe with the drained bog in which the axe was found.

Figure 29 shows the EDS spectrum recorded from the point 41 inside the crack that is propagating from the surface inwards. The SEM electron image shows a porous region where the point measurement was conducted and shows presence of silver signal. The spectrum 45 recorded on point 45 shows pure Cu signal and a relatively smooth and preserved region.

Concluding the SEM results, it can be seen that the surface on both clean and dirty sides consists of silver. However, the dirty side additionally consists of containments from the soil as well such as Fe. Furthermore, the core of the axe does not show any any silver content. Silver might be present as trace element but it is not resolved by SEM EDS in the core of the cross section. However, silver signal are not only detected on the surface of the axe but also along the cracks propagating inwards from the surface of the axe. For more detailed information, the TEM analysis from the FIB slices is displayed as follows.

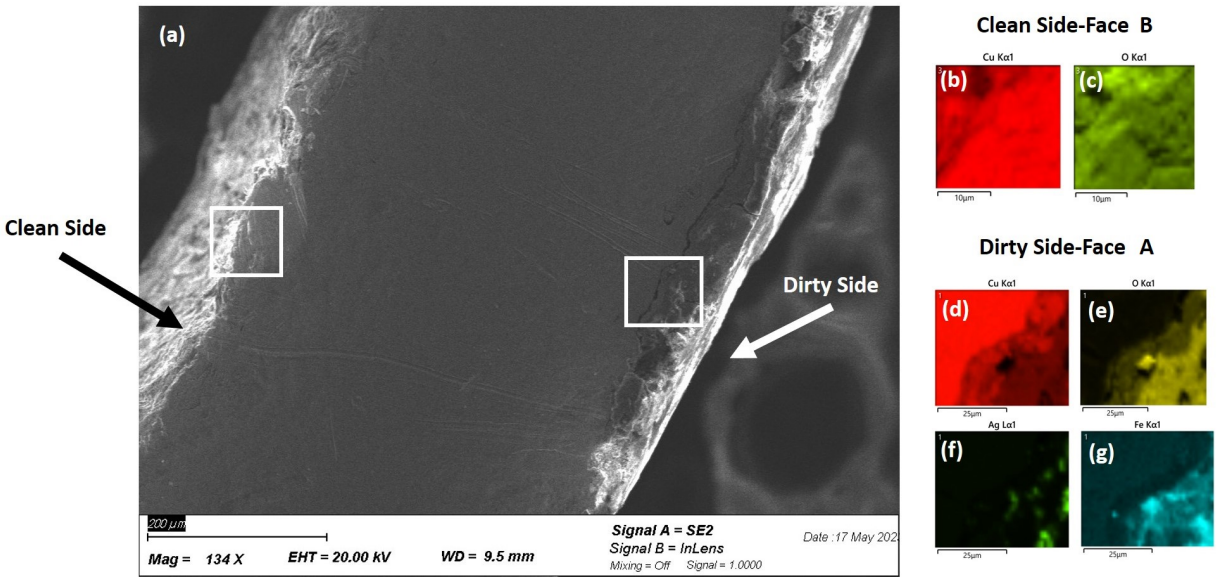

Figure 28: (a) SEM electron image recorded showing both sides of the cross section (b-c) EDX elemental map from clean side-Face B and (d-g) dirty side-Face A (By K. Saleem)

TEM analyses from the surface of the axe:

Both the lamellae are taken from the clean side as the lamellae from dirty side could not stay intact. The lamellae from the clean side are lamella A and B. The TEM results from lamella A are shown in Figure 30 and from the lamella B are shown in Figure 31. The first figure shows the HAADF image, showing higher Z elements bright whereas the second figure shows bright field electron image, with higher Z elements shown as darker contrast. The alphabetical markings on the images represent the regions where STEM EDS point measurements for elemental compositions were taken to attain the chemical information from the contrasting micro-structural features. The elemental composition at those points are displayed in Table 7 and 8, respectively. The dark field image in Figure 30 is taken from the lamella A. The lamella is significantly porous and the presence of Cu, Ag, Fe, P, O and Ca can be observed in the image. It can also be seen that the silver micro particles are agglomerated in regions within the lamella and are surrounded by matrix of Cu_2O. This observation is confirmed by the electron diffraction pattern shown in Figure 32 taken from lamella B. The point measurements taken from two areas near the surface show the presence of heavy oxidation (ca. 56 at.%), large amount of Fe (ca. 8.7 at%), P (ca. 6.6 at%) and Ca (ca. 4 at. %). The bright contrasting region in the dark field image of the lamella B shows high atomic percentage of Ag (ca. 83 at%).

So TEM results confirm the presence of silver micrparticles which are inhomogenously distributed over the whole lamella. It should be noted once again that even though the FIB cuts are taken from the clean side and this side also remained in soil for long period

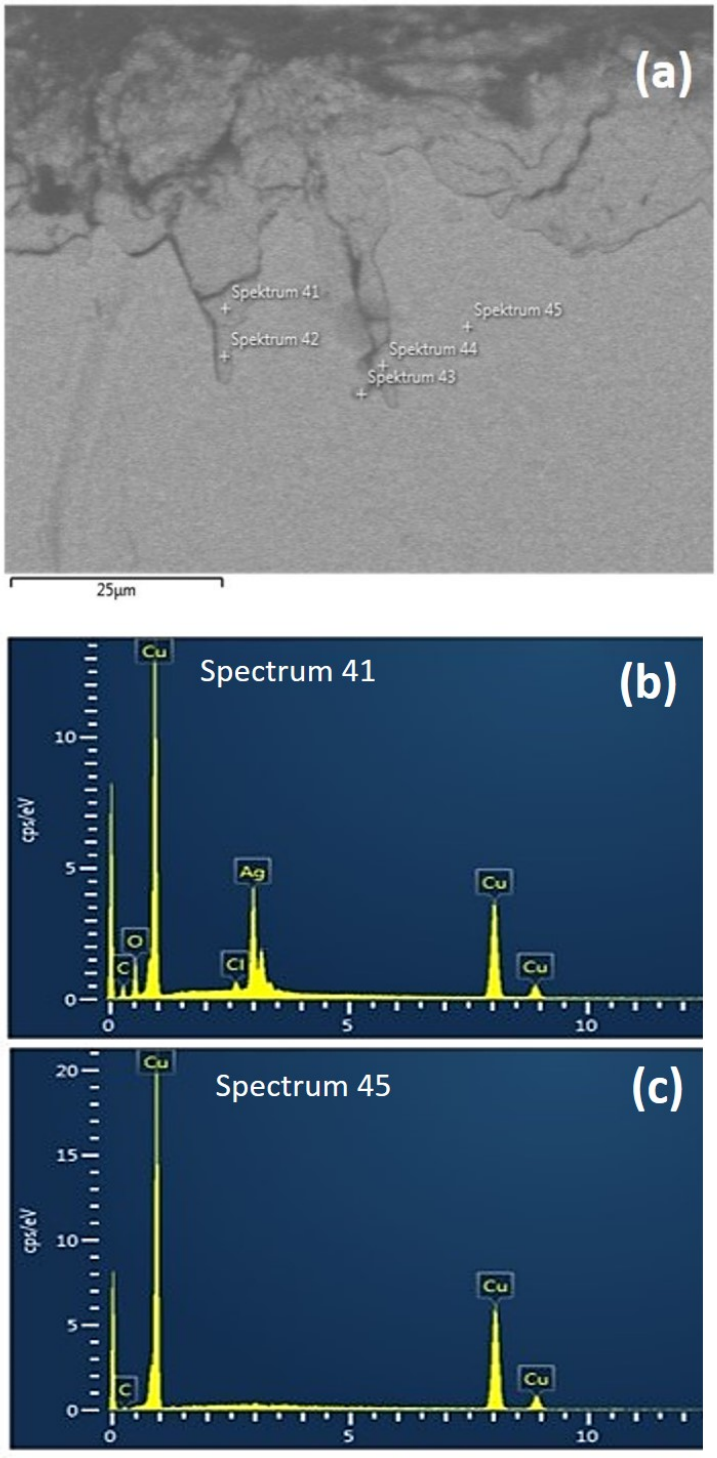

Figure 29: SEM measurements on the cross section of the axe with (a) electron image (b) EDS point measurement from the corrosion layer- spectrum 41 and (c) core- 45 (By K. Saleem)

of time. So a corrosion layer is expected on the side of the axe as well. Although some areas enriched in silver are present but in comparison to the average quantity of Cu, they are still in very less quantities (i.e. when compared with the amount of copper present over the whole lamella. So comparing the SEM and TEM EDS analyses, it is documented that a copper depleted region exists on the surface with signals of silver. The signals of silver are not detected within the core because they are very less. But the silver traces are present in the core as trace elements since Fahlore type copper ore is used to cast this axe as established by Horn et al. (2017) in their initial analysis. Depletion of Ag, Sn or other such metals is a known phenomenon documented by other researchers as well due to copper surface corrosion.

To further test this hypothesis of copper depletion on the surface as a result of corrosion. Some experiments are conducted and explained in the following section.

Table 7: Representative result of STEM EDS point measurements at different areas on lamella A, side B.

STEM EDX Point Measurement from lamella A (at. %)

Area	Cu	Ag	C	O	Fe	P	Ca
A	11.3	52.3	36.2	-	-	-	-
B	5.9	-	18	56.6	8.7	6.6	4
C	41	44.3	7.2	2	-	5	-
D	97.1	-	-	2.8	-	-	-
E	96.3	-	1.9	1.7	-	-	-

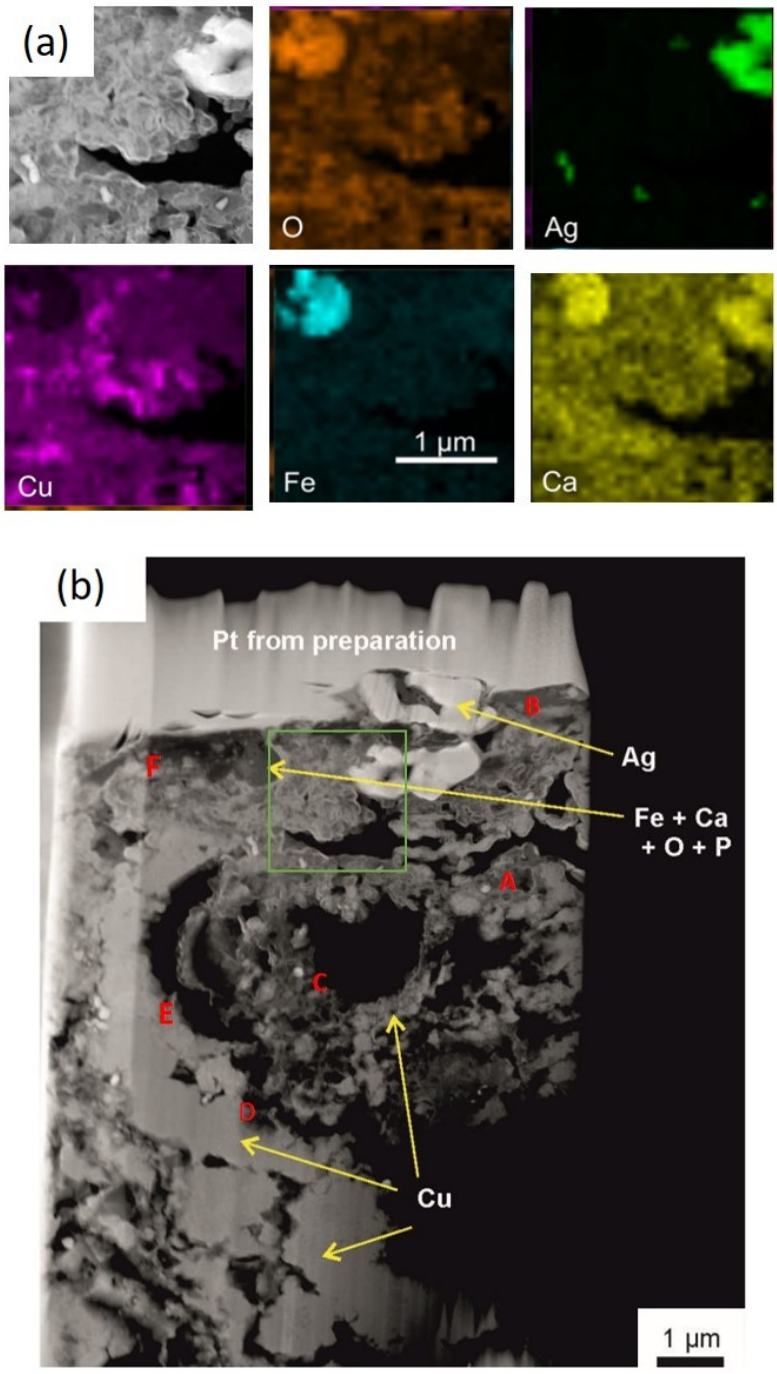

Figure 30: (a) STEM EDX elemental map of the region of interest taken from the marked square in the dark field image (b) HAADF image of the FIB lamella A, side B and the point measurements conducted from regions marked with alphabets (analysis credit: Ulrich Schürmann, CAU Kiel)

Table 8: Representative result of STEM EDS point measurements at different areas of lamella B, side B.

STEM EDX Point Measurement from lamella B (at. %)

Area	Cu	Ag	C	O	Fe	P	Ca
A	0.7	83.8	15.3	-	-	-	-
B	26.8	64.8	6.5	1.7	-	-	-
C	83	-	4.1	12.7	-	-	-
D	98	-	-	1.9	-	-	-

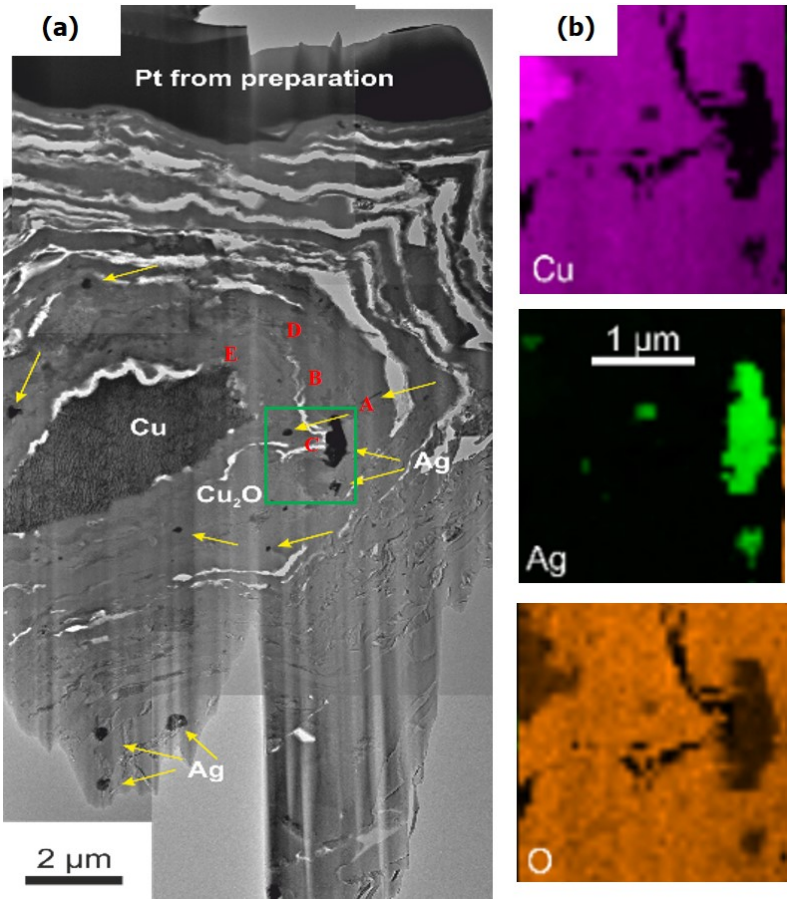

Figure 31: (a) Bright field image of the FIB lamella B, side B and the point measurements conducted from the regions marked with alphabets (b) STEM EDX elemental map of the region of interest taken from the marked square in the dark field image (analysis credit: Ulrich Schürmann, CAU Kiel)

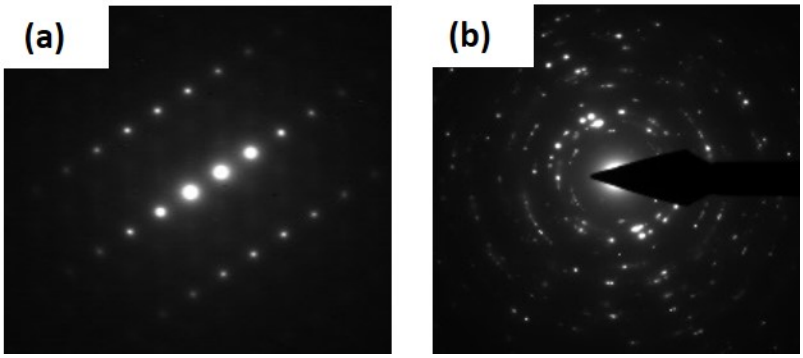

Figure 32: Electron diffraction patterns recorded in SAED mode confirming the presence of (a) regions of pure copper and (b) copper oxide from lamella B, side B. (analysis credit: Ulrich Schürmann CAU Kiel)

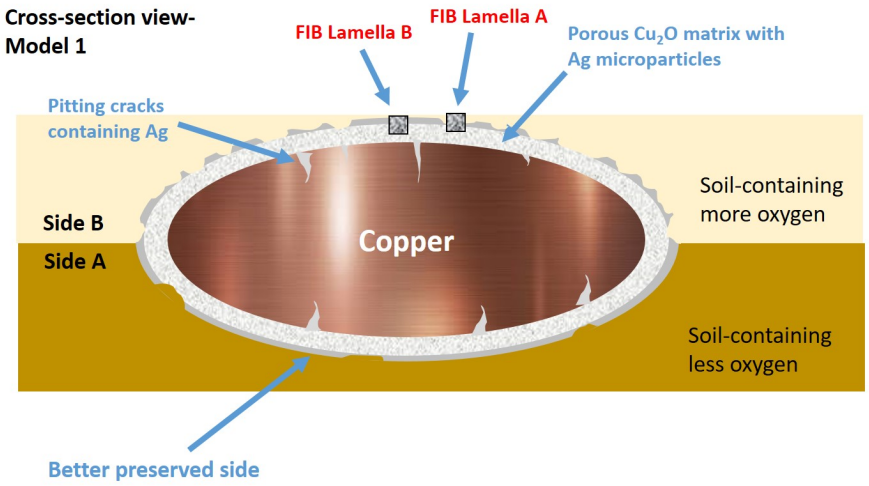

Figure 33: The devised model of the cross section of the axe by the author (K. Saleem)

5.6 Axe's Corrosion Process Simulation

To experimentally simulate the corrosion process, a study was conducted in the scope of this thesis, in which the copper silver alloy was prepared (95 at. % of copper and 5 at. % of silver) and a corrosion experiment was conducted in an electrolyte which resembles the soil-like composition. The following process was followed for the preparation of the alloy.

The total weight of the alloy was about 5 g. The silver wire was cut into smaller pieces, dipped in nitric acid (HNO_3) for 5 minutes to clean the surface contaminations. Sim-

ilarly, the copper beads were measured on a weighing scale and washed in nitric acid (HNO_3) for 5 minutes. Both the metals were then packed in a glass ampoule. The ampoule was vacuum sealed using a heating stove. This ampoule was then placed in the furnace at 1200 ℃ for 5 hours. Then sample were left in the furnace to cool down overnight. The ampoule was then broken and the prepared alloy was retrieved. This oval shaped alloy was then sectioned in two parts. An image from the flat side of the alloy is shown in the Figure 34. The halved-alloy has indentations which are deliberately made to mark the changes in the morphology of the same area after the corrosion experiment.

Figure 34: Cross section view of the prepared alloy with Cu 95 at. % and Ag 5 at. %.

To conduct the corrosion experiment, a solution of Humic acid with 56 mg/L in distilled water was prepared. The test solution was prepared in order to replicate conditions, similar to the soil environment. Humic acids (HA) are natural poly-electrolytes that occur in soil and natural waters because of the decay of plants and animal compounds, together with other biological species such as microorganisms in the environment [54].

Finally, the specimen was dried at room temperature, then degreased by acetone, rubbed with cotton wool, soaked in ethanol, dried at room temperature again and immediately immersed into the prepared solution. The prepared specimen remained immersed in the HA solution for 20 days at a room temperature. On the 20 th day, the sample was taken

out of the test solution, weighted and left to dry at room temperature. The specimen was then mounted onto the SEM stage and analysed for the surface examination.

5.6.1 Effects of Electrolyte on the Alloy

Figure 35 shows the EDX elemental mapping recorded on the indented area on the prepared alloy (a) before the corrosion experiment and (b) after the corrosion experiment. It is demonstrated from the images that a higher signals of silver is reported on the specimen after the corrosion experiment compared to pristine Cu/Ag specimen. The map shows certain pockets where the copper content is decreased when pristine and corroded specimen are compared. To quantify the elements present on the surface, EDX point measurements were recorded from 6 regions on the flat side of the specimen. These quantities are averaged out and shown in the Table 9. The average values show increase in the silver content from 5.2 at. % in the pristine specimen surface to 12.3 at. % in the surface of the specimen after the corrosion test. The copper signals have decreased from 94.3 at. % to 83.5 at. %. Moreover, the oxygen quantity is increased from very low 0.4 at. % to 12.3 at. %. It can be stated that substantial changes in the surface morphology of the specimen have been observed after the corrosion test where surface is relatively copper depleted compared to the uncorroded alloy. This comparison also displayed as a bar chart (FIgure 36) between corroded and uncorroded alloy elements.

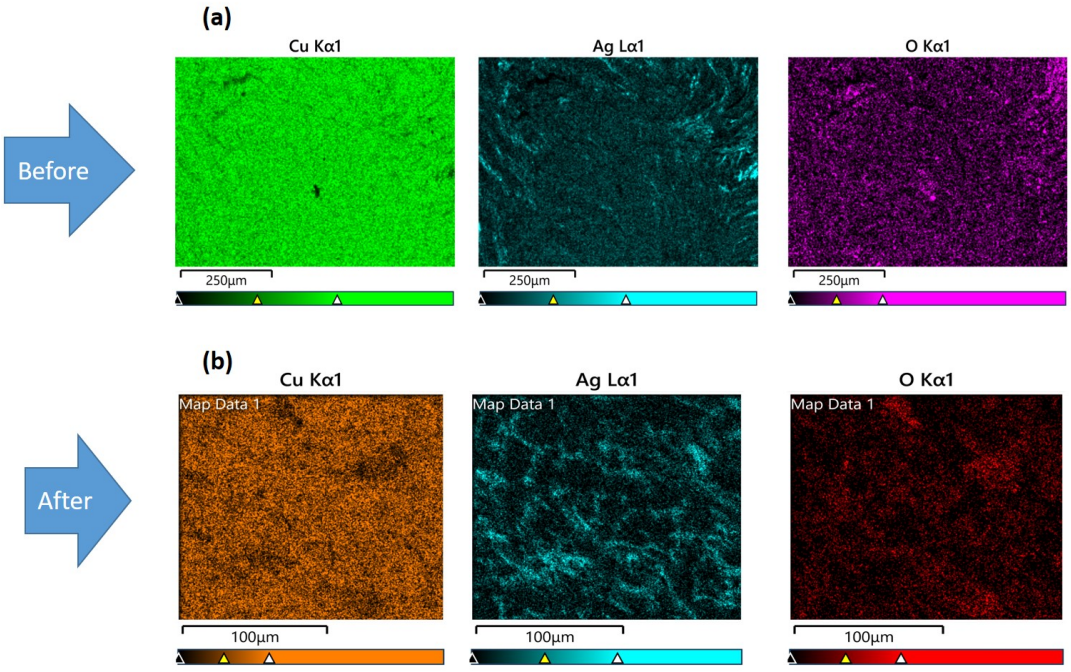

Figure 35: SEM EDX elemental mapping on the CuAg alloy (a) before the corrosion experiment (b) after the corrosion experiment

Table 9: SEM EDX point measurements from six different positions recorded on the copper and silver alloy represented in atomic percentage.

Pristine	Specimen	Pos1	Pos2	Pos3	Pos4	Pos5	Pos6	Average
	O	0.2	0.8	0.3	0.2	0.3	0.4	0.4
	Cu	96.3	95	94.7	95.1	94.5	94.1	94.3
	Ag	3.3	4.1	4.8	4.6	5.1	5.4	5.2
Corroded								
	O	14.5	3.9	8.81	2.3	0.7	2.5	4
	Cu	70.4	85.9	61.6	89.1	94.9	88.7	83.5
	Ag	15	10	29.5	8.5	4.3	8.7	12.3

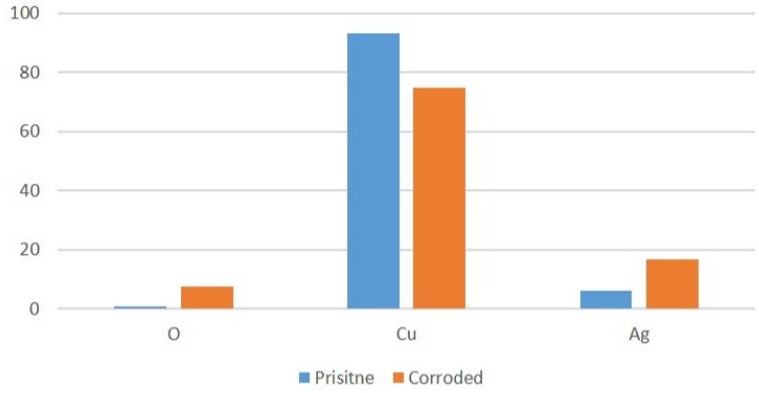

Figure 36: Comparison between the surface composition of pristine and corroded CuAg alloy.

5.7 Discussion

From the SEM results of the axe, it is illustrated that there is a copper core which is surrounded by the oxidised zone and possibly basic copper compounds. This result is confirmed by the elemental mapping drawn at the cross section of the axe. Furthermore, the EDX spectrum shown in Figure 29 demonstrates presence of silver particles as far as the cracks have penetrated inside from the surface inwards of the axe's surface. This phenomenon is possibly following the pitting corrosion phenomenon explained in Section 2.3.

There is a presence of Ag microparticles signal over the whole FIB lamella apparently taken from the layer in contact with the core. However, these silver particles are possibly less than 2%, when it is compared with the region where pure copper signal is recorded. These silver particles seem to be agglomerated in certain areas on the lamellae where they remain in pure form. The surface layer contains a matrix of copper oxide, Ag beads and crystals of pure copper as demonstrated more clearly from the devised model shown in Figure 33. As it was documented by the initial metallographic analysis that fahlore

type copper ore was suggested to have been used in the production of this Eskilstorp axe. Pernicka et al. (2016) argues that the fahlore type copper ore is comprised of small amounts (i.e. <1%) of impurities such as antimony, silver, arsenic and at times nickel. The silver signal is surrounded by highly oxidised copper. So the initial axe which contained Ag impurities from the ore used, has now a copper depleted and silver enriched regions in the corrosion layer. The copper from the surrounding regions of the silver possibly leached out and dissolved and leaving oxidation compounds of copper where due to more noble nature of Ag it stayed on the surface. Arnoldussen et al. (2022) also argues in his study on the prehistoric (c. 2200 BCE-AD) bronze alloy compositional analyses on metals and corrosion layers, that the corrosion process is the most probable reason for observed elevated concentrations of Ag (present as ore impurity) in the corrosion layer [55]. Orfanou et al. (2015) explains Sn enrichment of copper based artefacts due to the possibility of selective dissolution of copper from the surface due to corrosion, present at the interface of the environment [56].

Copper is a less noble metal with a standard reduction potential of 0.34 V and silver is more noble metal with a potential of 0.79 V [57]. Thus, copper is more susceptible to dissolution in water than silver. The solubility of copper in water depends on the pH, temperature, and the presence of other dissolved species. Generally, copper ions are more soluble in water than silver ions. Copper ions can form complex ions and hydroxides that are more soluble than silver ions, therefore copper has a higher solubility in water. However, the rate of dissolution will also depend on the specific conditions, such as the presence of oxygen or other dissolved species that can affect the redox potential of the water. Furthermore, silver compounds are less stable and transform into elemental silver overtime. Silver is possibly washed away from the side which is facing upwards whereas it stays in a metastable state in the cleaner side and possibly does not have enough energy to dissolution into the soil. Hence, caution remains in terms of representativity, and critical evaluation of results studied especially when the chemical analyses is surface limited. The study presented here also underlines the importance of examining the corrosion layer along with the core of the sample.

5.8 Section Conclusion

It can be concluded from our studies on the copper axe in the course of this thesis work that the category of the axe remains as primitive low flanged axe. Like other locally produced axes from South Scandinavia, this axe does not contain decorative layer of silver. We argue that the axe is casted using fahlore type copper ore which contains impurities of silver. As the axe remained buried under the soil for roughly 4000 year, the selective leaching of the copper resulted in copper depleted and silver enriched surface regions. However, more axes from the late Neolithic and early bronze age time period should be analysed in future to further solidify and draw further cross correlations between the commonalities in the axes. Another low flanged axe is received from Sweden dating to the similar time period and will be analysed for the comparison in future.

6 Pilot Study 3 Routes of Amber: An attempt on provenance and environmental effects study on amber

6.1 Overview

Amber is a complex tree resin which fossilised over millions of years through polymerisation and cross-linking of long carbon chains. The resins are sticky plant secretions made up of viscous liquid that composes volatile terpenes and non-volatile solids, making it thick and sticky. These resins harden on atmospheric exposure over millions of years and have been found with coal and other sedimentary rocks. Fossil resins are chemically water insoluble mixture of compounds such as terpenes, terpenoids and their derivatives [58]. It has been utilised in wide variety of applications ranging from its traditional use in jewellery, art and craft objects to ingredient of perfume, as decorative artefact and as folk medicine. A less mature form of amber is copal (sometimes referred to as immature amber) that has not gone through the entire fossilisation process. Amber obtained from similar locations may vary in molecular composition, could originate from distinct plants and undergo different fossilisation processes [59]. The difference from one deposit to another can be derived based on physicochemical properties as well as presence of organic or inorganic inclusions. The properties of amber reflect on the evolution of the resin from its initial botanical source to the present fossil form. The most abundantly available and common type of amber is extracted from the Baltic sea and is referred to as "Baltic amber" and sometimes as succinate. The Baltic amber contains succinic acid which is a finger print to discover Baltic amber [60]. Imitations of amber have been made since 600 years to produce fake amber using substances like synthetic polystyrenes, epoxy resins, celluloid, plastics, bakelite and coloured glass. Distinguishing authentic amber from its imitations is possible with chemical and physical tests. These tests include floating in salt water for testing specific gravity, checking melting point and conducting Rockwell hardness test. However, when dealing with ancient artefacts with historical relevance, it is not possible to compromise the samples integrity. The colour of amber ranges from often pale to golden yellow or orange. Natural amber has been appreciated for its colour and natural beauty since Paleolithic era.

In our research, amber samples of various ages and from different localities (Denmark and Russia) were investigated with Raman spectroscopy and fourier transform infrared spectroscopy (FTIR). The excitation wavelength for Raman was 735 nm. Based on the Raman and FTIR analyses the resins were differentiated on basis of their age and geographical origin and an attempt to observe the related age of the amber was made. Furthermore, since the chemical fingerprint of amber could change after being exposed to the heat from the environment. In this study, heat and UV light experiments are conducted on amber to identify changes in the FTIR and Raman spectra. Finally, the potential of Raman and FTIR spectroscopy as a tool for quick and non-destructive analysis of amber identification and classification is discussed.

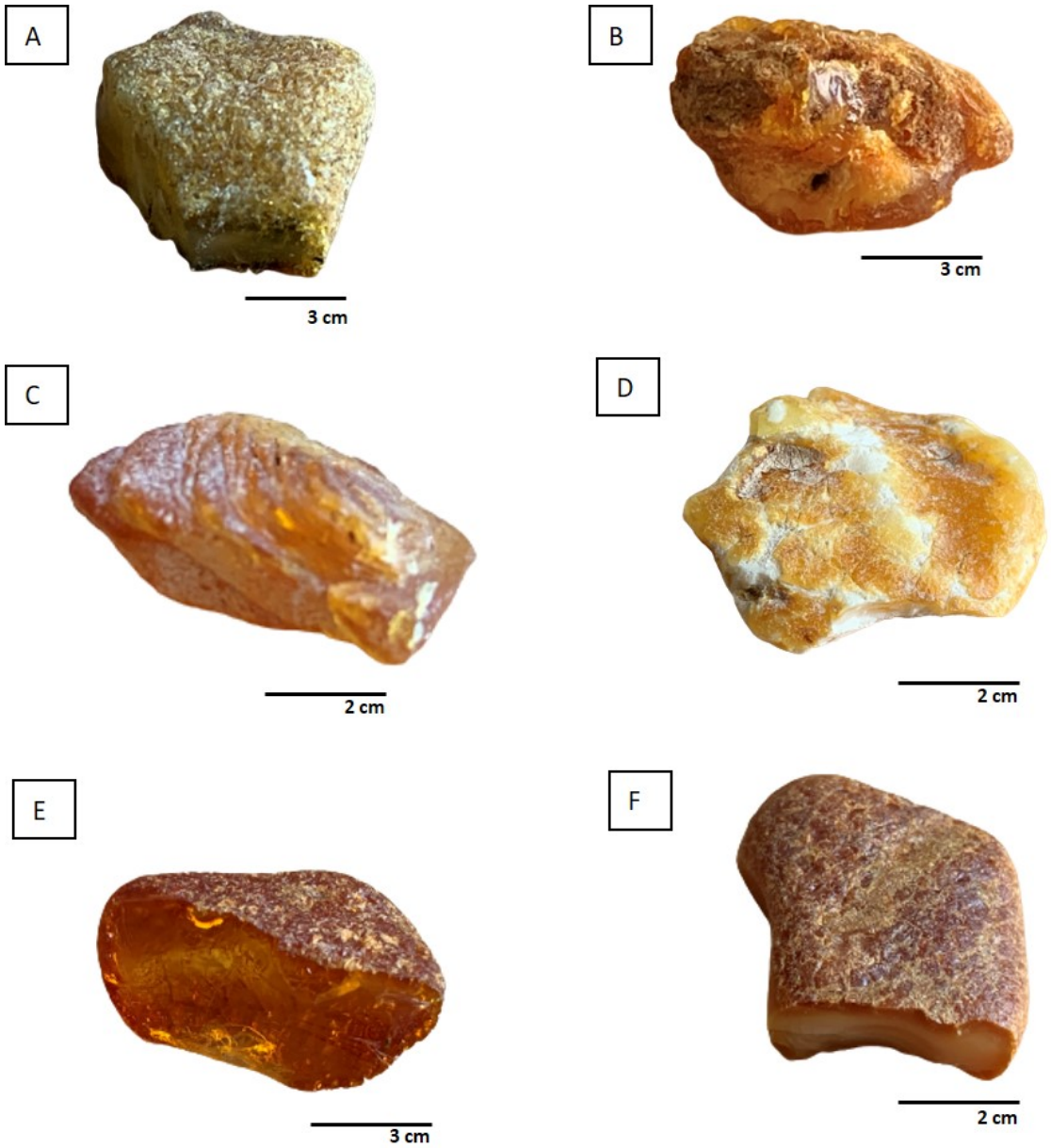

Figure 37: Amber Samples A, B, C from Kaliningrad in Russia and D, E, F from Skallingen Vejers in Denmark (photo credit: K. Saleem)

6.2 Sample Group

The samples subjected to analysis came from Kaliningrad (Russia) and Skallingen Vejers (Denmark) and were provided by centre for Baltic and Scandinavian Archaeology (ZBSA). They are not archaeological artefacts but samples collected as stray finds, therefore, less is know about their origin.

6.3 Analytical Methods

The unambiguous identification and classification of fossil resins remain challenging. The doubts related to the resins' origin, botanical source and alteration in the geological environment exists and requires utilisation of advanced analytical techniques. Therefore, development and usage of advanced analytical methods in fossil resin investigation is important to fill the knowledge gaps. Amber can be analysed using several analytical techniques such as scanning electron microscopy, Raman spectroscopy, infrared spectroscopy, UV-Vis spectroscopy and gas chromatography-mass spectroscopy and variety of other techniques. These techniques are popular for analysing amber mainly because of the non-destructive sample handling.

Raman spectroscopy is a molecular spectroscopic technique that has been often used for non-destructive analysis of historical materials. Some fossil resins can easily be identified using Raman. The technique provides information about chemical structure of the resin. The chemical structure consists of cyclohexane/cyclopentane derivates, aromatic rings and exocyclic CH_2 and CH_3 groups [59]. Since, the shape of Raman spectra is affected by resins degradation and by maturation degree, the Raman spectra has been occasionally used to correlate with the age of the specimen. Winkler et al. (2001) utilised Raman spectroscopy to find age of the amber samples by taking intensity ratios of bands at 1646 and 1450 cm $^{-1}$ (I = 1646/1450). They confirmed that the intensity ratio for immature copal and for mature amber are different [61]. Nielson et al. (2006) report that the peaks in the range of the ratios occur pre-dominantly for Baltic Amber with different geographical regions demonstrating different spectral ranges [62]. Jehlicka et al. (2009) reported the fluorescence interferences making it hard to obtain spectra of fossil resins with 785 nm excitation laser [63]. The problems associated with the fluorescence could be mitigated by utilising near infrared light source. Zhifan et al. (2013) investigated natural amber, copal resin and colophony by UV-VIS, infrared and Raman spectroscopy. Colophony is a brittle solid form of resin produced by heating away the volatile liquid terpenes. Copal, amber and colophony show very similar refractive indices when measured with UV-fluorimeter. The Infrared spectra typically show peaks at 3448, 2930, 2870, 1742, 1447, 1378, 1154, 1015 and 887 cm^{-1} with similarities between Copal and Amber. However, the peak at 887 cm^{-1} is more clear in copal than natural amber. Copal resin has two additional peaks at 700 and 637 cm $^{-1}$ due to C-C bond stretching. The infrared spectroscopy peaks for colophony are at 3435, 2955, 2867, 1708, 1464, 1385, 1166, 1041, 885 and 827 cm $^{-1}$. The obvious difference are at peaks 1166, 1041, 885 and 827 cm $^{-1}$, can be used to distinguish between copal and amber. Infrared spectroscopy is a useful technique however; the sample has to be powdered which is typically not allowed for arte-

facts. With the infrared spectroscopy, it was discovered that amber from Baltic region has a characteristic feature identified by a shoulder in the wavelength region 1250-1175 cm $^{-1}$ on the band at 1150 cm $^{-1}$. It still remains a challenging task since the fossil resins, in the course of their maturation process, are affected by degradation processes of various kinds which results in affected spectroscopic fingerprints. Various analytical methods in fossil resin investigation are needed together with a geological, palaeogeographical and palaeoclimatic background for understanding fossilization processes associated with the transformation of resins from plant exudates to present, fossil forms [64].

6.3.1 Aims and Objectives

The aims of the study involves chemically identifying the amber included in this thesis. To see if it can be categorised as Baltic amber on the basis of the analysis. Moreover, to identify characteristic features of Baltic amber in FTIR and Raman spectra. Another part of this research work involves studying the degradation and weathering on the amber in heat and UV light from the environment. For this reason, amber samples were heat treated artificially in the lab and the changes from the non heated samples and heat treated samples in accordance to the FTIR and Raman spectra are recorded. The work in this section can can be subdivided into the following two primary and secondary aims:

1) The primary goal of the study is to examine the origins of the amber by sampling and analyzing the compositions.

2) A secondary aim is to analyse specimens that undergo degradation to ascertain whether the specific treatment might interfere with the provenance process.

The results of the amber analyses are displayed in the following sections.

6.4 Results and Observations

6.4.1 Raman Spectroscopy

A comparison between the representative Raman Spectra of amber samples from Kallingrad Russia and Skallingen Vejers are shown in Figure 38. The spectra shows bands at 715, 940, 1201, 1293, 1448, 1651 and 2929 cm^{-1}. Additionally, there is a shoulder at 2871 cm^{-1}. The bands at 715 and the ratio of intensity between bands at 1450 and 1650 cm^{-1} (I_{1650}/I_{1450}) have been used to estimate the age of the amber. The spectra shows the characteristic peaks as mentioned above. Only sample 6, from Skallingen Vejers, has an additional peak at 1583 cm^{-1}. The spectra show identical bands corresponding to the Baltic amber chemical fingerprint. There is a difference in the peaks' intensities at bands 1651 and 1448 cm^{-1} respectively. Hence, there is an indication of the difference in the relative age or exposure to different paleoclimatic conditions.

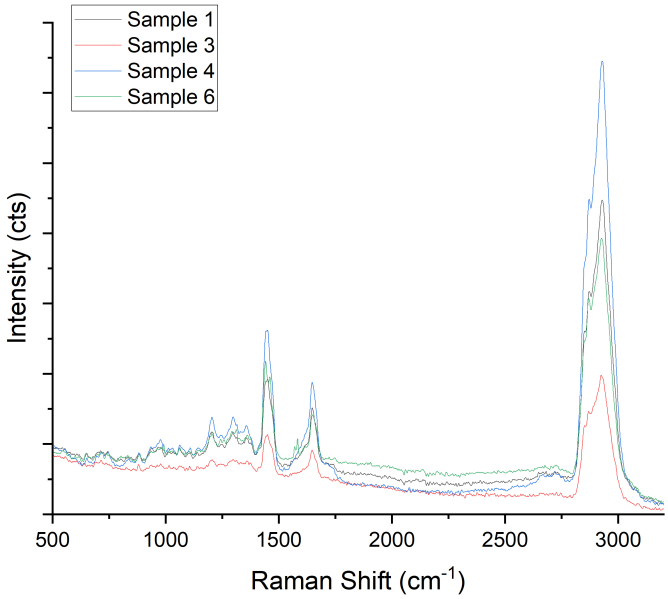

Figure 38: Raman spectra comparing all amber samples from Kaliningrad, Russia and Skallingen Vejers, Denmark

6.4.2 FTIR Spectroscopy

Figure 39 shows the FTIR spectrum of the Amber sample from Kaliningrad, Russia and Skallingen Vejers, Denmark. The spectrum shows the peaks at approximately around 884, 986, 1010, 1153, 1378, 1456, 1702, 2862 and 2935 cm^{-1}, respectively. Additionally, shoulders at 1259, 1641 and 1635 cm^{-1} are also visible. With minor differences, the spectrum of samples from Kaliningrad is very similar. The spectra from Skallingen Vejers all show the similar bands as stated for the amber from Kaliningrad. The FTIR Identification of the Amber is based upon the presence of characteristic absorption bands located at 2926, 2867 and 2849 cm^{-1} which are due to C-H stretching modes of the CH_2 and CH_3 groups. The carbonyl peaks between 1739 and 1700 cm^{-1} region are assigned to the ester and acid groups. Meanwhile the bands at 1260 and 1157 cm^{-1} are assigned to CO-O-modes of the succinate group. The peaks at 3080, 1643 and 888 cm^{-1} are representative of C-H and C=C stretching and bending of the rings and exocyclic methylene group. Importantly, the characteristic distinguishing feature, the so-called 'Baltic Shoulder' occurs at 1250-1150 cm^{-1} due to activity of axial and equatorial ester groups [65]. The band around 884 cm^{-1} shows the strongest peak for Sample 3 and weakest for Sample 1. Both these samples are from Kaliningrad Russia. This band signifies exocyclic methylene absorption and is used to differentiate between non-fossilised Copal and Balitc amber and Simetite. Simetite comes from the amber deposits in Sicily, Italy. An intermediate band strength (for both the samples), as in our case, is typical for Balitic Amber. Further, except sample 5, all other samples showed a peak around and a shoulder at 980 cm^{-1}.

The Baltic shoulder at around 1245 cm^{-1} is evident for all the samples. The Baltic shoulder is followed up by two peaks at around 1374 and 1439 cm^{-1}. The intensity of the peak at 1439 cm^{-1} is higher then 1374 for almost all the samples. Then, there is a very strong band at 2935 cm^{-1} with a shoulder at around 2850 cm^{-1} for all the samples. The FTIR spectrum of Semitite (Sicilian) amber is compared from the works of Dorothe et at. (2016) [66]. A distinct carboxylic acid carbon-oxygen stretch at 1238 cm^{-1} is observed, rather than flat shoulder as seen in the Baltic amber. Other rather intense bands present at 1174 and 1108 cm^{-1} and also a weak shoulder at 973 cm^{-1} are present in the Semitite and absent in the Baltic amber. Furthermore, the peaks at 1641 and 887 cm^{-1}, that are present in the Baltic amber are not present in the FTIR spectra of Sicilian amber.

Hence, clearly FTIR spectra can be used to differentiate between the Baltic and Sicillan amber chemically. In further section, heat and UV treatment experiments are conducted to observe the differences in the chemical fingerprints.

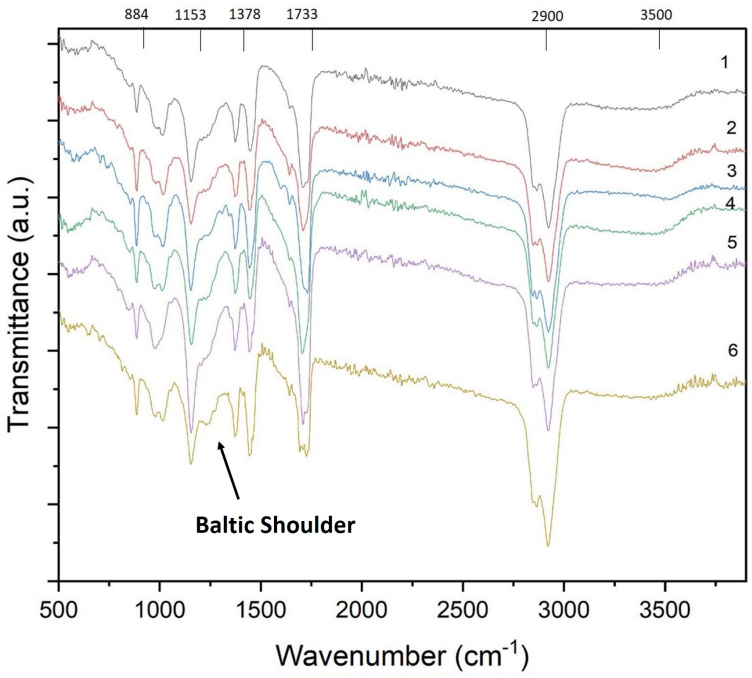

Figure 39: FTIR spectra of all amber samples from Kaliningrad, Russia and Skallingen Vejers, Denmark

6.5 Weathering and Degradation Experiments

For the degradation experiments amber sample from Kaliningrad was selected with a homogeneous translucency. The specimen did not have any visible organic or inorganic

inclusions. A section of the amber sample was smashed using a hammer in order to obtain fragments which could be used for analyses. Amber sample of size 2 cm x 3 cm x 1 cm from Kaliningrad was subjected to heat treatment experiments. The amber samples were enclosed in a glass tube sealed with parafilm. The tube was suspended in a beaker filled with 1 litre of vegetable oil covered with a teflon lid. To maintain a homogeneous temperature a magnetic stirrer was also placed inside the beaker. This whole assembly was placed on a IKA (r) C-Mag HS hotplate stirrer. The amber was heated to 120°C for 96 hours. Additionally, a piece of amber sample 1 cm x 2 cm x 1 cm was selected for the UV ageing experiment. To expose the sample to accelerated ageing under the UV lamp with a wavelength in the range of 365 nm emitted by the lamp. The ageing environment was kept at room temperature to separate the degradation effects of heat from the light: a temperature of approximately 25±2°C with around 50-70 % of humidity. the ageing of the specimen lasted for 39 days, after which they were stored and analysed under FTIR to see the changes.

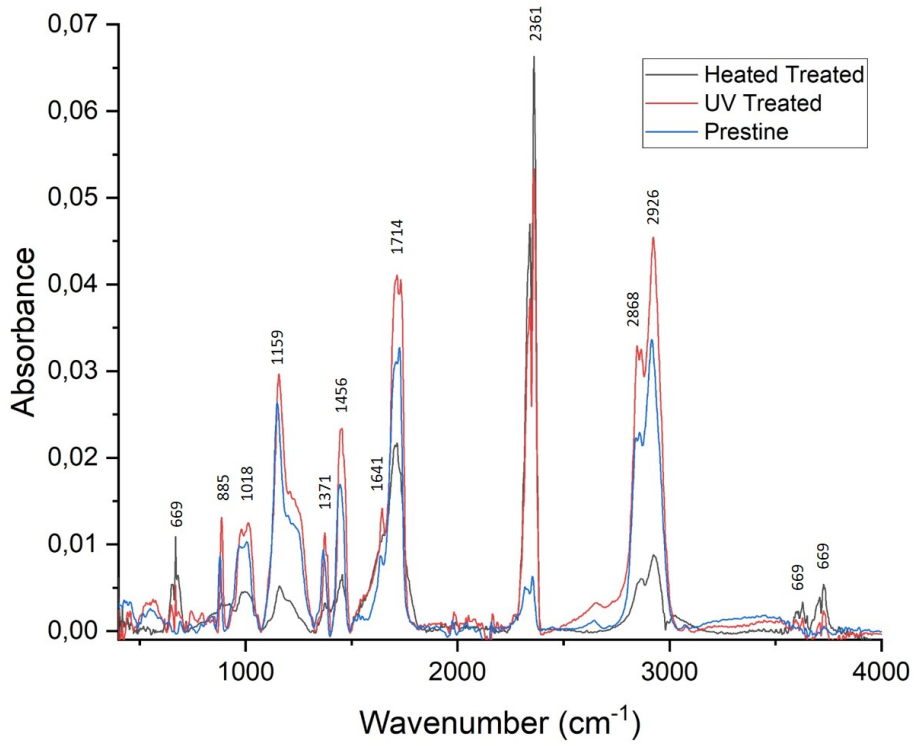

Figure 40: FTIR spectra of the amber Heat Treated, UV-Treated and Pristine from Kaliningrad Russia

ATR-FTIR was collected using the Bruker Vertex 70v with an accessory for holding the

bulk or powdered samples fitted with a crystal supplied with a pressure pin 3 mm in diameter to press the sample against the crystal. The absorbance spectra was acquired in the range of 400-4000 cm^{-1} with 32 scans. Figure 40 shows the comparison between the FTIR of the amber treated under heat and UV light with the prestive sample. The heated sample shows a very strong peak at 2361 cm^{-1}. However, the peaks at 885 and 1018 cm^{-1} are weak and missing the shoulder. Moreover, peak 1641 cm^{-1} which is quite evidently clear in spectra of UV treated amber, is very weak in the heat treated sample. Oxidation levels are measured by ratio between absorbance values of C=O (carbonyl group) and C-H bands, observed at 1700-1735 cm^{-1} and 1430-1470 cm^{-1}, respectively. From Figure 40 a higher intensity ratio (1735/1450) in the absorbance band representing carbonyl groups (C=O) i.e. 3.8 can be seen in heat treated amber compared to the UV treated amber which was of 1.8. This is attributed to the increase in concentration of the carbonyl groups due to formation of carboxylic acids. UV treated amber (royal blue colour in the Figure 40) shows similarities with the pristine amber . This may show that the Baltic amber is not sensitive to UV light. There is also evidence of changes in the ester groups that are assigned to the Baltic shoulder. This includes decrease in the C-O group located between 1250-1150 cm^{-1}. There are also changes in the exocyclic methylene peaks at 2929, 1643 and 885 cm^{-1}, they decreased possibly due to oxidation or isomerization mechanism in the heated sample. Measurements of the ratio of C=C groups to CH_2 groups (I_{1646}/I_{1448}) for amber in UV and heated sample suggested degradation had taken place. A reduction in C=C group was measured in the heat treated sample with a 0.18 to 0.60 ratio. The ratios of intensities are demonstrated in the Bar chart shown in the Figure 41 shows the clear affects of heat on the amber.

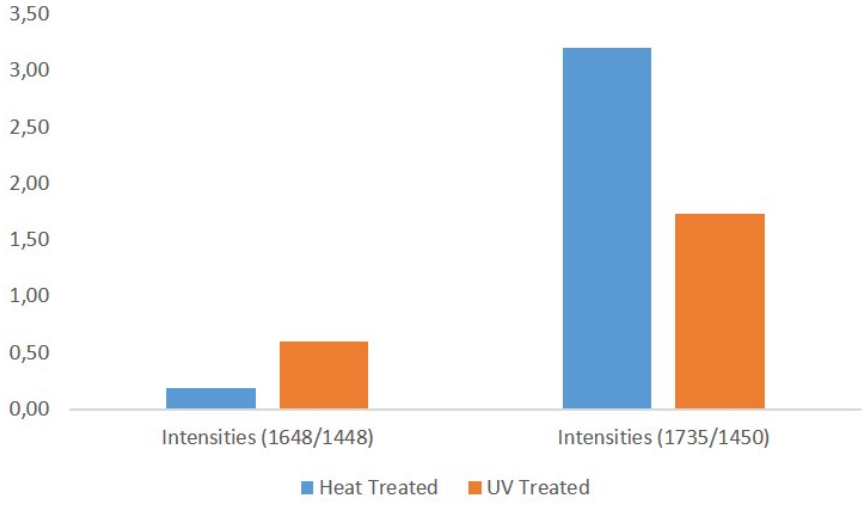

Figure 41: Comparison of intensities at (1646/1448) and (1735/1450) for Heat and UV treated amber samples

6.6 Section Conclusion

Both Raman and ATR-FTIR spectroscopies are effective and largely non-destructive techniques for the analysis of the amber. However, the bulk samples have to be flat to maintain a uniform contact with the underlying crystal in the ATR-FTIR holder. We could clearly identify the Baltic Shoulder in the FTIR spectra of the ambers from both the regions. The main peaks positioned at 715, 1447 and 1650 cm^{-1} in case of Raman and the presence of Baltic shoulder in FTIR spectra was in accordance with chemical profile of typical Baltic amber. The overlapping of the peaks in case of amber from Kaliningrad, Russia and Skelengen Vejers, Denmark inferred that the amber has come from the same source. Both the techniques helped reliably to distinguish between the Baltic from other classes of amber based on the chemical fingerprint. Furthermore, the intensity ratio between peaks 1447 and 1650 cm^{-1} in Raman spectra provided relative degree of maturity among all the ambers. The relative degree of maturity could arise from the number of years, the amber stayed in the environment. However, it could also indicate extreme whether conditions on one amber compared to the other. While using the data for age estimation, it should be noted that the absolute quantitative value of the age in not possible to estimate but rather a relative age can be stated when measuring a group of amber found within the same atmospheric conditions. By observing the 1640/1440 Raman band ratios, we identified the amber from Skelengen Vejers older from the amber of Kaliningrad. On the other hand, ATR-FTIR is a reliable technique for the detection and quantification of the degradation of the amber. The ATR-FTIR spectroscopy suggested that thermal ageing under ambient conditions had an impact on the amber and increase in the concentration of carbonyl groups was noted while ageing under UV-365 nm light either had no influence or acts slow to the reaction.

7 Pilot Study 4 Shaping the late Neolithic Stones: Tracing knapping tool remnants on flint

7.1 Overview

This study is about searching for traces of metal tool that was utilised during the production of late Neolithic Nordic flint daggers. Chipped stone tools are made by knapping, that is, hitting the raw material (rock) with a hammer in such a way that fragments with specific sizes and shapes are extracted from it. The chunk of rock from which the flakes are detached is called a core whereas the large flakes that are removed from the core are called blanks. Depending on the requirement of precision in knapping, there are different knapping processes that knappers employed such as direct percussion, indirect percussion and pressure flaking. In general, flint knapping involves striking a piece of flint with a hammerstone to produce sharp-edged tools and weapons. The force and angle of each blow determine the shape and size of the resultant fragments. Through subsequent refining, these fragments are transformed into functional tools like arrowheads, blades, and scrapers.

Studies were conducted in order to gain more insight regarding the production processes and types of tools used during production of late Neolithic stones. This is done by means of experimental flint knapping replicas', comparative macroscopic analysis and chemical analysis. The possibility of determining whether or not copper pressure-flaking tools were utilised to produce intricate shaped Late Neolithic flint daggers. It is possible that the analysis performed during this study will show that copper, or copper alloys were not only known and available but were tool of choice for production of flint, sharpening and re-sharpening in dagger production areas of Denmark. The aim of this research is to study experimental flint replicas that show traces of copper knapping tool or copper-tipped flaking tool. This is done by a two step methodology that was developed to identify the copper traces on the flint. The two step methodology involves identifying regions on the flint which appears to contain the metal left-overs using digital microscope. As a second step it involves conducting elemental analysis using scanning electron microscope with energy dispersive spectroscopy detector to identify the actual element. This was done on the experimental replicas of the daggers produced by copper knapping tools to search for copper traces.

7.1.1 Aims and Objectives

The aims and objectives are to test whether microchemical analysis is a viable technique to identify the type of knapping tool used to shape the experimental flint replicas. The second part of the study aims at testing the method of identifying the knapping tool by trace element analysis and question the reliability of this technique. For this purpose heat treatment on experimental flint replicas is performed and analysed again to see if the trace remains even after the heat treatment. The aims and objectives of the technique

will be around following two points:

1. What kind of tools were used to produce flint experimental replicas by analysing surface of the experimental replicas?

2. Examining the surface of the heat treated flint experimental replica to check the authenticity of the methodology of the trace element analysis on ancient flint.

7.2 Methods

The flint and experimental replicas were each subjected to go through the analysis under the Andonstar ADSM302 digital microscope and SEM Zeiss Gemini Ultra55 Plus.

7.2.1 Sample Group

In total 35 experimental replicas were analysed using the digital microscope. The main criteria for analysing the replicas was the presence of perceived traces of copper on the surface, edge, or the sides. However, the traces may have been contaminated with trace elements or developed a patina. To account for this, obvious contamination spots on the samples were ignored and only marks that appeared to be copper from the perspective of flint knapping tool were considered.

From the initial analysis, 8 flint experimental replicas were selected for further analysis due to observation of potential metal tool traces on specific regions on the specimen and were selected for further analysis. Under the digital microscope, 10 of the selected experimental replicas exhibited traces what seemed like copper metal represented here with the IDs are as follows: R16, R5, R22, R24, R25, R29 and R32.

Each experimental replica was subjected to a full photographic analysis via digital microscope analysis which were consequently subjected to elemental analysis for further confirmation, or rejection.

7.3 Results and Observations

Here follows the visual representation of the experimental replicas. For the purpose of documentation, the specimen will be denoted by the IDs to correlate the specimen and its photographic analysis.

R16, the shiny trace was documented, having metal-like structure when brought under the digital microscope under zoom (1X, 4X). The possible trace is encircled with a mark of lead pencil, is clearly evident on the surface of the flint. The metal is engraved on the surface, very close to the cutting edge as shown by the digital microscope at 4X Zoom

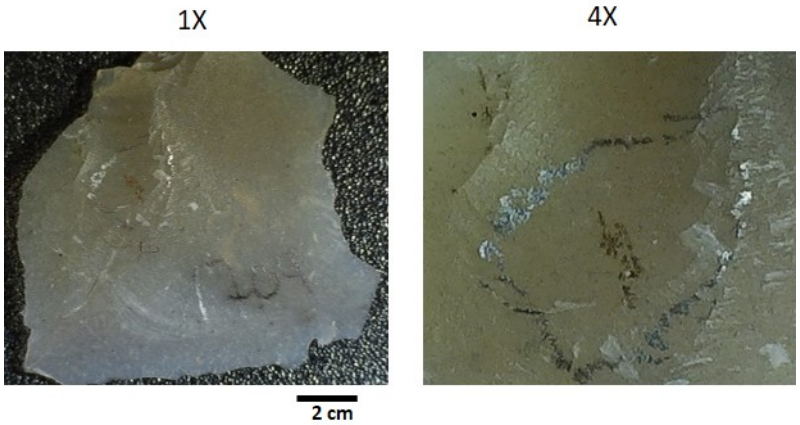

Figure 42: Experimental replica R16 of Late Neolithic flint tool knapped with copper knapping tool, photographic image with Digital Microscopy (By K. Saleem)

Figure 43: Experimental replica R5 of Late Neolithic Flint Tool knapped with copper knapping tool, photographic image with Digital Microscopy (By K. Saleem)

shown in Figure 42.

R5, the potential metal was photographically documented exhibiting gold luster when brought under the LED powered digital microscope under several zoom settings (1X, 2X, 4X). The metal trace shows the typical shiny behaviour reflecting the light and is found in the crevice in the central region of the surface. The trace can be more clearly seen when the flint is held vertically under the microscopy at 4X Zoom, Figure 43. Only R16 and R5 are included in the results section of the photographic analysis, the rest of the specimen along with their description are in the Index Section. The other specimen which also showed traces were R19 (Index Section, Figure 63), R22, R24, R25, R29, R31, R50 and R32. They are not included because their results were also similar and would not have provided any new knowledge.

7.4 Trace Analysis

The comparative analysis of photographic documentation for the traces helps draw parallels between experimental replicas. The trace remains on the specimen are a result of subsequent production steps elaborated further in the following part.

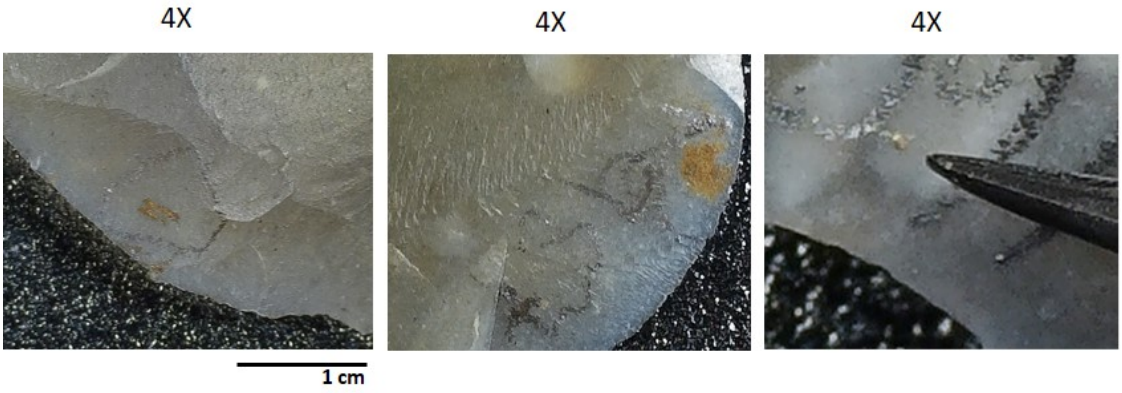

Figure 44: Experimental replicas left to right R22, R25 and R32 photographic image with Digital Microscopy (By K. Saleem)

The traces are left on the edge or close to the edge during the step of edge tapering or sharpening of the blade as a result of pressure removal techniques. The metallic traces often run horizontally across the blade and are short, present few millimetres inside the cutting edge due to the flake removal from the surface of the flint. This is unambiguously seen on the flint R22, R25 and R32 documented by the digital microscope shown in Figure 44.

The experimental replicas showed the so called "Step fracture" which occurs during the unsuccessful thinning of the flake causing a sudden step on the face of the flint. Rather

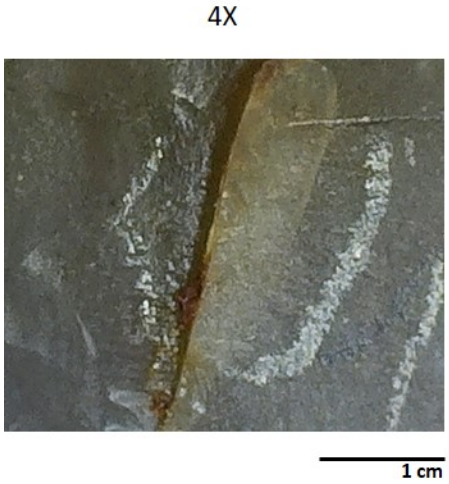

Figure 45: Experimental replica R5, photographic image with Digital Microscopy, showing step fracture (By K. Saleem)

than having a smooth surface, a step fracture has grown thicker as a result of subsequent thinning attempts during the preparation stages. Figure 45 presents such a step fracture which could not be removed and stacked the lustrous copper traces along the edge of the step, which kept piling up in subsequent steps during flaking of the flint.

7.5 Chemical Analyses

From the initial photographic analysis of 10 experimental flint replicas, several flint samples were short-listed which seemed appropriate to possess the metallic traces on the surface. The elemental analysis was carried out using SEM Zeiss Gemini Ultra55 Plus in Technical Faculty CAU, Kiel, more information in Section 3.5.2.

10 of the selected experimental replicas exhibited traces what seemed like copper metal as follows: R16, R5 , R19, R22, R24, R25, R50, R29, R32 out of 36 replicas. Each experimental replica was subjected to a full microscopic analysis via SEM electron imaging and SEM EDX analysis, including microscopic documentation of metal traces, with EDX spectrum and elemental mapping.

The chemical analysis starts with replica R16. The initial step in detecting the copper traces on R16 involved imaging the surface topography of the specimen under electron imaging mode. As shown in the Figure 46, the surface profile is recorded as a contrast between the regions at different heights as the reflections from the elevated regions are brighter. In the electron image certain regions appear brighter, corresponding to the original flaked surface of the flint, corresponding to Si and O as documented by the elemental mapping. Chemically, flint is a fine grained sedimentary rock made up of SiO_2

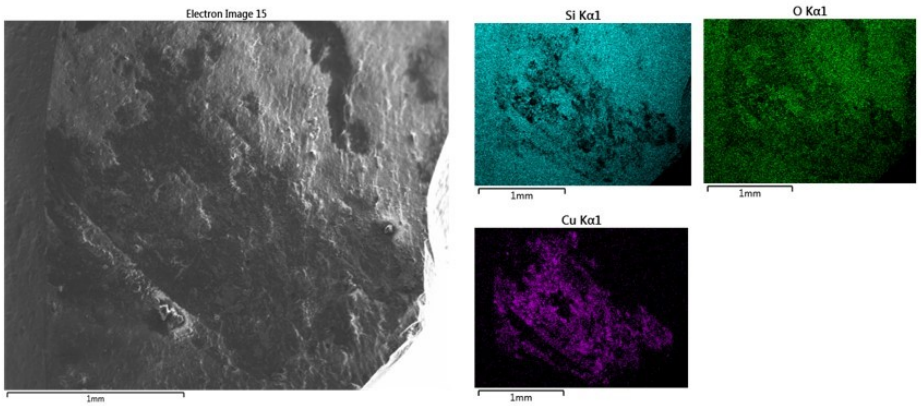

Figure 46: SEM EDX elemental mapping on experimental replica R16 showing the regions of Cu traces on flint (By K. Saleem)

with compositional proportions 1:2 (Si:O). The smooth regions with signals of Si and O in the elemental map are coming from SiO_2, as also confirmed with the help of the EDX spectrum, in Figure 47. As evident in the digital photographic image as well in the chemical analysis of R16 and R19 the copper remains from the knapping tool penetrated inside the surface, supposedly during flaking step are detectable.

The specimen R19 was documented with electron image demonstrating the surface topography of the flint experimental replica as shown in the Figure 47(a). The point measurement mode was used to check the elemental signals in various areas within region of interest. Out of 7 points measurements recorded, none had shown the copper trace signal, for a reference one of the recorded spectrum (spectrum 67) is also shown. The EDX spectrum only showed signals from flint and no metallic trace elements were detected. The digital image shows a brownish spot (Figure 48) is a false positive, even though it looked like copper metal trace.

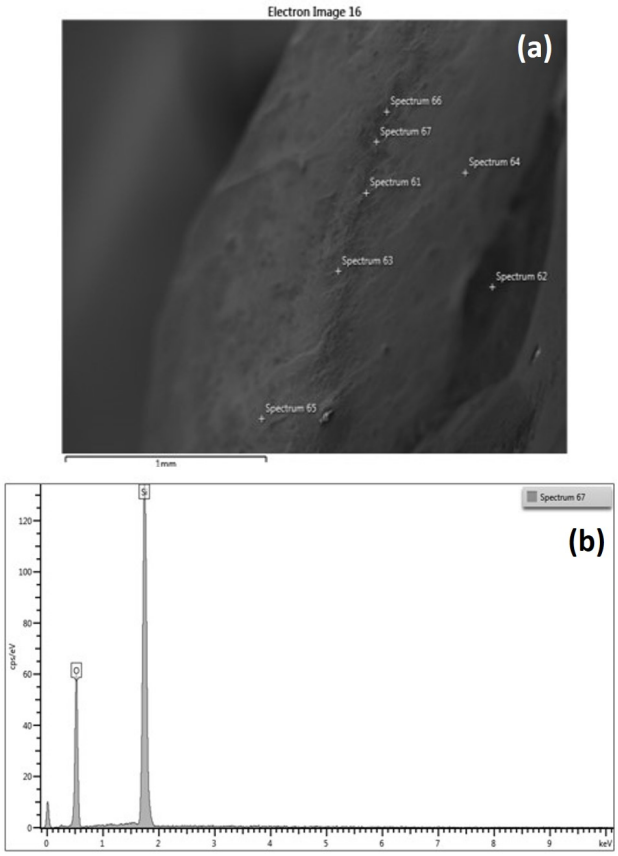

Figure 47: (a) SEM electron image on experimental replica R19 and (b) EDX spectrum showing atomic percentages of the detected elements on the right (By K. Saleem)

Further moving on with chemical analysis of specimen R50 The point measurement mode was used to check the elemental signals in various areas within the region of interest. Out of 4 points measurements recorded, none had shown the copper trace signal. The EDX spectrum only showed signals from flint and no metallic trace elements were detected. The digital image shows a brownish spot which is a false positive, even though it looked like a copper metal traces.

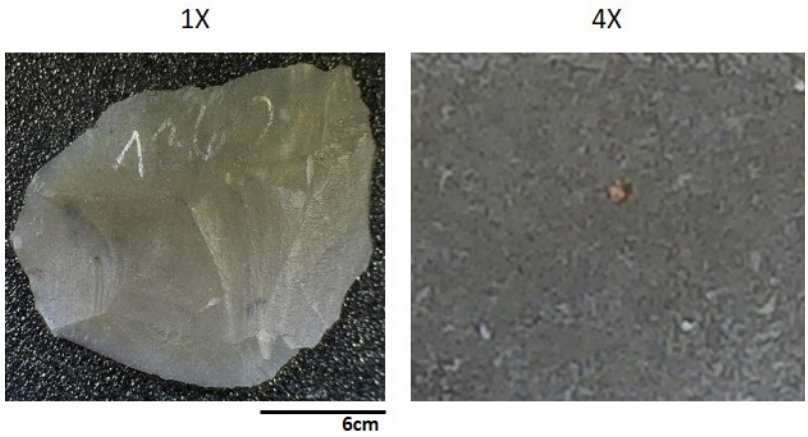

Figure 48: Experimental replica R50 of Late Neolithic Flint Tool knapped with copper knapping tool, photographic image with Digital Microscopy (By K. Saleem)

The electron image of the specimen R29 that was placed vertically inside the SEM chamber documents the surface topography as a results of the contrast between the features as shown in the Figure 50. The elemental map was recorded from the selected area marked within the rectangle to minimize the signals from the unresolved flatter regions of the specimen. The presence of SiO_2 on comparatively smoother region on the side is evident, as also confirmed by the EDS spectrum. The elemental map shows the presence of metallic copper ingrained within the selected region of analysis, which earlier showed sign of lustrous traces via photographic image (Figure 49).

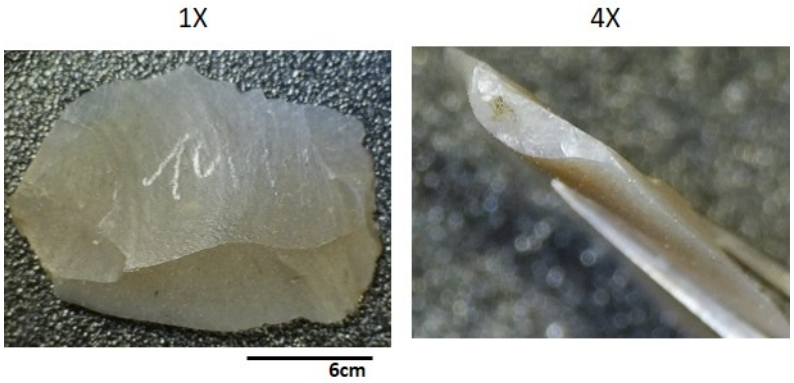

Figure 49: Experimental replica R29 of Late Neolithic Flint Tool knapped with copper knapping tool, photographic image with Digital Microscopy (By K. Saleem)

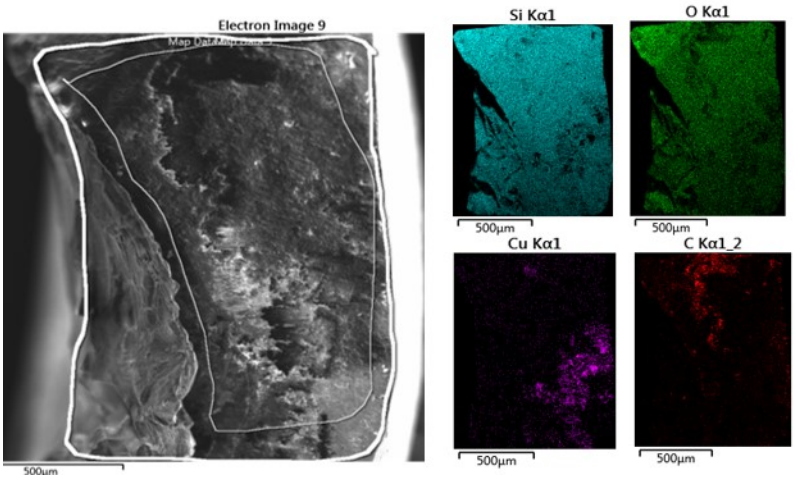

Figure 50: SEM-EDS elemental mapping on experimental replica R29 showing electron image on the left and corresponding elemental mapping on the right side (By K. Saleem)

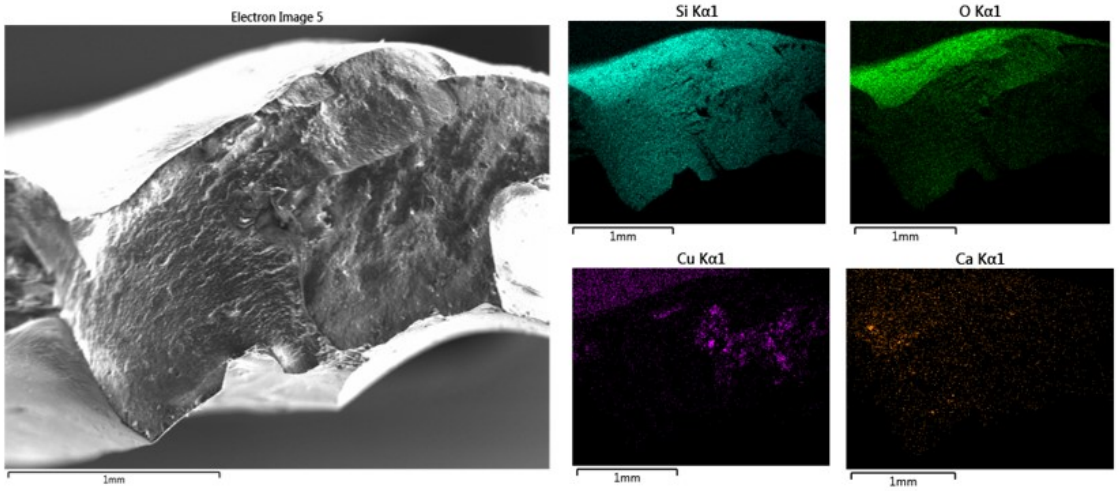

Figure 51: SEM EDS elemental mapping on experimental replica R51 showing electron image on the left and corresponding elements on the right (By K. Saleem)

Similarly, SEM EDS elemental mapping conducted on experimental replica number R51 confirmed the presence of copper traces on the regions documented by digital photographs. The image is displayed in the Figure 51 clearly showing the presence of copper metal traces.

7.6 Flint Sample Heat Treatment

This flint sample was heated to 600°C for 24 hours and at 600°C for 48 hours and analysed using SEM EDX before and after the experiment. The electron images are displayed in Figure 52 and shows the surface topography of flint before the heat treatment and after the heat treatment. Furthermore, the EDX point measurements from three areas on the flint were also recorded and are displayed in Table 10. The copper trace on the surface of the experiment flint replica is oxidised and the copper content is decreased. From the table it can be seen that the oxygen content is increased (pristine 23 at.%, 24 hours 64 at.% and 48 hours 83 at.%). One of the flint experimental replicas which showed traces of copper in photographic images were selected in this study. This experimental replica confirmed to have traces of copper via SEM EDS as well. The EDX elemental map recorded before and after the heat treatment shows that the oxidized copper partially fell from the surface after the heat treatment as displyed in Figure 53.

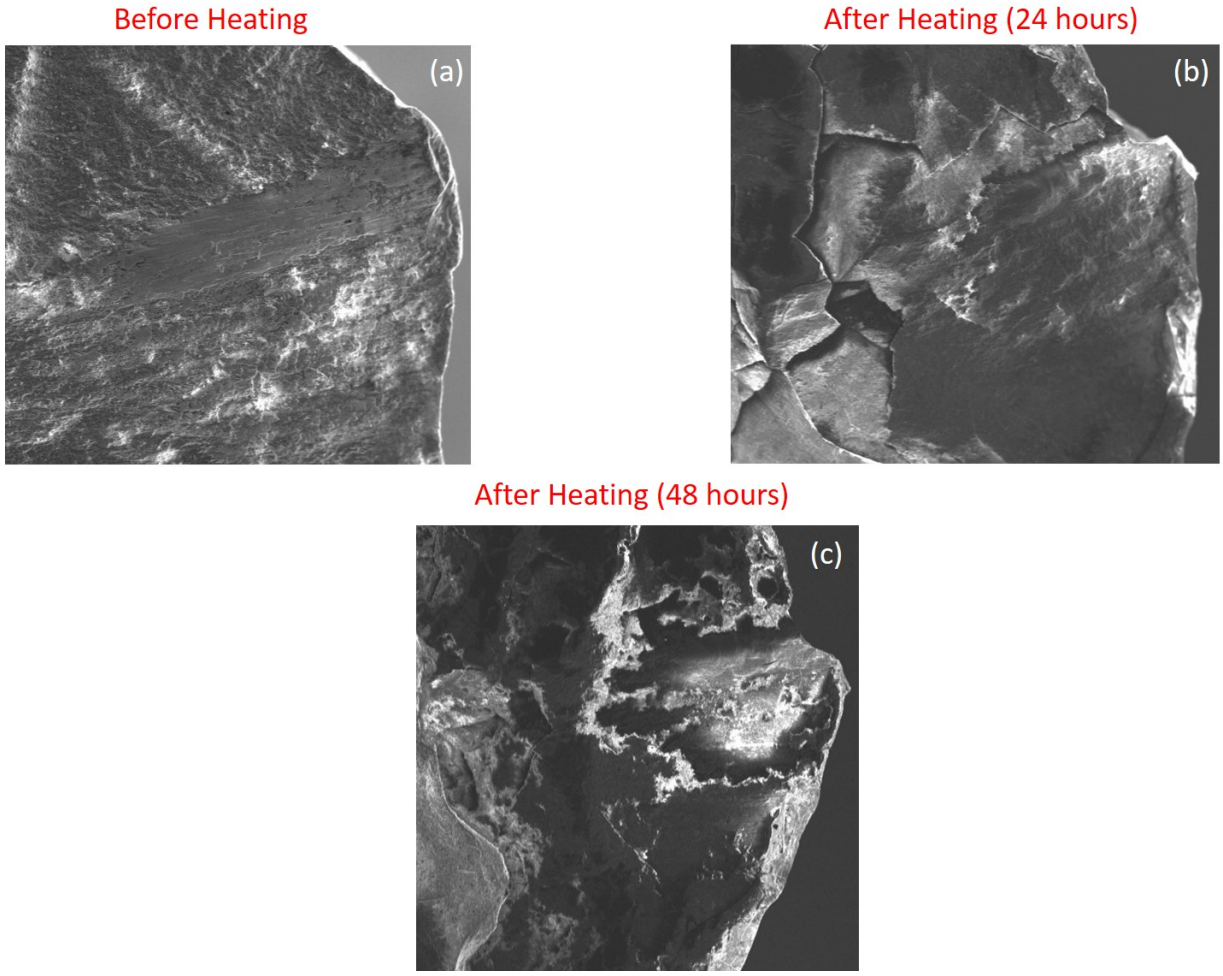

Figure 52: SEM electron images of heat treated flint at 600°C (a) before heating (b) after heating for 24 hours (c) after heating for 48 hours (By K. Saleem)

Table 10: SEM EDX point measurements before and after heating the flint experimental replica displayed in atomic percentage and averaged over three values

At.%	Before Heating	After Heating 24 Hours	After Heating 48 Hours
Cu	76 at.%	36 at.%	17 at.%
O	23 at.%	64 at.%	83 at.%

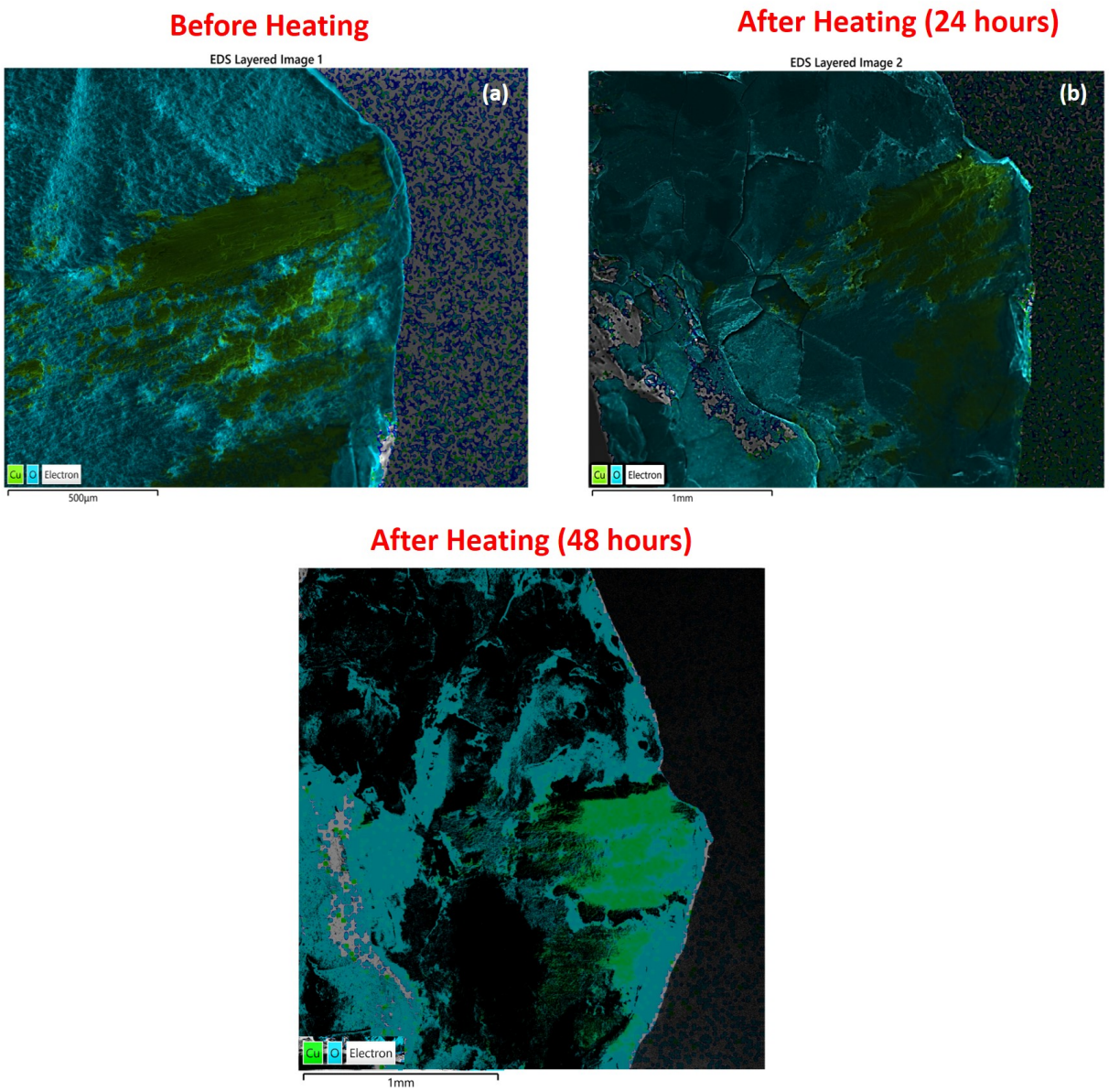

Figure 53: SEM EDX elemental map of experimental flint replica (a) before heating (b) after heating for 24 hours (c) after heating for 48 hours (By K. Saleem)

7.7 Section Conclusion

Bifacial experimental replicas imitating late Neolithic flint tools were analysed in this study. The bifacial tools were fabricated using the pressure flaking technique which created series of ridges along the edge with the tool. Besides creating ridges, it also leave the traces of the tool that was used to fabricate these flint samples. These elements can

serve as important indicator to identify the type of knapping tools available in the late Neolithic period. In the scope of this thesis, we successfully demonstrated the two step methodology to identify the remnants of knapping tool on the experimental replicas and the neolithic dagger. The methodology involved identifying the presence of traces by using the digital microscopy and in the second step confirming the chemical information of these trace elements using SEM EDS. The study also showed that it is important to not only rely on the digital microscopy results for the trace analyses because occasionally shiny dirt particles could give a false indication of the metal trace. So, a followed up analysis with SEM EDS can eliminate the possibility of false interpretations. Eventually, the copper traces were successfully identified in this study which confirmed that the copper knapping tool was used to shape the experimental replica. However, the second part of the study showed that the copper on the surface falls from the surface when it is oxidised. The archaeological flint is often cover with patina and quite possibly oxidises the copper traces on the surface as well due to environmental exposure. As a result the oxidised copper could fall from the surface. This brings us to the conclusion that care should be taken while making conclusions only on the basis of microchemial analyses. Where the presence of copper trace in microchemical analysis can confirm the usage of copper knapping tool but the absence of copper in the chemical analysis does not necessarily mean that copper knapping tool was not used to produce the flint.

8 Thesis Conclusion

The thesis work demonstrated attempts to answer various archaeological research questions on a plethora of artefacts and experimental replicas. It encompassed chronocultural history of the artefacts and also provided experimental evidence on identifying salient features and reliability of material science techniques. The connection between the population of East Baltic settlements and the Ostriv grave finds was tested. The metal analysis showed similarities in the production process, raw materials and similar stylistic attributes. Whereas, the properties and the suggestions about the choice of brass in medieval East Baltic and Ostriv cemetery population are documented. The study also showed the significance of materials analysis tools such as transmission electron microscopy, scanning electron microscopy and the focused ion beam for applications in archaeological items. The conclusions on the East Baltic and Ostriv artefacts pilot study are as follows:

a) Brass was the primary alloy of choice in the East Baltic and Ostriv artefacts, however, pure copper was also found attributed to the dezincification phenomenon.

b) The zinc content in Ostriv artefacts ranged between 8 to 20 at. %. Meanwhile, the zinc content in the brass artefacts of East Baltic was between 7 to 14 at at. %.

c) It was noted that the penannular brooches with the connected star-shaped terminals from Sambian Trentitten and Ostriv showed close stylistic and compositional attributes (Cu/Zn content as 87/11.5 and 88/11.2 at. %, respectively) providing an important evidence of the artefacts, which could be produced in the same region. But, we need some more archaeological arguments for those interpretations.

d) The variation in the copper and zinc ratios of 3-4 % are attributed to the complexities of brass production process in the medieval times and not a deliberate change.

e) Common origin of the populations is suggested based on the material analysis and stylistic commonalities. Also, evidence from archaeological studies are used in this conclusion, suggesting the historical Baltic tribes like Prussians, Curonians, Scalvians or Yatvingians interpreted as settlers (in Ostriv) and/or mercenaries during the reign of Yaroslav the Wise in the 11th Century.

Extending the usage of material analysis techniques, the pilot study on the late Neolithic copper axe was also instrumental. It helped understand the production mechanism of the primitive low flanged axes from South Scandinavia. It also helped differentiate between the primary and secondary alterations on the axe by the help of the material analysis techniques. The corrosion layer and its constituents from the environment and the actual base alloy composition of the axe were established. And via experimental replicas it was shown that the axe consisted of silver enriched regions on the surface because of the selective dissolution of copper. The conclusions are listed in following points:

a) Transmission electron microscopy along with scanning electron microscopy helped distinguish between the surface containments from the original base alloy. The analysis showed a ring of copper oxide matrix with silver microparticles and core of fahlore type copper (established via initial analysis).

b) Corrosion experiment in the Hemic Acid showed selective dissolution of copper from the surface of Cu/Ag alloy. Which left a silver enriched surface regions.

c) From the silver whiskers, copper depleting phenomenon reported by recent literature and also the corrosion experiment, evidence showed secondary alterations on the surface for copper depleted and silver enriched regions.

d) The primitive low flanged axe from South Scandinavia contains silver on the surface originating from the primary fahlore type copper ore used to cast the axe which contains silver as an impurity.

e) Hence, it was demonstrated that primitive low flanged axes do not possess decorative silver surface layer.

Similarly, material analysis approach proved instrumental in organic archaeological samples as well. The FTIR and Raman spectroscopy successfully helped identify the chemical features of Baltic amber. It helped compare the Baltic amber from different regions of Europe (Russia, Denmark and Sicily). And helped identify differences in chemical structures. Moreover, the changes arising from the paleoclimatic conditions were demonstrated via laboratory experiments. The changes in the chemical structure of the Baltic amber were observed and noted when subjected to heat experiments. Hence, it was shown how relative age of the amber can be chemically estimated.

Applying material analysis technique further in an attempt to identify knapping tools by trace element analysis, flint experimental replicas were analysed. It was demonstrated that the metal trace elements can be identified on the surfaces of flint. It was demonstrated by using the photographic imaging and chemical analysis via SEM EDS. The study also contained testing the reliability of the technique on the ancient artefacts. It was shown via experimental replica heat treatment that there is a possibility of oxidised metal traces to not be detected on the artefacts. As the oxidised metal traces can fall from the surface of the flint items and the metal might not be detected even if the metallic knapping tools were used on it. Hence, the chemical analysis can confirm the presence of copper knapping tool used but its absence does not directly mean that the copper tool was not used. Furthermore, care should also be exercised on false positives from the photographic imaging of the flint as well.

Where materials analysis techniques helped identify important features in archaeological research, it should be noted that the number of artefacts analysed should be increased from East Baltic and Ostriv population, Neolithic copper axe, including more amber from

non-Baltic regions and flint from archaeological excavations. This work provides a good basis for further applications of materials science techniques in the field of archaeology based on the demonstrated methodologies involving transmission electron microscopy, focused ion beam, fourier transform infrared spectroscopy and Raman spectroscopy.

9 Summary

This work provides an interdisciplinary approach of material science analysis and field of archaeology. Microchemical analysis and stylistic analysis has been carried out on heritage materials which are correlated to the stylistic attributes as well. The methodology for the comparative analysis of the metallic artefacts involved selecting chrono-culturly identical artefacts by tracing similarities and differences in raw materials, production mechanism, material properties etc. Hence, a detailed analysis of the stylistic attributes followed by the microchemical analysis was used in the scope of this thesis. In this study, artefacts from East Baltic locations, Central Ukraine and South Scandinavia are analysed. The timeline of the artefacts are from 2200 BC to 1200 AD. The primary objective of the research is to provide a framework for material analysis using advanced characterisation methods on archaeological objects. The research questions and methods used differed for each pilot study included in this thesis. The analysis on the Ukrainian and East Baltic artefacts was carried out in order to find origins of the population buried at Central Ukrainian cemetery. Whereas, the Neolithic copper axe from the South Scandinavia was examined to identify whether a decorative silver layer existed on the surface of the axe. The axe belonged to the Pile type hoard and dated back to 2200 BC. The flint samples were also part of this thesis work which belonged to South Scandinavia as well. The research on the flint was to document trace metals on the surface of the flint and to link it with the material of the knapping tool used to shape the flint. Lastly, organic specimen (amber) were also included in this study. The analysis on the amber was an attempt to differentiate Baltic amber chemically and compare the relative ages of the amber. For the analysis of the metal artefacts transmission electron microscopy was used first the first time on East Baltic and Ostriv artefacts. Transmission electron microscopy in combination with scanning electron microscopy was used on Neolithic copper axe as well. Ion milling was used to produce extremely minimally invasive specimen for TEM analysis. Scanning electron microscopy was also used to analyse flint samples. In the scope of this thesis, the main findings showed a cross-correlation between the artefacts from the East Baltic and Central Ukrainian populations. The Neolithic copper axe's silver enrichment on the surface is attributed to the corrosion phenomenon and a secondary alteration. The traces on the flint samples are successfully analysed. Chemical analysis is a viable tool to identify the trace on flint, however, not finding the traces does not directly correspond to unavailability of metal knapping tools. And lastly, the amber artefacts showed differences in chemical finger prints of Baltic amber which showed further changes in the spectra when degraded.

The results imply that comparative analysis based on typological analysis and microchemical analysis provided strong basis of common origins of East Baltic and Ostriv population. Hence, the migrants buried at Ostriv cemetery possibly migrated from East Baltic regions and settled in Central Ukraine during 11-12th AD. The results of the Neolithic copper axe imply that the axe was not imported and instead produced locally without silver decoration layer. Some of the limitations are also encountered when analysing archaeological artefacts. It should be noted that dimensional limits, keep-

ing the process non-destructive and differentiating between the intrinsic and extrinsic corrosion compounds were the challenges faced during the research work. The modern analytical techniques and sample preparation method demonstrated in this thesis work can open new viewpoints on the interpretation of historic events and could be refereed during future studies.

11 Future Prospects

The outcomes of the chemical and stylistic evaluations of artifacts originating from the Ostriv and East Baltic regions exhibit promising prospects, contributing to the ongoing comprehension of the populations buried at Ostriv. However, to enhance the validity of the hypotheses pertaining to connection of Baltic regions with the Ostriv population, a more extensive analysis of the artifacts is proposed. Aligning with the methodological framework of this thesis, further investigations via artifact comparison are recommended. It is suggested that additional samples be subjected to analysis, from both the Prussian Collection and the Ostriv region, in the context of future research endeavors.

In this regard, a new series of 10 samples, represented by fragments extracted from the artifacts, have been received from the Ostriv (Ukraine) region. This collection of artifacts encompasses a diverse array, including ring brooches, penannular brooches with connected star-shaped terminals, spiral neck rings, bracelets, and cross-shaped flat fibula. Correspondingly, a compilation of samples originating from the East Baltic regions (Prussian Collection) has been collected to facilitate a thorough comparative analysis of both material and stylistic attributes further. These East Baltic samples, sourced from a variety of 22 artifacts obtained from the Olsztyn Museum, signify an ancient Prussian Collection, originating from the Polish and Sambian sides. These pieces, which were not transported to Berlin during the years 1943-44, exhibit remarkable stylistic commonalities with the artifacts retrieved from Ostriv, thereby furnishing a sound foundation for a comprehensive comparison opportunity of stylistic and chemical composition analysis.

Expanding the analytical research directed towards the Neolithic Eskilstorp Axes from Sweden, specifically targeting the inquiry regarding the presence of a decorative coating on this copper axe. A suggestion to chemically study a second axe has been put forth. Belonging to the Pile type hoard, akin to the axes studied within the scope of this thesis, this particular axe also dates back to 1800-2200 BC. Preliminary metallographic findings reveal the existence of a copper core surrounded by a matrix of corroded copper enriched with silver. The forthcoming materials analysis of this new axe stands to increase the number of chemically assessed axes from the Pile type hoard, thereby fortifying the hypotheses advanced within the context of this thesis through the utilization of complementary material analysis techniques. The hypothesis described the presence of silver in the matrix as originating from the copper ore used to cast the axe and resulting on the surface as a result of selective dissolution of the copper from the surface leaving silver enriched surface.

In conclusion, the ongoing investigation into artifacts from the Ostriv and East Baltic regions holds promise, necessitating the continued expansion of sample analyses. The assessment of artifacts not only advances our understanding of ancient populations buried in central Ukrainian region but also underscores the significance of cross-analysis of material and stylistic attributes methodology further in the archaeological research. Furthermore, the analyses of the surface of the axe will increase the number of axes analysed from

the pile type hoard which will also serve to reach more concrete conclusions about the category of the axes.

References

[1] Luc Robbiola and Richard Portier. A global approach to the authentication of ancient bronzes based on the characterization of the alloy-patina-environment system. *Journal of Cultural Heritage*, 7(1):1–12, 2006.

[2] Roman Shiroukhov, Vyacheslav Baranov, Vsevolod Ivakin, Artem Borysov, Claus Von Carnap-bornheim, Lorenz Kienle, John Meadows, Khurram Saleem, Ulrich Schuermann, Žydrūnė Miliauskienė, Artem Borysov, Claus Von Carnap-bornheim, Lorenz Kienle, Ben Krause-kyora, Khurram Saleem, Ulrich Schuermann, Justina Kozakaitė, and Žydrūnė Miliauskienė. Baltic Migrants in the Middle Dnipro Region : A Comparative Study of the Late Viking Age Archaeological Complex of Ostriv , Ukraine Baltic Migrants in the Middle Dnipro Region : A Comparative Study of the Late Viking Age Archaeological Complex of Ostriv ,. *Medieval Archaeology*, 66(2):221–265, 2022.

[3] Paul T. Craddock. The composition of the copper alloys used by the Greek, etruscan and Roman civilisations. 2. The Archaic, Classical and Hellenistic Greeks. *Journal of Archaeological Science*, 4(2):103–123, 1977.

[4] Wenli Zhou, Marcos Martinón-Torres, Jianli Chen, Haiwang Liu, and Yanxiang Li. Distilling zinc for the Ming Dynasty: The technology of large scale zinc production in Fengdu, southwest China. *Journal of Archaeological Science*, 39(4):908–921, 2012.

[5] F. J. Fortes, M. Cortés, M. D. Simón, L. M. Cabalín, and J. J. Laserna. Chronocultural sorting of archaeological bronze objects using laser-induced breakdown spectrometry. *Analytica Chimica Acta*, 554(1-2):136–143, 2005.

[6] C. Deeb, P. Walter, J. Castaing, P. Penhoud, and P. Veyssière. Transmission electron microscopy (TEM) investigations of ancient Egyptian cosmetic powders. *Applied Physics A: Materials Science and Processing*, 79(2):393–396, 2004.

[7] Klaas Jan Van Den Berg, Maude Daudin, Ineke Joosten, Bill Wei, Rachel Morrison, and Aviva Burnstock. A comparison of light microscopy techniques with scanning electron microscopy for imaging the surface cleaning of paintings. *(th International Conference on NDT of Art*, (May):1–11, 2008.

[8] Otilia Mircea, Ion Sandu, Viorica Vasilache, and Ioan Gabriel Sandu. A study on the deterioration and degradation of metallic archaeological artifacts. *International Journal of Conservation Science*, 3(3):179–188, 2012.

[9] Hui Li, Xuan Wang, and Yong Zhu. Identification Characteristics for Amber and its Imitation. *Proceedings of the 5th International Conference on Information Engineering for Mechanics and Materials*, 21(Icimm):483–488, 2015.

[10] Iana Verkhovskaia and Viktor Prokopenko. Raman scattering spectra of amber. *E3S Web of Conferences*, 164:1–7, 2020.

[11] D. Syvilay, X. S. Bai, N. Wilkie-Chancellier, A. Texier, L. Martinez, S. Serfaty, and V. Detalle. Laser-induced emission, fluorescence and Raman hybrid setup: A versatile instrument to analyze materials from cultural heritage. *Spectrochimica Acta - Part B Atomic Spectroscopy*, 140(December):44–53, 2018.

[12] Francesca Lionetto, Roberta Del Sole, Donato Cannoletta, Giuseppe Vasapollo, and Alfonso Maffezzoli. Monitoring wood degradation during weathering by cellulose crystallinity. *Materials*, 5(10):1910–1922, 2012.

[13] David A Scott and David A Scott. Artefacts. 50(3):179–189, 2020.

[14] Melania Di Fazio, Anna Candida Felici, Fiorenzo Catalli, and Caterina De Vito. Microstructure and chemical composition of Roman orichalcum coins emitted after the monetary reform of Augustus (23 B.C.). *Scientific Reports*, 9(1):1–11, 2019.

[15] L. Beck, S. Bosonnet, S. Réveillon, D. Eliot, and F. Pilon. Silver surface enrichment of silver–copper alloys: a limitation for the analysis of ancient silver coins by surface techniques. *Nuclear Instruments and Methods in Physics Research Section B: Beam Interactions with Materials and Atoms*, 226(1-2):153–162, 2004.

[16] Ricardo Fernandes, Bertil J.H. van Os, and Hans D.J. Huisman. The use of Hand-Held XRF for investigating the composition and corrosion of Roman copper-alloyed artefacts. *Heritage Science*, 1(1):1–7, 2013.

[17] W. Mohamed and S. Darweesh. Ancient egyptian black-patinated copper alloys. *Archaeometry*, 54(1):175–192, 2012.

[18] Geraldine Marchand, Elodie Guilminot, Stéphane Lemoine, Loretta Rossetti, Michelle Vieau, and Nicolas Stephant. Degradation of archaeological horn silver artefacts in burials. *Heritage Science*, 2(1):1–7, 2014.

[19] L. Beck, S. Bosonnet, S. Réveillon, D. Eliot, and F. Pilon. Silver surface enrichment of silver–copper alloys: a limitation for the analysis of ancient silver coins by surface techniques. *Nuclear Instruments and Methods in Physics Research Section B: Beam Interactions with Materials and Atoms*, 226(1-2):153–162, 2004.

[20] F. Mathis, S. Descamps, D. Robcis, and M. Aucouturier. Original surface treatment of copper alloy in ancient Roman Empire: Chemical patination on a Roman strigil. *Surface Engineering*, 21(5-6):346–351, 2005.

[21] J. Muller, G. Lorang, E. Leroy, B. Laik, and I. Guillot. Electrochemically synthesised bronze patina: Characterisation and application to the cultural heritage. *Corrosion Engineering Science and Technology*, 45(5):322–326, 2010.

[22] M. Aucouturier, F. Mathis, D. Robcis, J. Castaing, J. Salomon, L. Pichon, E. Delange, and S. Descamps. Intentional patina of metal archaeological artefacts: Non-destructive investigation of Egyptian and Roman museum treasures. *Corrosion Engineering Science and Technology*, 45(5):314–321, 2010.

[23] Giuseppe Capobianco, Adriana Sferragatta, Luca Lanteri, Giorgia Agresti, Giuseppe Bonifazi, Silvia Serranti, and Claudia Pelosi. μXRF mapping as a powerful technique for investigating metal objects from the archaeological site of ferento (Central Italy). *Journal of Imaging*, 6(7):1–17, 2020.

[24] Ellery Frahm. Applications in Archaeology. *Encyclopedia of Global Archaeology*, pages 6487–6495, 2009.

[25] Lee Sharon, Younan Hua, Siping Zhao, and Zhiqiang Mo. Studies on electron penetration versus beam acceleration voltage in energy-dispersive X-ray microanalysis. *IEEE International Conference on Semiconductor Electronics, Proceedings, ICSE*, pages 610–613, 2006.

[26] Bogdan Constantinescu, Viorel Cojocaru, Roxana Bugoi, and Alexandru Sasianu. SOME METALLURGICAL ASPECTS OF ANCIENT SILVER COINS DISCOVERED IN romania - original and imitations. *2nd International Conference Archaeometallurgy in Europe (Aquileia)*, (January 2009), 2007.

[27] W. Mohamed and S. Darweesh. Ancient egyptian black-patinated copper alloys. *Archaeometry*, 54(1):175–192, 2012.

[28] Steffen Orso. Structural and mechanical investigations of biological materials using a Focussed Ion Beam microscope. pages 13–58, 2005.

[29] E. Vindel, J. García, C. Gumiel, V. López-Acevedo, and M. Hernando. The Contribution of Transmission Electron Microscopy (TEM) to Understanding Pre-Columbian Goldwork Technology. *Archaeometry*, 60(2):342–349, 2018.

[30] Marcus A. Roxburgh and Bertil J.H. Van os. A Comparative Compositional Study of 7th- to 11th-Century Copper-Alloy Pins from Sedgeford, England, and Domburg, the Netherlands. *Medieval Archaeology*, 62(2):304–321, 2018.

[31] Vanda Morton. *Brass from the Past: Brass made, used and traded from prehistoric times to 1800: Appendix Metallurgical tables relevant to individual chapters.* 2019.

[32] Ewelina A. Mińta, Ryszard Diduszko, Aneta M. Gójska, Bartosz Kontny, Adrianna Łozinko, Dariusz Oleszak, and Grzegorz Żabiński. Material description of a unique relief fibula from Poland. *Archaeological and Anthropological Sciences*, 11(3):973–983, 2019.

[33] Ian Freestone, Nigel Meeks, Margaret Sax, and Catherine Higgitt. The Lycurgus Cup — A Roman nanotechnology. *Gold Bulletin*, 40(4):270–277, 2007.

[34] Andrey Drozdov, Maxim Andreev, Maxim Kozlov, Dmitriy Petukhov, Sergey Klimonsky, and Claudio Pettinari. Lycurgus cup: the nature of dichroism in a replica glass having similar composition. *Journal of Cultural Heritage*, 51:71–78, 2021.

[35] Stavros Nicolopoulos, Partha P. Das, Pablo J. Bereciartua, Fotini Karavasili, Nikolaos Zacharias, Alejandro Gómez Pérez, Athanassios S. Galanis, Edgar F. Rauch, Raúl Arenal, Joaquim Portillo, Josep Roqué-Rosell, Maria Kollia, and Irene Margiolaki. Novel characterization techniques for cultural heritage using a TEM orientation imaging in combination with 3D precession diffraction tomography: a case study of green and white ancient Roman glass tesserae. *Heritage Science*, 6(1):1–12, 2018.

[36] A. El Warraky, H. A. El Shayeb, and E. M. Sherif. Pitting corrosion of copper in chloride solutions. *Anti-Corrosion Methods and Materials*, 51(1):52–61, 2004.

[37] T H E Characterization, O F A Corroded, Bronze Statue, A Study, O F The, and Degradation Phenomena. of Conservation Science the Characterization of a Corroded Egyptian Bronze Statue and a Study. 2(2):95–108.

[38] Cem Zeren. Using Raman spectroscopy of counterfeit amber examinations. (February), 2016.

[39] S. Siano, L. Bartol, A. A. Mencaglia, M. Miccio, and J. Agresti. Use of neutron diffraction and laser-induced plasma spectroscopy in integrated authentication methodologies of copper alloy artefacts. *Nuovo Cimento della Societa Italiana di Fisica B*, 124(6):671–686, 2009.

[40] P. K.Andrew Hong and Ying Ying Macauley. Corrosion and leaching of copper tubing exposed to chlorinated drinking water. *Water, Air, and Soil Pollution*, 108(3-4):457–471, 1998.

[41] Bella H. Chudnovsky. Degradation of power contacts in industrial atmosphere: Silver corrosion and whiskers. *Electrical Contacts, Proceedings of the Annual Holm Conference on Electrical Contacts*, pages 140–150, 2002.

[42] Viorela Dan. Empirical and Non-Empirical Methods. (February), 2019.

[43] Daniel M. Seo, Paul D. Boyle, Roger D. Sommer, James S. Daubert, Oleg Borodin, and Wesley A. Henderson. Solvate structures and spectroscopic characterization of litfsi electrolytes. *Journal of Physical Chemistry B*, 118(47):13601–13608, 2014.

[44] Erez Ben-Yosef. Provenancing Egyptian metals: A methodological comment. *Journal of Archaeological Science*, 96(June):208–215, 2018.

[45] Tim Sandle. What the eye can see : Vision requirements for personnel who inspect injectable pharmaceuticals Author : Tim Sandle WHAT THE EYE CAN SEE : VISION REQUIREMENTS FOR PERSONNEL WHO INSPECT INJECTABLE PHARMACEUTICALS. (July), 2022.

[46] G. Bergerhoff, R. Hundt, R. Sievers, and I. D. Brown. The Inorganic Crystal Structure Data Base. *Journal of Chemical Information and Computer Sciences*, 23(2):66–69, 1983.

[47] P. Zhou, M. J. Hutchison, J. W. Erning, J. R. Scully, and K. Ogle. An in situ kinetic study of brass dezincification and corrosion. *Electrochimica Acta*, 229:141–154, 2017.

[48] Edward E. Igelegbai, Oluwaseun A. Alo, Adefemi O. Adeodu, and Ilesanmi A. Daniyan. Evaluation of Mechanical and Microstructural Properties of α-Brass Alloy Produced from Scrap Copper and Zinc Metal through Sand Casting Process. *Journal of Minerals and Materials Characterization and Engineering*, 05(01):18–28, 2017.

[49] Ernst Pernicka. Trace element fingerprinting of ancient copper: a guide to technology or provenance? *Metals in Antiquity, BAR INTERNATIONAL SERIES*, pages pp. 163–171, 1999.

[50] Christian Horn. Korta meddelanden A silver-coated copper axe from Late Neolithic Scania :. (January 2016), 2020.

[51] Christian Horn and Isabella C.C. von Holstein. Dents in our confidence: The interaction of damage and material properties in interpreting use-wear on copper-alloy weaponry. *Journal of Archaeological Science*, 81(May):90–100, 2017.

[52] Helle Vandkilde. Bronze age beginnings – A scalar view from the global outskirts. *Proceedings of the Prehistoric Society*, 85(August 2019):251–272, 2019.

[53] Heide W. Nørgaard, Ernst Pernicka, and Helle Vandkilde. *Correction: On the trail of Scandinavia's early metallurgy: Provenance, transfer and mixing (PLoS ONE (2019) 14: 7 (e0219574) DOI: 10.1371/journal.pone.0219574)*, volume 14. 2019.

[54] N. Souissi. Comparison of early stages of copper corrosion in sulfate, chloride, humic and soil media. *Surface Engineering and Applied Electrochemistry*, 49(1):73–77, 2013.

[55] S. Arnoldussen, D. J. Huisman, B. van Os, B. Steffens, L. Theunissen, and L. Amkreutz. A not so isolated fringe: Dutch later prehistoric (c. 2200 BCE-AD 0) bronze alloy networks from compositional analyses on metals and corrosion layers. *Journal of Archaeological Science: Reports*, 46(October):103684, 2022.

[56] V. Orfanou and Th Rehren. A (not so) dangerous method: pXRF vs. EPMA-WDS analyses of copper-based artefacts. *Archaeological and Anthropological Sciences*, 7(3):387–397, 2015.

[57] D. B. Short, P. Badger, A. Lorenzi, B. Mentzer, H. Bearer, P. S. Graves, J. V. Harris, K. E. Mahoney, A. M. Schwaderer, C. M. Shennan, A. Siters, and C. Warner. Fast food premium toys as a significant source of lead and chromium to the environment. *Journal of Toxicology and Environmental Health Sciences*, 8(7):68–75, 2016.

[58] J. O. Grimalt, B. R.T. Simoneit, P. G. Hatcher, and A. Nissenbaum. The molecular composition of ambers. *Organic Geochemistry*, 13(4-6):677–690, 1988.

[59] Beata Naglik, Maja Mroczkowska-Szerszeń, Magdalena Dumańska-Słowik, Lucyna Natkaniec-Nowak, Przemysław Drzewicz, Paweł Stach, and Grażyna Żukowska. Fossil resins–constraints from portable and laboratory near-infrared raman spectrometers. *Minerals*, 10(2), 2020.

[60] Ivana Angelini and Paolo Bellintani. The use of different amber sources in Italy during the Bronze Age: new archaeometric data. *Archaeological and Anthropological Sciences*, 9(4):673–684, 2017.

[61] W. Winkler, E. Ch Kirchner, A. Asenbaum, and M. Musso. A Raman spectroscopic approach to the maturation process of fossil resins. *Journal of Raman Spectroscopy*, 32(1):59–63, 2001.

[62] Yvonne Shashoua, Mai Britt Lund Degn Berthelsen, and Ole Faurskov Nielsen. Raman and ATR-FTIR spectroscopies applied to the conservation of archaeological Baltic amber. *Journal of Raman Spectroscopy*, 37(10):1221–1227, 2006.

[63] J. Jehlička, P. Vítek, H. G.M. Edwards, M. Hargreaves, and T. Čapoun. Rapid outdoor non-destructive detection of organic minerals using a portable Raman spectrometer. *Journal of Raman Spectroscopy*, 40(11):1645–1651, 2009.

[64] Joseph B. Lambert, Jorge A. Santiago-Blay, and Ken B. Anderson. Chemical signatures of fossilized resins and recent plant exudates. *Angewandte Chemie - International Edition*, 47(50):9608–9616, 2008.

[65] Herant Khanjian, Michael Schilling, and Jeff Maish. FTIR and PY-GC/MS Investigation of Archaeological Amber Objects From the J. Paul Getty Museum. *e-Preservation Science*, 10:66–70, 2013.

[66] Inez Dorothé, Van Der Werf, Daniela Fico, Giuseppe Egidio, De Benedetto, and Luigia Sabbatini. The molecular composition of Sicilian amber . *Microchemical Journal*, 125:85–96, 2016.

10 Activities and Contributions

-Contribution in Electron Microscopy Conference Berlin: Analytical TEM Methods for Neolithic Materials (2019).

-Sankt Peter-Ording excursion-Amber samples collection by the shores, 20th Jan (2020).

-Retreats-Schloss Gottorf-identification of interrelated subprojects within Subclusters and over arching ROOTS project-framework for inter and intra subclusters communication (2020-2022).

-Organisation of phD Teaching on Material Science Analysis Techniques (2020-2021) .

-Differences and similarities in material of East Baltic and Ukrainian cemetery artefacts from Medieval period using electron microscopy-Preliminary results of the project were presented at the European Association of Archaeologists (EAA) 2021.

-Contribution in Electron Microscopy Conference Vienna: Comparative Material Analysis on Vikings age brass ornaments by TEM and SEM (2021).

-Three Workshop-Material Science Analysis-Theoretical presentations and physical tour to the laboratories (TEM, SEM, XRD, Raman, FIB) (2020-2022).

-Focus Group Material Science Analysis (FGMSA I to VII)- Seven sessions took place (2020-2022).

-Contribution in the ROOTS of routes and Waste booklets (2021 and 2022).

-Contribution in Electron Microscopy Conference Darmstadt: TEM investigation comparing heritage materials of Former Prussia and central Europe (Ukraine)(2023).

-Contribution in EAA 23-Material analysis of medieval artefacts from East Baltic region and Ostriv (Ukraine) using Transmission Electron Microscopy and Scanning Electron Microscopy (2023)

1. Publikation/Manuskript: Metal on Metal: Comparative material analysis of medieval artifacts from eastern Baltic and central Ukrainian cemeteries using transmission electron microscopy (TEM) and scanning electron microscopy (SEM) techniques

Submitted to Journal of Archaeologia Baltica (2023)

Autoren: Khurram Saleem, Roman Shiroukhov, Ulrich Schürmann, Vyacheslav Baranov, Vsevolod Ivakin, Claus von Carnap-Bornheim, Lorenz Kienle

Konzeptionierung	Planung	Durchführung	Manuskripterstellung
hoch	hoch	hoch	hoch

2. Publikation/Manuskript: Decorative coating or corrosion product? TEM and SEM Study on a Late Neolithic Axe to find origins of silver metal on the surface

Uploaded to ArXiv (2023)

Autoren: Khurram Saleem, Ulrich Schürmann, Lena Grandin, Christian Horn, Johannes Müller, Claus von Carnap-Bornheim, Lorenz Kienle

Konzeptionierung	Planung	Durchführung	Manuskripterstellung
hoch	hoch	hoch	hoch

3. Publikation/Manuskript: Baltic Migrants in the Middle Dnipro Region: A Comparative Study of the Late Viking Age Archaeological Complex of Ostriv, Ukraine.

Journal of Medieval Archaeology, Page 221-265, Vol 66, issue 2 (2022)

Autoren: Roman Shiroukhov, Vyacheslav Baranov, Vsevolod Ivakin, Oleksandra Kozak, Artem Borysov, Claus von Carnap-Bornheim, Lorenz Kienle, Ben Krause-Kyora, John Meadows, **Khurram Saleem**, Ulrich Schürmann, Justina Kozakaitė and Žydrūnė Miliauskienė.

Konzeptionierung	Planung	Durchführung	Manuskripterstellung
niedrig	mittel	mittel	mittel

Declaration of authorship

I hereby confirm that my dissertation entitled *Examination of ancient artefacts from Europe (2200 BC-1200 AD) using material analysis techniques* is the result of my own work. I have received no help or support from commercial consultants. All sources and/or materials used herein are listed and specified in the thesis. Furthermore, I assure that this work has not been submitted in the same or similar form before in any other examination procedure and has been prepared in compliance with the safeguarding of good scientific practice of the German Research Foundation. I further declare that no academic degree has been withdrawn from me.

Kiel, 29.08.2023

Ort, Datum, Unterschrift Doktorand

12 Index

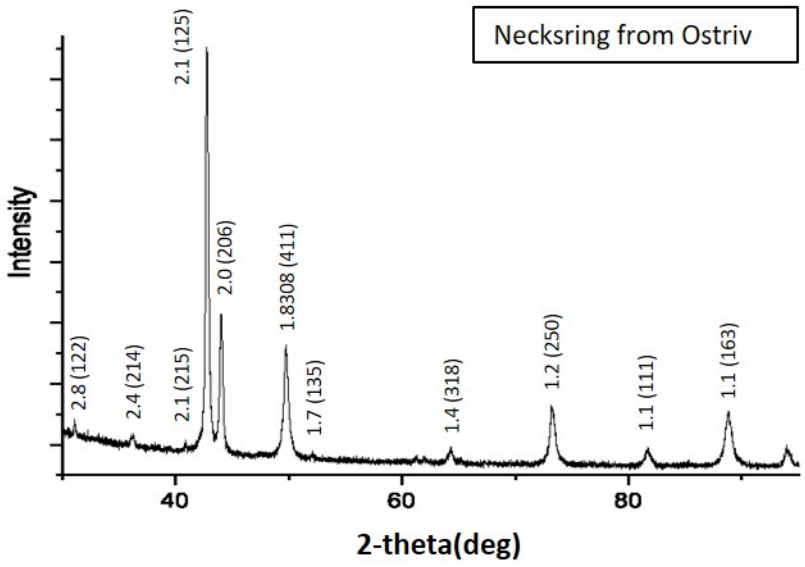

Figure 54: Neck Ring fragment from Ostriv (2403)-X-ray Diffraction (XRD) for large scale structural analysis

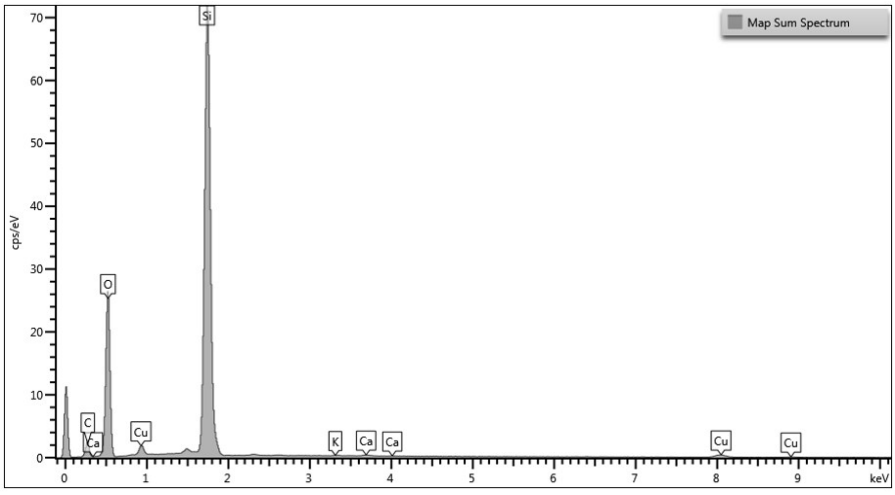

Figure 70: SEM EDS spectrum on experimental replica R29 of the detected elements

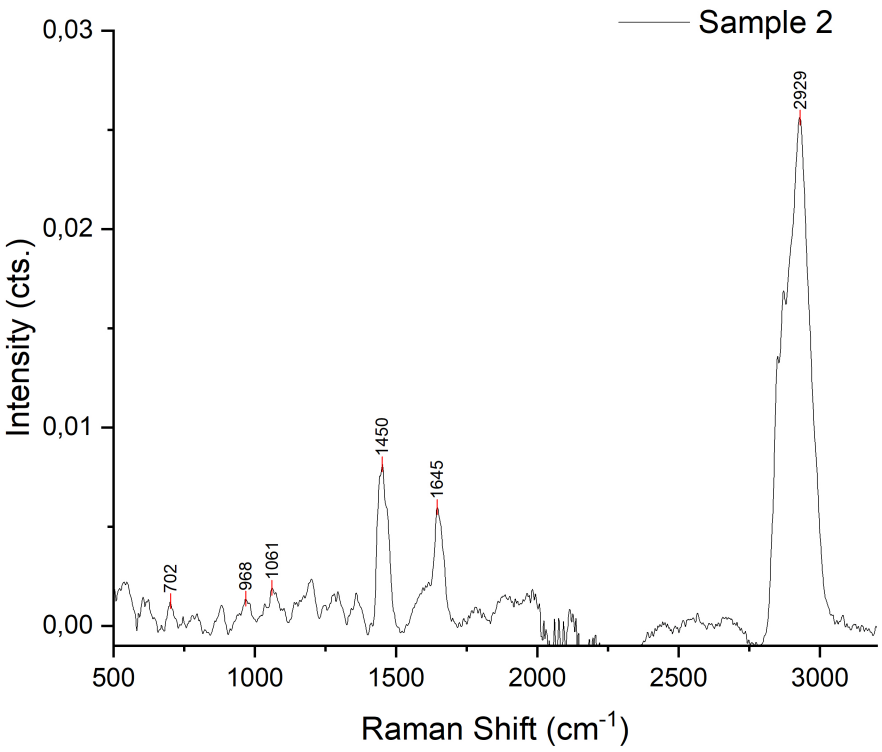

Figure 55: Raman spectra of the Amber sample from Kaliningrad, Russia

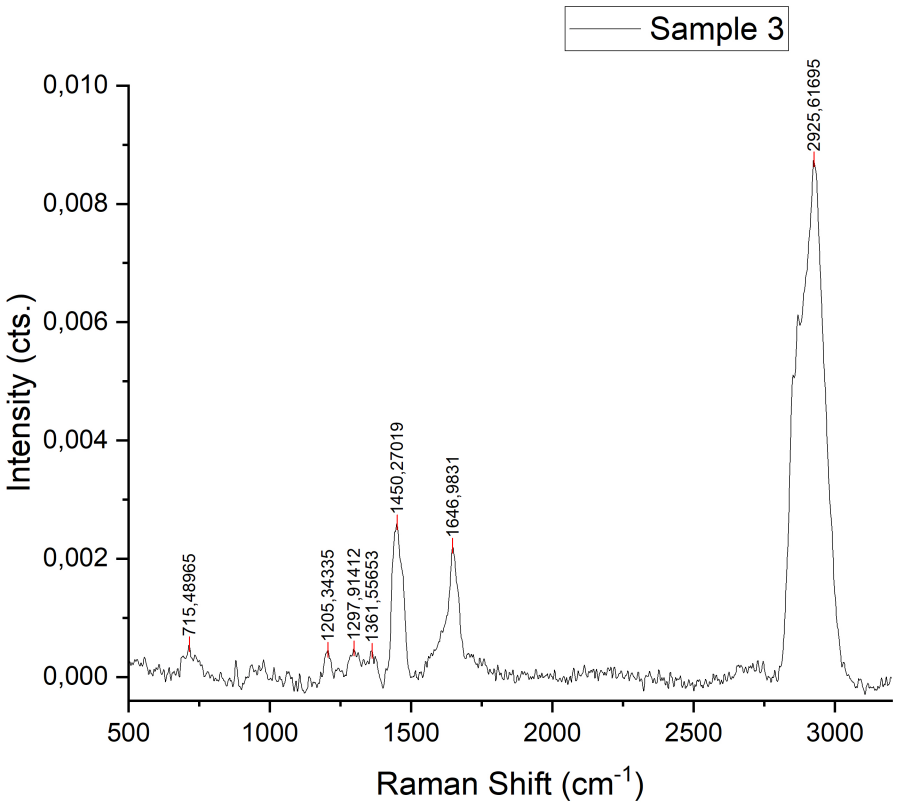

Figure 56: Raman spectra of the Amber sample from Kaliningrad, Russia

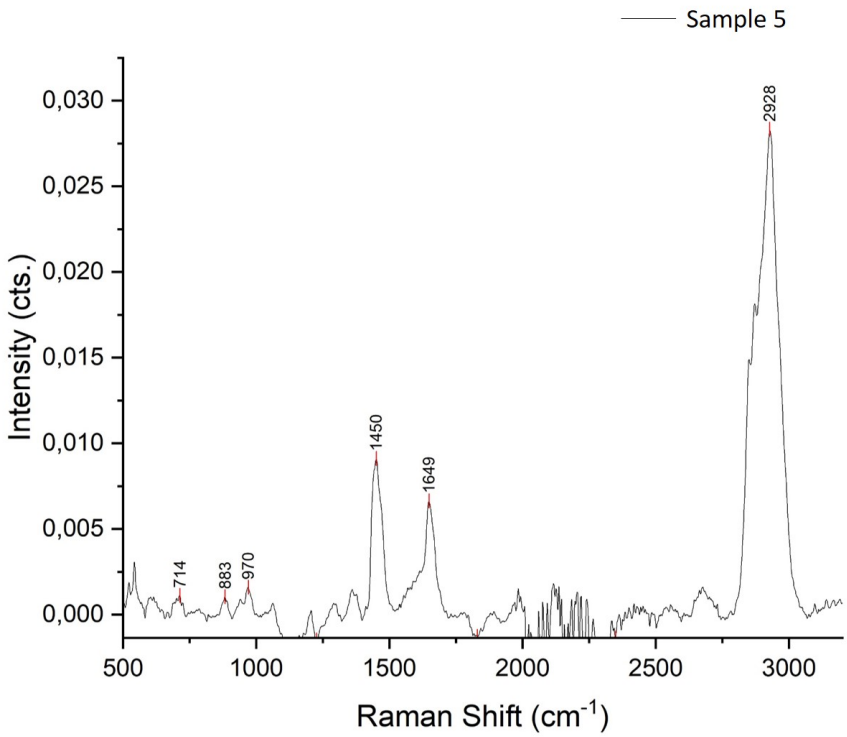

Figure 57: Ramam spectra of the Amber sample from Skallingen Vejers, Denmark

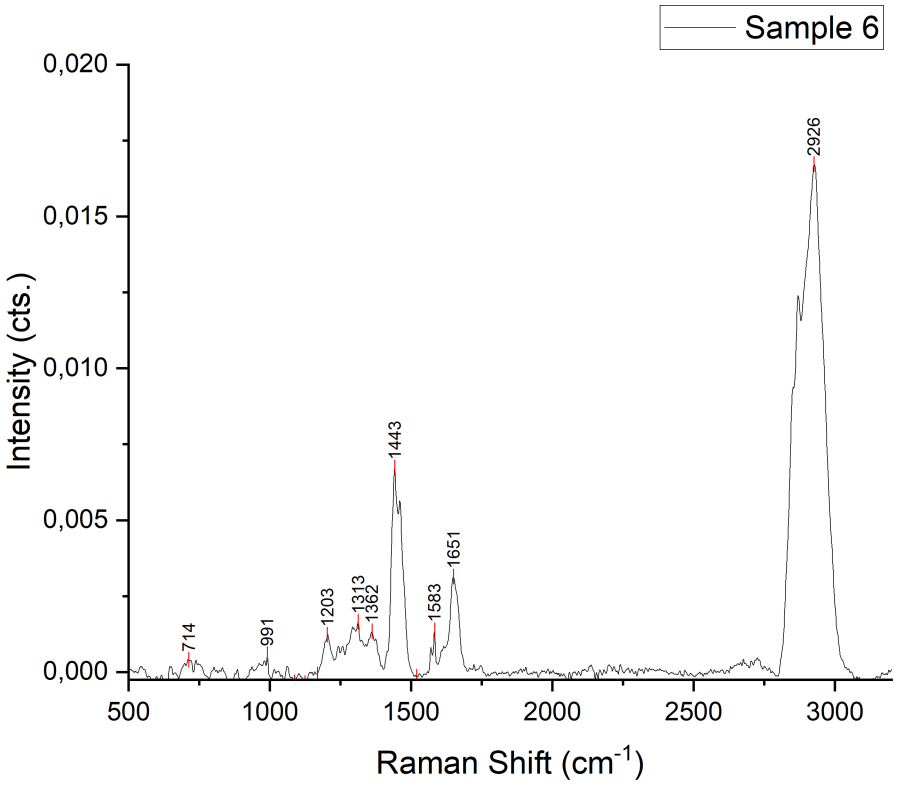

Figure 58: Ramam spectra of the Amber sample from Skallingen Vejers, Denmark

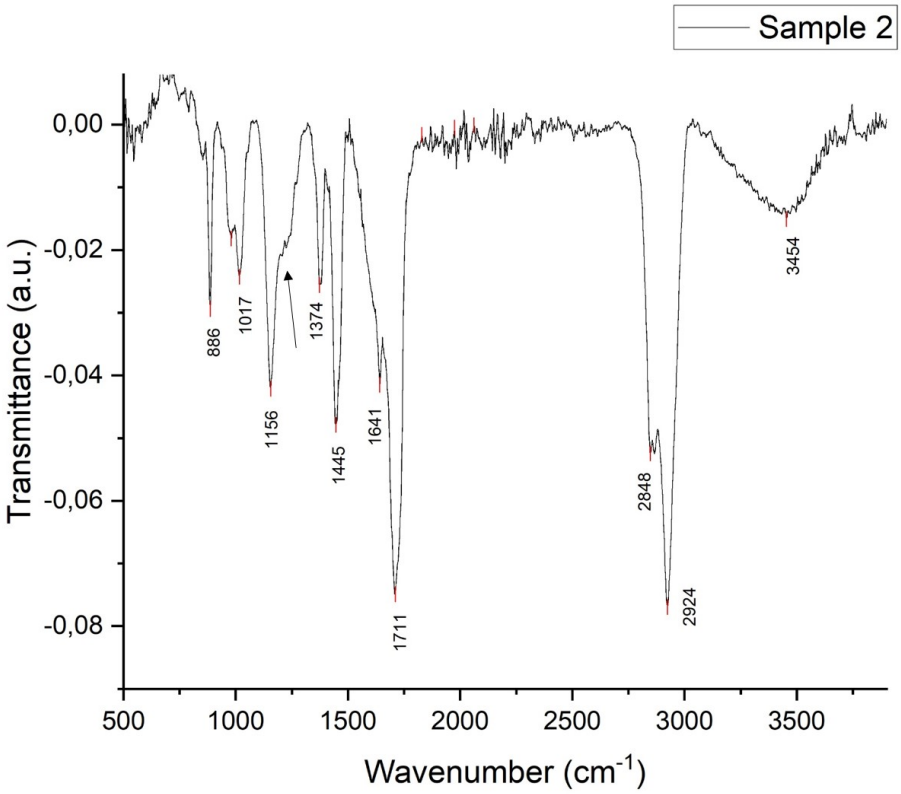

Figure 59: FTIR spectrum of amber from Kaliningrad, Russia, note the arrow between 1250 and 1180 cm^{-1} represents 'Baltic shoulder'

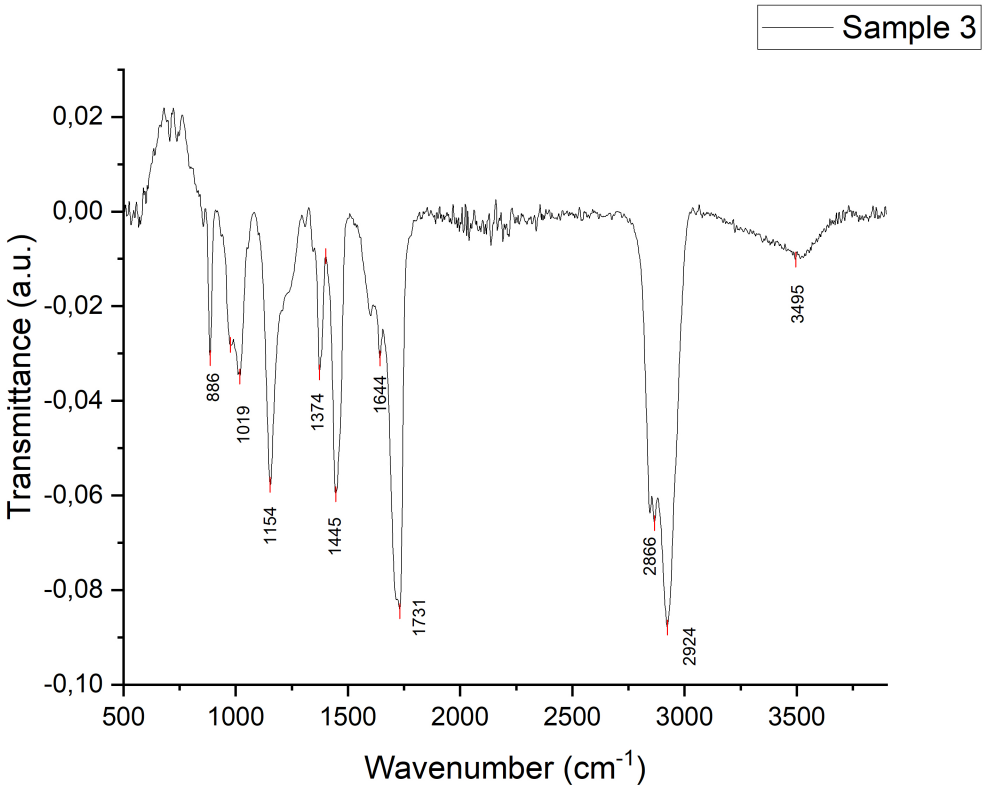

Figure 60: FTIR spectrum of amber from Kaliningrad, Russia, note the arrow between 1250 and 1180 cm^{-1} represents 'Baltic shoulder'

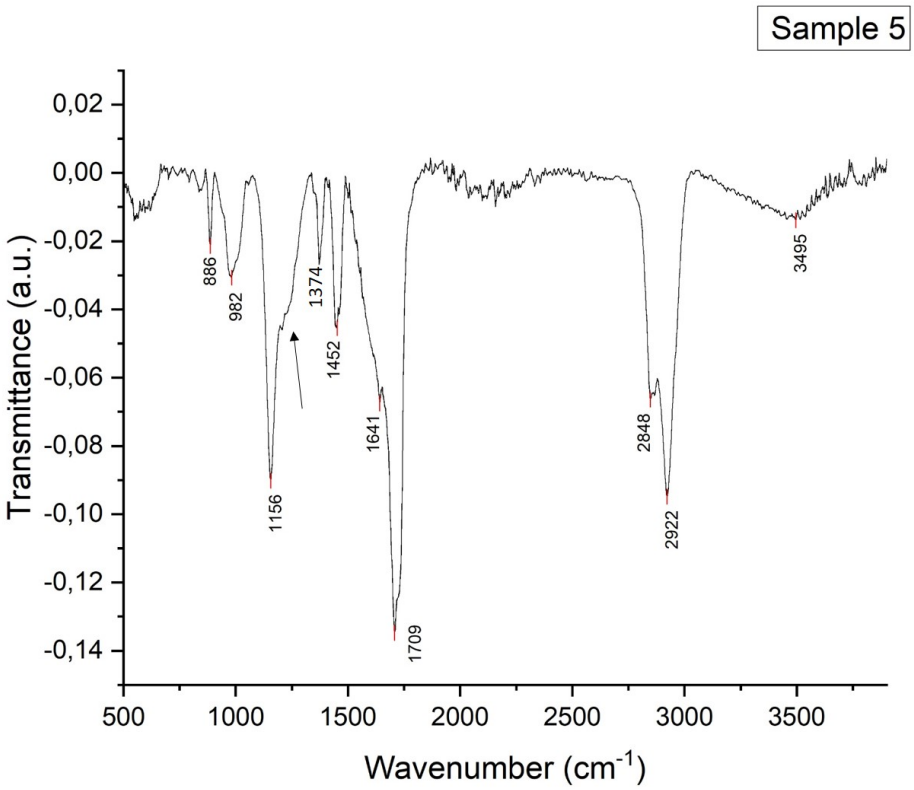

Figure 61: FTIR spectrum of amber from Skallingen Vejers, Denmark, note the arrow between 1250 and 1180 cm^{-1} represents 'Baltic shoulder'

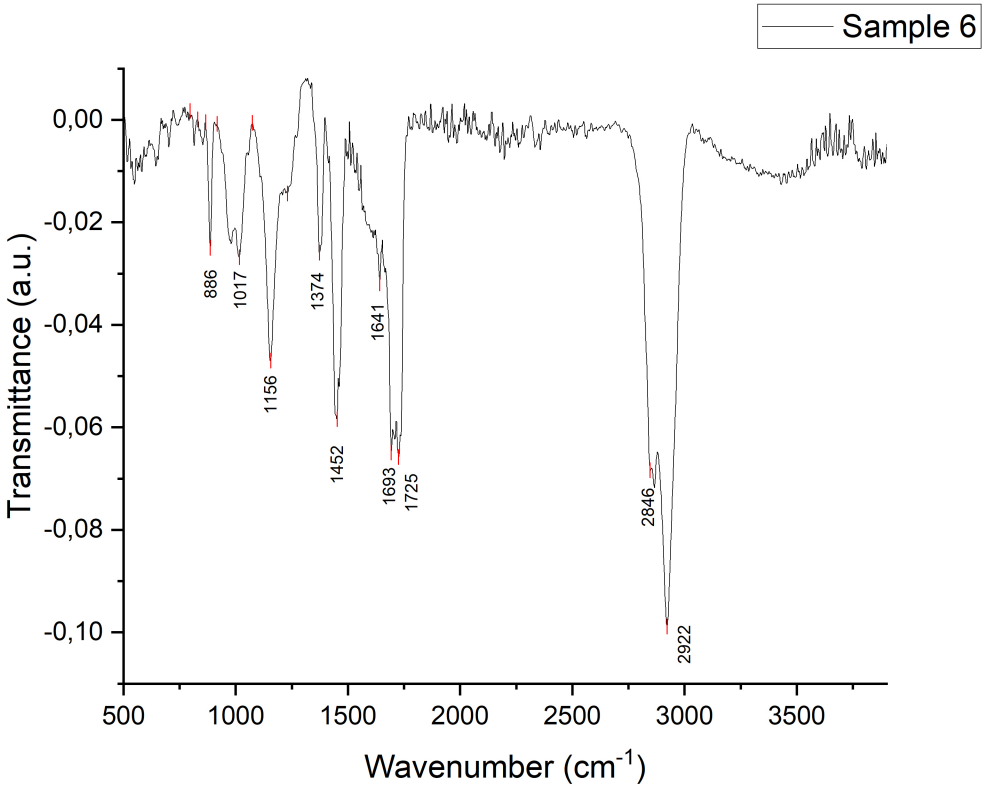

Figure 62: FTIR spectrum of amber from Skallingen Vejers, Denmark, note the arrow between 1250 and 1180 cm^{-1} represents 'Baltic shoulder'

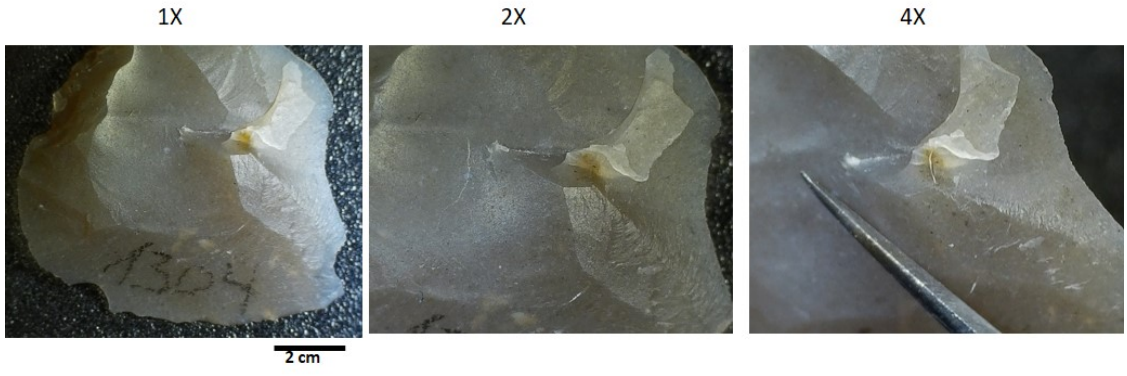

Figure 63: Experimental replica R19 of Late Neolithic Flint Tool knapped with copper knapping tool, photographic image with Digital Microscopy.

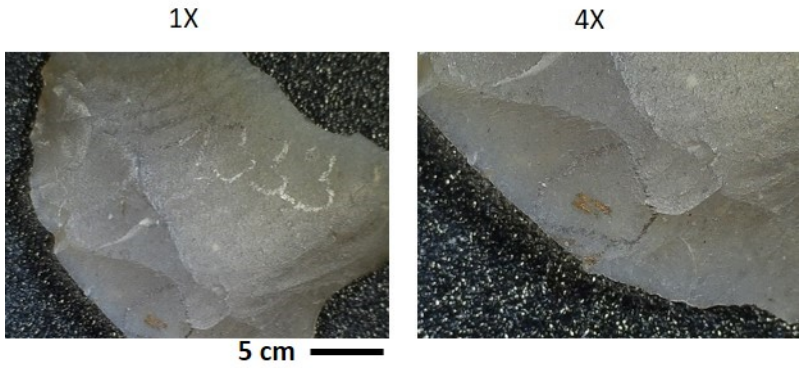

Figure 64: Experimental replica R22 of Late Neolithic Flint Tool knapped with copper knapping tool, photographic image with Digital Microscopy.

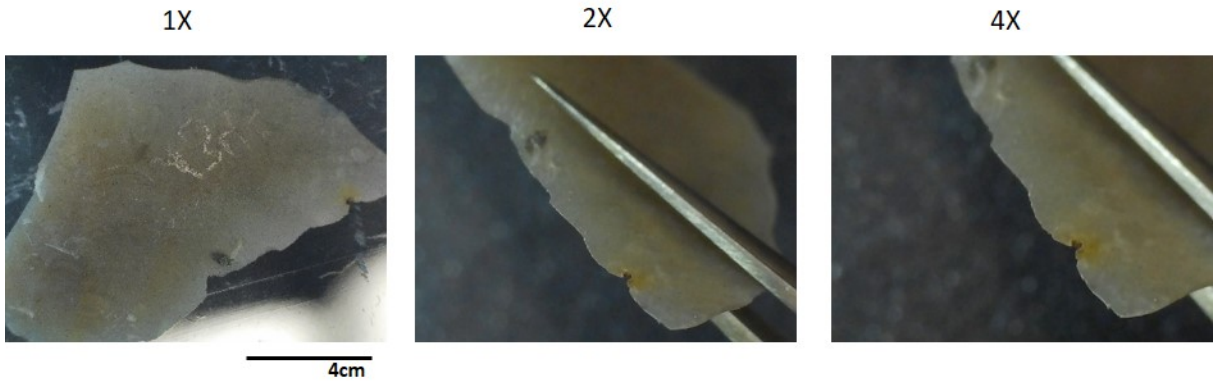

Figure 65: Experimental replica R24 of Late Neolithic Flint Tool knapped with copper knapping tool, photographic image with Digital Microscopy.

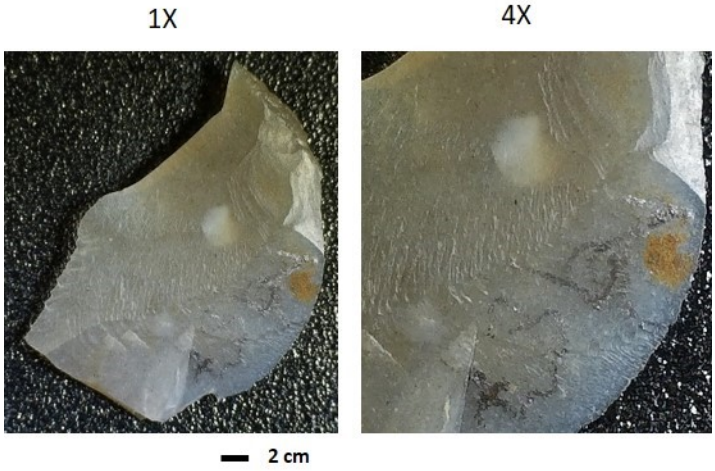

Figure 66: Experimental replica R25 of Late Neolithic Flint Tool knapped with copper knapping tool, photographic image with Digital Microscopy.

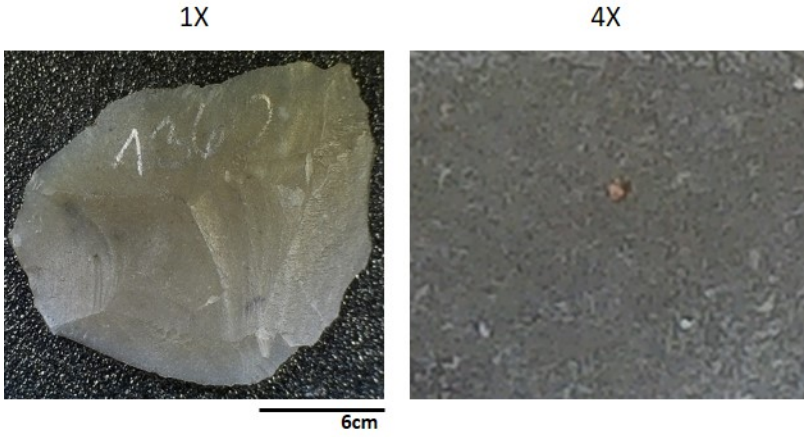

Figure 67: Experimental replica R50 of Late Neolithic Flint Tool knapped with copper knapping tool, photographic image with Digital Microscopy.

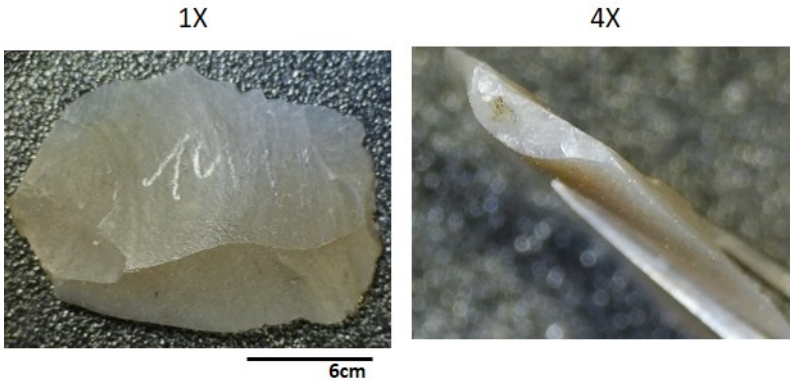

Figure 68: Experimental replica R29 of Late Neolithic Flint Tool knapped with copper knapping tool, photographic image with Digital Microscopy.

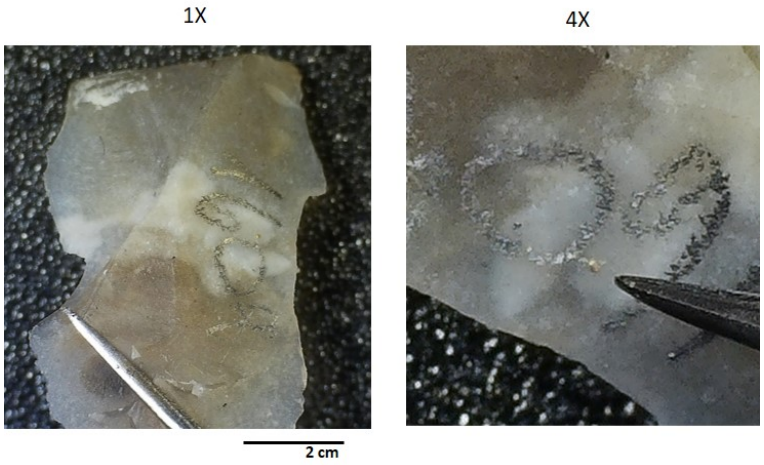

Figure 69: Experimental replica R32 of Late Neolithic Flint Tool knapped with copper knapping tool, photographic image with Digital Microscopy.

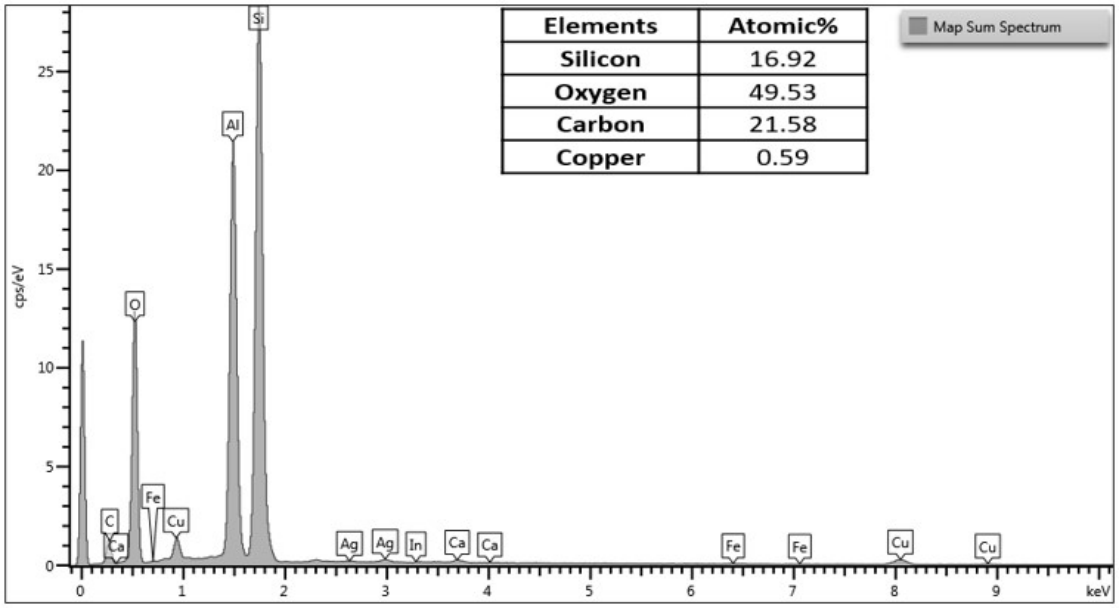

Figure 71: SEM-EDS spectrum on experimental replica R51 showing the detected elements

Specimen R24

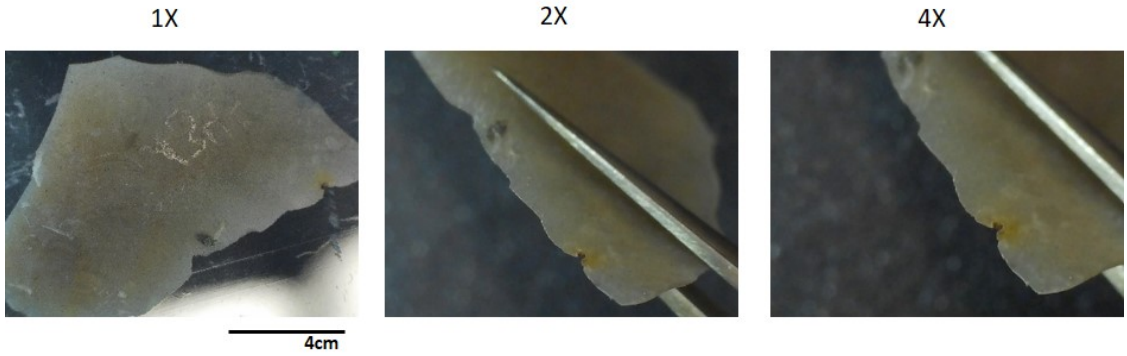

Figure 72: Experimental replica R24 of Late Neolithic Flint Tool knapped with copper knapping tool, photographic image with Digital Microscopy.

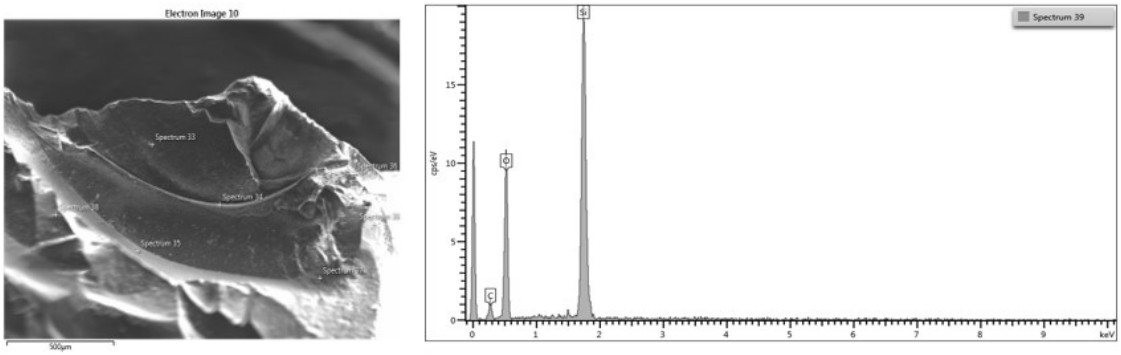

Figure 73: SEM electron image on experimental replica R24 on the left and EDS spectrum showing atomic percentages of the detected elements on the right